

**DOKUZ EYLÜL UNIVERSITY**  
**GRADUATE SCHOOL OF NATURAL AND APPLIED**  
**SCIENCES**

**NANOTECHNOLOGIC METHODS FOR WATER**  
**TREATMENT**

by  
**Ruti Ruth POLİTİ**

**April, 2014**  
**İZMİR**

# **NANOTECHNOLOGIC METHODS FOR WATER TREATMENT**

**A Thesis Submitted to the  
Graduate School of Natural and Applied Sciences of Dokuz Eylül University  
In Partial Fulfillment of the Requirements for the Degree of Master of  
Science in Environmental Engineering**

**by**

**Ruti Ruth POLİTİ**

**April, 2014**

**İZMİR**

**M.Sc THESIS EXAMINATION RESULT FORM**

We have read the thesis entitled “NANOTECHNOLOGIC METHODS FOR WATER TREATMENT” completed by RUTİ RUTH POLİTİ under supervision of PROF. DR. AYŞEGÜL PALA and we certify that in our opinion it is fully adequate, in scope and in quality, as a thesis for the degree of Master of Science.

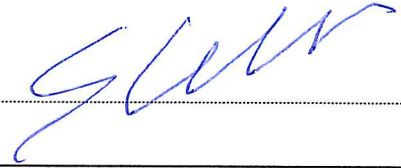


Prof. Dr. Ayşegül PALA

Supervisor



Prof. Dr. Delia SPONZA



Prof. Dr. Erdal ÇELİK



Prof.Dr. Ayşe OKUR

Director

Graduate School of Natural and Applied Sciences

## ACKNOWLEDGMENTS

I would like to state my special thanks to my advisor Professor Dr. Ayşegül PALA, for her priceless advices, invaluable experiences, continous supervision, considerable support and significant concern to carry out this study. It was pleasure to work with her.

I would like to also express Prof. Dr. Erdal ÇELİK for supervising this study, with his valuable suggestion, supports in the metallurgical and material step of this project and extend my appreciation to the crew of EMUM.

I am thankful to Research Assistant Mustafa EROL for his advices and comments. I am also appreciated to Fatma BAKAL for her valuable helps in metallurgical and material steps of the thesis.

This work is supported by TÜBİTAK (The Scientific and Technological Research Council of Turkey) 1001 - The Support Program for Scientific and Technological Research Project. The number of the project is 112Y162. In addition, Dokuz Eylül University Department of Scientific Research Project (BAP) provided support. The number of the project was 2010.KB.FEN.0302010111.

I also want to thank to my project partners Gülek ÖNER and Güneş KURŞUN, for their helps in various steps of the thesis and support.

A special thanks to my family for their moral support, motivation and encouragement.

Ruti Ruth POLİTİ

# NANOTECHNOLOGIC METHODS FOR WATER TREATMENT

## ABSTRACT

The main objective of this study is to see the photocatalytic degradation efficiencies of the persistent compounds in wastewater by using new generation photocatalytic materials (potassium lanthanum titanates). And also the influence of pH, pollutant concentration and light intensity are investigated. Newly developed layered perovskite structures are produced by sol-gel method. Sol-gel technique is a process to generate colloidal nanoparticles from liquid phase. The production of advanced nanomaterials and coatings are improving day by day. Today, water pollution problem is an important and increasing issue. Especially domestic and industrial wastes and natural pollutants create many problems. The disadvantage of the current treatment methods is the sludge formation. A nanotechnological method called sol-gel is applied to produce newly developed photocatalysts, to avoid the sludge formation and to oxidize the pollutants. To increase the crystallographic harmony, buffer layer application was applied. Cerium oxide was selected for a buffer layer. DTA, FTIR, XRD and SEM analyses were performed to find the structural and morphological characterization processes of the photocatalysts (KLTO), respectively. Phenol (organic matter), methylene blue (azo dye) and cyanide (inorganic matter) photocatalytic performance experiments were carried out in a solar box ATLAS SUNTEST CPS+ which is simulating natural radiation.

As a result of the study, the phenol and methylene blue experiments can be fitted to a second order reaction law. On the other hand, cyanide can be fitted first order reaction law. KLTO is more effective to treat cyanide and methylene blue than phenol.

Thin film photocatalysts are more environmentalist and less harmful than particulate catalysts. The difficulties of particulate catalysts are the separation of the particles from wastewater. For this reason, this study is realized.

**Keywords:** Sol-gel technique, photocatalytic, nanotechnology, KLTO, phenol, methylene blue, cyanide.

## SU ARITIMINDA NANOTEKNOLOJİK METODLAR

### ÖZ

Bu çalışmanın en önemli amacı yeni nesil fotokatalizörlerle (potasyum lantanyum titanat) suyun içinde zor parçalanmış bazı bileşiklerin fotokatalitik parçalanma verimlerinin araştırılmasıdır. Bu çalışmada pH, kirletici konsantrasyonu ve ışık şiddetinin etkileri incelenmiştir. Yeni gelişen katmanlı perovskit yapıdaki fotokatalizör sol-jel yöntemiyle üretilmiştir. Sol-jel tekniği koloidal nano partiküllerin sıvı fazdan oluşturulmasıdır. Nanomalzemelerin ve kaplamaların üretimleri gün geçtikçe ilerlemektedir. Bugün, en önemli ve sürekli artan problem su kirliliğidir. Su kirliliği evsel ve endüstriyel atıklar ile doğal kirleticilerden meydana gelmektedir. Mevcut arıtma yöntemlerindeki en önemli problem çamur oluşumudur. Çamur oluşumunu önlemek amacıyla nanoteknolojik bir yöntem olan sol - jel yöntemi ile üretilen yeni nesil fotokatalizörler kirleticinin oksidasyonu için kullanılmıştır. Kristografik harmoniyi arttırmak için buffer layer uygulaması ile katalizör geliştirilmiştir. Seryum oksit buffer layer olarak seçilmiştir. Üretilen filmlerin yapısal ve morfolojik karakterizasyon işlemleri DTA, FTIR, XRD ve SEM analizleri yapılmıştır. Fenol (organik madde), metilen mavisi (azo boyar madde) ve siyanür (inorganik madde) gibi kirleticiler kullanılarak fotokatalitik oksidasyon ile güneş simülatörü (ATLAS SUNTEST CPS+) yardımıyla performans testleri yapılmıştır.

Üretilen filmlerle yapılan deneyler sonucunda, fenol ve metilen mavisi ikinci derece reaksiyon kinetiğine uyduğu görülmüştür. Siyanür testlerinin sonucunda ise siyanür birinci derece reaksiyon kinetiğine uyduğu çıkmıştır. KLTO siyanür ve metilen mavisi arıtımında fenol arıtımından daha başarılı olmuştur.

Yüzey kaplaması ile üretilen katalizörlerin partikül haldeki katalizörlere göre daha çevreci ve insan sağlığı açısından daha az zararlı olması sebebiyle böyle bir çalışma yapılmasına karar verilmiştir.

**Anahtar Kelimeler:** Sol - jel tekniği, fotokatalitik, nanoteknoloji, KLTO, fenol, metilen mavisi, siyanür.

## CONTENTS

	Page
M.Sc THESIS EXAMINATION RESULT FORM.....	ii
ACKNOWLEDGMENTS .....	iii
ABSTRACT.....	iv
ÖZ .....	v
LIST OF FIGURES .....	x
LIST OF TABLES .....	xiii
<b>CHAPTER ONE - INTRODUCTION .....</b>	<b>1</b>
<b>CHAPTER TWO - FUNDAMENTAL ASPECTS OF PHOTOCATALYSTS AND PHOTOCATALYTIC SYSTEM .....</b>	<b>6</b>
2.1 Introduction .....	6
2.2 Photocatalysis .....	7
2.2.1 Photocatalytic Systems .....	10
2.3 Band Theory and Semiconductor Structure .....	11
2.4 Hole Conduction.....	17
2.5 Photocatalytic Degradation Mechanisms .....	18
2.6 Photocatalysis of Water with Layered Compounds .....	19
2.6.1 Layered Transition Metal Oxides .....	20
2.6.2 Layered Perovskite Oxides .....	20
2.6.2.1 Dion – Jacobson Series .....	21
2.6.2.2 Ruddlesden – Popper Series.....	21
2.7 $K_2La_2Ti_3O_{10}$ .....	21
2.7.1 Crystalline Structure .....	22
2.7.2 Photocatalytic Mechanisms of $K_2La_2Ti_3O_{10}$ .....	23

2.8 The Synthesis Methods of Semiconductor Photocatalysts (Sol–Gel) .....	23
2.9 The Coating Techniques for Producing Thin Films .....	26
2.9.1 Dip Coating Techniques .....	26
2.9.2 Spray Coating Techniques .....	27
2.9.3 Spin Coating Techniques .....	27
<b>CHAPTER THREE - MATERIAL AND METHOD.....</b>	<b>28</b>
3.1 The Aim of the Study .....	28
3.2 Materials .....	29
3.3 Production Process .....	30
3.4 Characterization.....	33
3.4.1 The Aim of Characterization .....	33
3.4.2 Solution Characterization .....	33
3.4.2.1 Turbidity Tests .....	33
3.4.2.2 pH Values of Solutions .....	34
3.4.2.3 Rheological Tests .....	34
3.4.2.4 Contact Angle Measurement.....	34
3.4.3 Process Optimization .....	35
3.4.3.1 Differential Thermal Analysis/Thermogravimetry (DTA/TG).....	35
3.4.3.2 Fourier Transform Infrared (FTIR).....	35
3.4.4 Material Characterization .....	35
3.4.4.1 X – Ray Diffraction (XRD) .....	35
3.4.4.2 Scanning Electron Microscopy – Energy Dispersive Spectrophotometer (SEM - EDS).....	36
3.4.4.3 Elemental Analysis-X-Ray Photoelectron Spectrophotometer(XPS). 36	
3.4.4.4 Surface Roughness - Atomic Force Microscope (AFM) .....	36



3.5 The Pollutants and the Properties .....	36
3.5.1 Phenol .....	36
3.5.2 Methylene Blue.....	41
3.5.3 Cyanide .....	43
3.6 Method.....	45
3.6.1 Photocatalytic Method .....	45
3.6.2 Statistical Method - Factorial Experimental Design.....	46
3.6.3 Reaction Kinetic Method .....	48
3.7 Atlas Suntest CPS+ .....	49
<b>CHAPTER FOUR - RESULTS AND DISCUSSION .....</b>	<b>51</b>
4.1 Solution Properties .....	51
4.1.1 Turbidity Values .....	51
4.1.2 pH Values .....	51
4.1.3 Rheological Properties.....	52
4.1.4 Contact Angle Measurement .....	53
4.2 Process Optimization.....	53
4.2.1 Differential Thermal Analysis/Thermogravimetry (DTA/TG) Analysis...	53
4.2.2 Fourier Transform Infrared (FTIR) .....	54
4.3 Film Characterization .....	55
4.3.1 XRD Analysis .....	55
4.3.2 SEM - EDS Analysis .....	57
4.3.3 Elemental Analysis and XPS Results .....	60
4.3.4 Surface Roughness - AFM Analysis.....	60
4.4 Photocatalytic Degradation Results.....	61
4.4.1 Photodegradation Results of Phenol .....	61

4.4.2 Photodegradation Results of Methylene Blue .....	72
4.4.3 Photodegradation Results of Cyanide.....	77
4.5 Kinetic Studies of Photodegradation Results with Synthetic Wastewaters .....	83
4.6 Factorial Experimental Design Studies .....	92
<b>CHAPTER FIVE - CONCLUSION AND RECOMMENDATIONS.....</b>	<b>97</b>
5.1 General Results.....	97
5.2 Recommendations .....	103
<b>REFERENCES .....</b>	<b>104</b>
<b>APPENDICES .....</b>	<b>115</b>

## LIST OF FIGURES

	<b>Page</b>
Figure 1.1 Typical photocatalytic reactions for water decomposition: (a) Ni(NiO) - SrTiO <sub>3</sub> , (b) Ni-K <sub>4</sub> Nb <sub>6</sub> O <sub>17</sub> , and (c) Ni(NiO)-K <sub>2</sub> La <sub>2</sub> Ti <sub>3</sub> O <sub>10</sub> .....	4
Figure 2.1 A comparison between photosynthesis and photocatalysis .....	8
Figure 2.2 Electromagnetic spectrum. ....	9
Figure 2.3 The mechanism of photocatalyst. ....	10
Figure 2.4 The mechanism of photocatalytic system.....	11
Figure 2.5 Insulator, conductor and semiconductor band energy levels.....	12
Figure 2.6 Semiconductor particle .....	13
Figure 2.7 A wall,(a) without coating of photocatalyst and (b) after the coating process .....	15
Figure 2. 8 Some metal oxides valence band energies.....	15
Figure 2.9 TiO <sub>2</sub> phases (a) rutile, (b) anatase, (c) brokite.....	16
Figure 2.10 The three types of semiconductors: (a) Intrinsic semiconductors, (b) n-type semiconductors, (c) p-type semiconductors.....	17
Figure 2.11 K <sub>2</sub> La <sub>2</sub> Ti <sub>3</sub> O <sub>10</sub> crystalline structure .....	22
Figure 2.12 K <sub>2</sub> La <sub>2</sub> Ti <sub>3</sub> O <sub>10</sub> energy band gap.....	23
Figure 2.13 Sol–gel technologies and their products. ....	25
Figure 2.14 Stages of the dip coating process.....	26
Figure 2.15 A schematic demonstration of spin coating technique. ....	27
Figure 2.16 The three sol gel method: (a dip coating, (b)spin coating and (c)spray coating.....	27
Figure 3.1 A schematic representation of the Photoreactor. ....	29
Figure 3.2 Production flow chart. ....	30
Figure 3.3 A schematic figure of buffer layer technique. ....	31
Figure 3.4 The flow chart of the production of CeO <sub>2</sub> . ....	31
Figure 3.5 CeO <sub>2</sub> heat treatment process.....	32
Figure 3.6 KLTO Film. ....	33
Figure 3.7 Dimensions of phenol.....	38
Figure 3.8 The chemical structure of methylene blue.....	42
Figure 3.9 The chemical structure of cyanide.....	44

Figure 3.10 ATLAS Suntest CPS+ images. ....	50
Figure 4.1 The change of the modulus of elasticity and viscous (25°C). ....	52
Figure 4.2 DTA/TG curves of KLTO powder xerogel. ....	54
Figure 4.3 FTIR spectrums of the KLTO xerogels. ....	55
Figure 4.4 XRD pattern of the optimum phase (specimen 9). ....	56
Figure 4.5 SEM micrographs of $K_2La_2Ti_3O_{10}$ thin films ....	59
Figure 4.6 The spectrum of $K_2La_2Ti_3O_{10}$ from XPS. ....	60
Figure 4.7 AFM images of KLTO films from different areas. ....	60
Figure 4.8 Schematic experiment apparatus. ....	61
Figure 4.9 Phenol concentration vs.time results( $C_0=10$ mg/l, $250$ W/m <sup>2</sup> , pH=7). ....	63
Figure 4.10 Phenol removal efficiencies(%)( $C_0 = 10$ mg/l, $250$ W/m <sup>2</sup> , pH = 7). ....	63
Figure 4.11 Phenol concentration vs.time results ( $C_0=100$ mg/l, $250$ W/m <sup>2</sup> , pH=7). ....	65
Figure 4.12 Phenol removal efficiencies(%)( $C_0 = 100$ mg/l, $250$ W/m <sup>2</sup> , pH=7). ....	65
Figure 4.13 Phenol concentration vs.time results( $C_0=10$ mg/l, $750$ W/m <sup>2</sup> , pH = 7). ....	67
Figure 4.14 Phenol removal efficiencies (%) ( $C_0 = 10$ mg/l, $750$ W/m <sup>2</sup> , pH=7). ....	67
Figure 4.15 Phenol concentration vs.time results( $C_0=100$ mg/l, $750$ W/m <sup>2</sup> , pH=7). ....	69
Figure 4.16 Phenol removal efficiencies(%)( $C_0 = 100$ mg/l, $750$ W/m <sup>2</sup> , pH=7). ....	69
Figure 4.17 Methylene blue removal absorbance vs. time ( $C_0 = 10^{-5}$ M, $250$ W/m <sup>2</sup> and pH = 3). ....	73
Figure 4.18 Methylene blue removal efficiencies (%) ( $C_0 = 10^{-5}$ M, $250$ W/m <sup>2</sup> and pH = 3). ....	73
Figure 4.19 Cyanide concentration vs. time results( $C_0=100$ mg/l, $250$ W/m <sup>2</sup> and pH = 10). ....	78
Figure 4.20 Cyanide removal efficiencies(%)( $C_0=100$ mg/l, $250$ W/m <sup>2</sup> , pH = 10). ...	78
Figure 4.21 Cyanide concentration vs. time results ( $100$ mg/l, $750$ W/m <sup>2</sup> and pH = 10). ....	80
Figure 4.22 Cyanide removal efficiencies(%)( $C_0=100$ mg/l, $750$ W/m <sup>2</sup> , pH=10). ...	80
Figure 4.23 Concentration vs. time for second order degradation of phenol (KLTO Surface Coating). ....	84
Figure 4.24 Concentration vs. time for zero order degradation of phenol (KLTO Surface Coating). ....	85

Figure 4.25	Concentration vs. time for first order degradation of phenol (KLTO Surface Coating).....	86
Figure 4.26	Concentration vs. time for zero order degradation of phenol (KLTO Surface Coating).....	87
Figure 4.27	Concentration vs. time for first order degradation of cyanide (KLTO Surface Coating).....	88
Figure 4.28	Concentration vs. time for zero order degradation of cyanide (KLTO Surface Coating).....	89
Figure 4.29	Concentration vs. time for second order degradation of methylene blue (KLTO Surface Coating).....	90
Figure 4.30	Concentration vs. time for zero order degradation of methylene blue (KLTO Surface Coating).....	91
Figure 4.31	Some photos from experimental studies.....	96

## LIST OF TABLES

	<b>Page</b>
Table 3.1 Raw materials and its properties .....	29
Table 3.2 Materials used in the production of CeO <sub>2</sub> .....	31
Table 3.3 Spin coating parameters .....	32
Table 3.4 Water pollution control regulations - phenol limits.....	38
Table 3.5 Chemical and biological treatment methods for phenol according to the literature .....	39
Table 3.6 A summary table for the photocatalytic treatment methods of phenol according to the literature .....	40
Table 3.7 Water pollution control regulations - methylene blue limits .....	42
Table 3.8 A summary table for the photocatalytic treatment methods of methylene blue according to the literature .....	43
Table 3.9 Water pollution control regulations - cyanide limits .....	44
Table 3.10 A summary table for the photocatalytic treatment methods of cyanide according to the literature .....	44
Table 3.11 Properties of SUNTEST CPS+ .....	49
Table 3.12 Sunlight measurements of ATLAS SUNTEST CPS+ .....	50
Table 4.1. Solutions turbidity value .....	51
Table 4.2 pH values of Ce based solutions .....	51
Table 4.3 pH values of K, La, Ti - based solutions.....	52
Table 4.4 Thermal treatment analysis phase .....	54
Table 4.5 Thin film codes .....	56
Table 4.6 The efficiencies of phenol experiment (10 mg/l, 250 W/m <sup>2</sup> and pH=7)....	62
Table 4.7 The efficiencies of phenol experiment (100 mg/l, 250 W/m <sup>2</sup> and pH=7) .	64
Table 4.8 The efficiencies of phenol experiment (10 mg/l, 750 W/m <sup>2</sup> and pH=7) ...	66
Table 4.9 The efficiencies of phenol experiment (100 mg/l, 750 W/m <sup>2</sup> and pH=7) .	68
Table 4.10 Summary of phenol experiments .....	70
Table 4.11 Summary of phenol degradation efficiencies (%).....	71
Table 4.12 The efficiencies of methylene blue experiment (10 <sup>-5</sup> M, 250 W/m <sup>2</sup> and pH = 3) .....	72

Table 4.13 The efficiencies of methylene blue experiment ( $10^{-5}$ M, $750 \text{ W/m}^2$ and pH = 5) .....	74
Table 4.14 Summary of methylene blue experiments.....	75
Table 4.15 Summary of methylene blue degradation efficiencies (%).....	76
Table 4.16 The efficiencies of cyanide experiments (100 mg/l, $250 \text{ W/m}^2$ and pH = 10) .....	77
Table 4.17 The efficiencies of cyanide experiments (100 mg/l, $750 \text{ W/m}^2$ and pH = 10).....	79
Table 4.18 Summary of cyanide experiments.....	81
Table 4.19 Summary of cyanide degradation efficiencies (%).....	82
Table 4.20 The reaction order types of phenol (10 mg/l, $250 \text{ W/m}^2$ , pH = 7).....	84
Table 4.21 The reaction order types of phenol (100 mg/l, $250 \text{ W/m}^2$ , pH = 7).....	85
Table 4.22 The reaction order types of phenol (10 mg/l, $750 \text{ W/m}^2$ , pH = 7).....	86
Table 4.23 The reaction order types of phenol (100 mg/l, $750 \text{ W/m}^2$ , pH = 7).....	87
Table 4.24 The reaction order types of cyanide (100 mg/l, $250 \text{ W/m}^2$ , pH = 10) .....	88
Table 4.25 The reaction order types of cyanide (100 mg/l, $750 \text{ W/m}^2$ , pH = 10) .....	89
Table 4.26 The reaction order types of methylene blue ( $10^{-5}$ M, $250 \text{ W/m}^2$ , pH=3) .	90
Table 4.27 The reaction order types of methylene blue ( $10^{-5}$ M, $750 \text{ W/m}^2$ , pH=3) .	91
Table 4.28 Variables for phenol experimental design .....	93
Table 4.29 Variables for cyanide experimental design .....	93
Table 4.30 Variables for methylene blue experimental design.....	93
Table 4.31 A briefly comparison of the variables and their effects by KLTO Surface Coating .....	95
Table 5.1 Summary table of the reaction order.....	101

## **CHAPTER ONE**

### **INTRODUCTION**

The water pollution problem is an important and increasing issue. That is why; the rise of the environmental consciousness becomes more significant in national and international levels. Especially domestic and industrial wastes create many problems. The major pollutant of surface water and underground water is industrial wastewaters. The upward trend of water contamination causes many environmental problems. There are many different treatment processes such as mechanical, biological, physical and chemical which are usually used separately or together for industrial wastewater treatment facilities. But none of them could treat persistent and toxic organic matters with high removal rates. Chemical coagulation, flocculation and sedimentation are conventional methods to remove toxic and persistent matters, but their efficiencies are very low. Different methods for the treatment of these substances are distillation and adsorption. These methods have high removal rates but they are very expensive. For these reasons advanced treatment methods are developed. To remove persistence and toxic matters, "Advanced Treatment Methods" are improved. Photocatalytic oxidation processes are suggested to treat this polluted water. Photodegradation is a method for the treatment of toxic and bioresistant pollutants (D'Oliveria et al., 1990; Kochany, 1993). The principal of photodegradation is hydroxyl radical ( $\text{OH}^{\bullet}$ ) formation. With this method high removal rates of organic pollutant can be obtained, but the amount of the chemicals (e.g.  $\text{H}_2\text{O}_2$ ) which are used and energy requirements (to obtain UV light) are very high. For this reason, a natural source as sunlight has been using. The utilization of sunlight is still not only sufficient for removing organic contaminants exactly. In addition, for the purification of wastewater, other different methods are existed which are remaining residue called sludge and that is why the problem is not finishing. To avoid the sludge formation, a nanotechnological method is applied. Sol-gel method is a new photocatalytic technique.



In recent years, photocatalytic specialized materials and devices are increased not only in academic case but also in industrial applications. This dramatic rise accompanies with the population growth and wastes which are increased by them.

New technological improvements are invented continuously. Owing to the environmental pollution, these new approaches ought to be nature - friendly. In 1969, according to a Japan researcher called Fujishima, photocatalysts had used for the treatment process. The name of his study called Honda – Fujishima effect. Honda - Fujishima realized a prototype: Fine powders which are doped with metal and/or metal oxide particles were used as a photocatalyst in chemical reactions. These fine powders were semiconductor. Photocatalytic reactions with using  $\text{TiO}_2$  were discovered by them. Among these years many research have been done to improve the photocatalytic systems (Kodama & Suzuki, 2007).

Photocatalytic semiconductors drew attention because of the ability to remove the pollutants. Photocatalysis is a substance which creates chemical oxidation reaction with the presence of light like chlorophyll in photosynthesis process. When photocatalysis is exposed to the light like photosynthesis process, the activation of the photocatalysis will occur (Khakpash, Simchi & Jafari, 2011).

The most powerful and cheap photocatalyst known is titanium dioxide ( $\text{TiO}_2$ ) and the semiconductor structure provides this photocatalytic function. It has high chemical stability, non-toxicity and high oxidation power. Three types of  $\text{TiO}_2$  exist such as anatase, rutile and brookite. Two of them (anatase and rutile) are the most used, but anatase phase has higher photocatalytic activity than the others. For this reason anatase phase is using widely. Neither chemically nor biologically it is active.  $\text{TiO}_2$  is not entering the reaction and it exists without any change. Although it is very active with light, light cannot degrade it. The anatase phase's band gap is 3.2 eV and the rutile phase's is 3.0 eV. The wavelengths are 388 and 410 nm, respectively (Khakpash, Simchi & Jafari, 2011).

Photocatalytic process is started with the absorption of light by the presence of the semiconductor structure. Semiconductors are constituted with an energy gap which are separated two energy band called valance and conductivity band. If photocatalysis which is exposed to photon energy is on the own energy gap, it gives its energy to an electron which is in valance band and electron is reached to the conductivity band. At the end of this reaction, electron – hole pairs occur. Electron – hole pairs which are located in valance and conductivity band become power supply. The size of energy gap and position effects photocatalytic reactions (Kaneko & Okura, 2002).

Photocatalytic activity of  $\text{TiO}_2$  is investigated by many researchers thanks to their band gap donors and acceptors, for instance cationic or anionic dopants. To improve photocatalytic activity, some anions or transition metals can be doped to  $\text{TiO}_2$ .

After the improvements of  $\text{TiO}_2$ , new approaches are enhanced like perovskite type layered materials. It has been realized that these types are more active than  $\text{TiO}_2$ . Ion exchange occurs immediately with perovskite type layered structures in terms of the geometry. One of them is very popular among researchers and they are continuing to their study to find some new properties. This is called lanthanum – titanates ( $\text{K}_2\text{La}_2\text{Ti}_3\text{O}_{10}$ ).  $\text{Ln}_2\text{Ti}_3\text{O}_{10}^{2-}$  octahedral perovskite layers and substitutional K ions constitute the structure. This structure provides hydration of toxic and persistent organic matters in aqua solutions with the presence of UV light; in this way it presents high photocatalytic activity (Takata et al., 1997).

New photocatalysts for water splitting are invented which are ion – exchangeable layered compounds such as  $\text{K}_4\text{Nb}_6\text{O}_{17}$ ,  $\text{KCa}_2\text{Nb}_3\text{O}_{10}$ ,  $\text{K}_2\text{La}_2\text{Ti}_3\text{O}_{10}$  and  $\text{KTiNbO}_5$ . Photocatalytic activity is enhanced by the combination of some dopants like Ni or Pt. Because of the structural properties, bulk – type photocatalysts such as  $\text{TiO}_2$  and  $\text{SrTiO}_3$  decompose water on the external surface, layered photocatalysts might use each individual layered surface for water splitting. Figure 1.1 illustrates the three types of photocatalysts which show the mechanism of  $\text{H}_2\text{O}$  decomposition: (a) Ni(NiO) -  $\text{SrTiO}_3$ , bulk-type photocatalyst; (b) Ni- $\text{K}_4\text{Nb}_6\text{O}_{17}$ , a layered photocatalyst

with two different types of interlayer space (I and II); and (c) Ni(NiO)-K<sub>2</sub>La<sub>2</sub>Ti<sub>3</sub>O<sub>10</sub>, a layered perovskite photocatalyst with only one type of interlayer space (Kakahana & Domen, 2000).

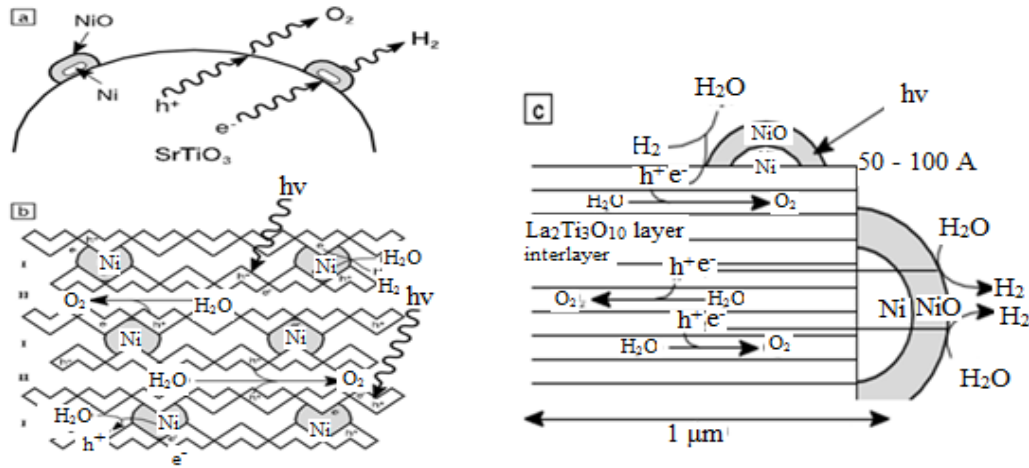


Figure 1.1 Typical photocatalytic reactions for water decomposition: (a) Ni(NiO) - SrTiO<sub>3</sub>, (b) Ni-K<sub>4</sub>Nb<sub>6</sub>O<sub>17</sub>, and (c) Ni(NiO)-K<sub>2</sub>La<sub>2</sub>Ti<sub>3</sub>O<sub>10</sub> (Kakahana and Domen, 2000).

According to the literature studies, some ion additives enhance lanthane - titanate structure. K ion which is located between the layers or Ti ions replaced the other dopants.

Yuelin et al. (2008) investigated the effect of the Ta addition in K<sub>2-x</sub>La<sub>2</sub>Ti<sub>3-x</sub>Ta<sub>x</sub>O<sub>10</sub> (x=0.1–1.0) which was produced by high temperature solid state sintering. As a result of this study, it can be reported that when the Ta ratio increases, photocatalytic effect is increasing.

Yahui et al. (2006) doped B to K<sub>2</sub>La<sub>2</sub>Ti<sub>3</sub>O<sub>10</sub> structure and examined the photocatalytic variation. In consequence of the study, B addition enhances the photocatalytic effect.

Lui et al. (2010) were produced Ce - based K<sub>2</sub>La<sub>2</sub>Ti<sub>3</sub>O<sub>10</sub> structure by solid state reaction and characterized by using XRD, UV-Vis DRS, TEM and XPS. The photocatalytic activity was examined by visible light region.

Cui et al. (2006) were produced layered perovskite  $K_2La_2Ti_3O_{10}$  by high temperature solid state sintering and characterized by XRD and UV-Vis DRS. Ni and Pt dopants were added to understand the effectiveness.

Yang et al. (2009) were produced  $K_2La_2Ti_3O_{10}$  by sol-gel method and by doping with Vanadium (V). V was risen the photocatalytic activity.

According to the literature, there are very few studies on thin film  $K_2La_2Ti_3O_{10}$  application.

One of the big problems generally encountered in the synthesis of  $K_2La_2Ti_3O_{10}$  was to find the effective phase. Several researches were done to solve the structure and necessary phase. At once powders have been tested in treatment experiences. After this process, suitable phase was found. New generation photocatalytic thin films production is accelerated. Buffer layer method is used to enhance the efficiency.

A laboratory study was performed to examine the effectiveness of  $K_2La_2Ti_3O_{10}$ , and the photocatalytic degradation of phenol, methylene blue and cyanide. The selection of the pollutants is special. Phenol is an organic matter, methylene blue is an azo dye and cyanide is an inorganic substance. The effect of various parameters such as the concentration of wastewater, pH and the light intensity were selected. The efficiency of photocatalytic degradations was studied. Based on the approaches, this thesis is focused on as follows:

- To produce  $K_2La_2Ti_3O_{10}$  photocatalysts with using nanotechnologic method,
- To see the influence of concentration of wastewater, pH and light intensity with ATLAS SUNTEST CPS+ by using  $K_2La_2Ti_3O_{10}$  photocatalysis,
- To understand the effectiveness of  $K_2La_2Ti_3O_{10}$ , make a degradation comparison of  $K_2La_2Ti_3O_{10}$ , arbitration specimen and  $TiO_2$ ,
- To examine the effectiveness of the parameters under favor of ANOVA tests.

## CHAPTER TWO

### FUNDAMENTAL ASPECTS OF PHOTOCATALYSTS AND PHOTOCATALYTIC SYSTEM

#### 2.1 Introduction

During the century, titanium dioxide and its effects on water treatment has been subjected to the several studies. Researches focused on hydrogen photoevolution from water or organic wastes. At first, researches had been done to learn the properties of semiconductors and its modifications. While the development of the new branch of chemistry was occurring, investigations was interested in semiconductors such as titania and the reactions which were occurring. In aqueous TiO<sub>2</sub> suspensions, the generation of •OH radical and their effect was studied out by Bard and co – workers. After the discovery of •OH radical effects on TiO<sub>2</sub>, photocatalytic oxidation of organic compounds has been studied by many scientists. In recent years, photocatalytic degradation/mineralization of organic/inorganic pollutants studied and subjected to many reviews. An increasing demand was shown to enhance the photocatalytic activity of TiO<sub>2</sub> nanostructures via doping with midband gap donors or acceptors to raise the solar absorption (Sobczynski et al., 2003).

Fujishima and Honda were introduced the development of photocatalysis and mineralization by using TiO<sub>2</sub> in 1972. The photocatalytic reduction of water under favor of semiconductors under solar energy is very effective to generate hydrogen. Studies have been focused on TiO<sub>2</sub>, niobates, titanates, tantalates, ferrate and vanadate. Thus far photocatalytic materials were limited, but now the modifications have been improved with using solar energy or artificial energy source (Yang et al., 2009). Recently, the layered perovskite photocatalyst K<sub>2</sub>La<sub>2</sub>Ti<sub>3</sub>O<sub>10</sub> has drawn attention due to its unique properties, for example, optical properties, electrical transport properties, and especially its photocatalytic activity. In addition, a lot of derivatives of K<sub>2</sub>La<sub>2</sub>Ti<sub>3</sub>O<sub>10</sub> can be generated due to replace with other elements (Yang et al., 2007).

This thesis represents an approach to report the mechanism of phenol, methylene blue and cyanide with photocatalytic oxidation. Additionally, the kinetics of phenol, methylene blue, cyanide was estimated. The effectiveness of the parameters was examined by using ANOVA tests.

## **2.2 Photocatalysis**

Organic/inorganic pollutants can be found in wastewater from industrial or domestic sources. These chemicals must be removed before discharge to the environment. These pollutants may also be found in ground and surface waters which also require treatment to achieve acceptable drinking water quality (Lindner et al., 1995). The increased public concern with these environmental pollutants has prompted the need to develop novel treatment methods with photocatalysis which is gained a lot of attention in the field of pollutant degradation (Ziltner et al., 1996).

The natural treatment processes such as lagoons, ponds, streams, rivers and lakes are taken action in the presence of sunlight which initiating the degradation of organic compound into simpler molecules and finally convert to carbon dioxide and other mineral products. Some agents speed up the process. The utilization of 'colloidal semiconductors' and the introduction of catalysts to promote specific redox processes on semiconductor surfaces were developed in 1976 (Kalyanasundaram, 1983). Since then, laboratory studies have increased to create artificial medium to enhance semiconductors and solar purification process (Matthews, 1993). The photocatalytic degradation of wastewater is a combination of catalysis and solar technology (Zhang et al., 1994). At first, the only semiconductor photocatalysis was  $\text{TiO}_2$  to treat wastewaters. But now, illuminated semiconductors for degrading undesirable organic pollutants have improved and new materials are continuously invented (Beydoun, Amal, Low and McEvoy, 1999).

A catalyst is not changing during the reaction or being consumed or change the speed of reaction. Photo-catalysis is identified as "acceleration by the existence of catalyst". On another words, the same process of catalyst is occurred by the presence

of sunlight and semiconductor. The difference between catalytic and photocatalytic systems are the activated zones (Ohtani, 2010).

This explanation includes photosensitization. Chlorophyll of plants works like photocatalyst. In photosynthesis process, chlorophyll uses sunlight to turn water and carbon dioxide into oxygen and glucose, on the other hand, photocatalysis creates strong oxidation agent to deteriorate organic matters to carbon dioxide and water in the presence of photocatalyst, light and water (Nimetoğlu, 2011).

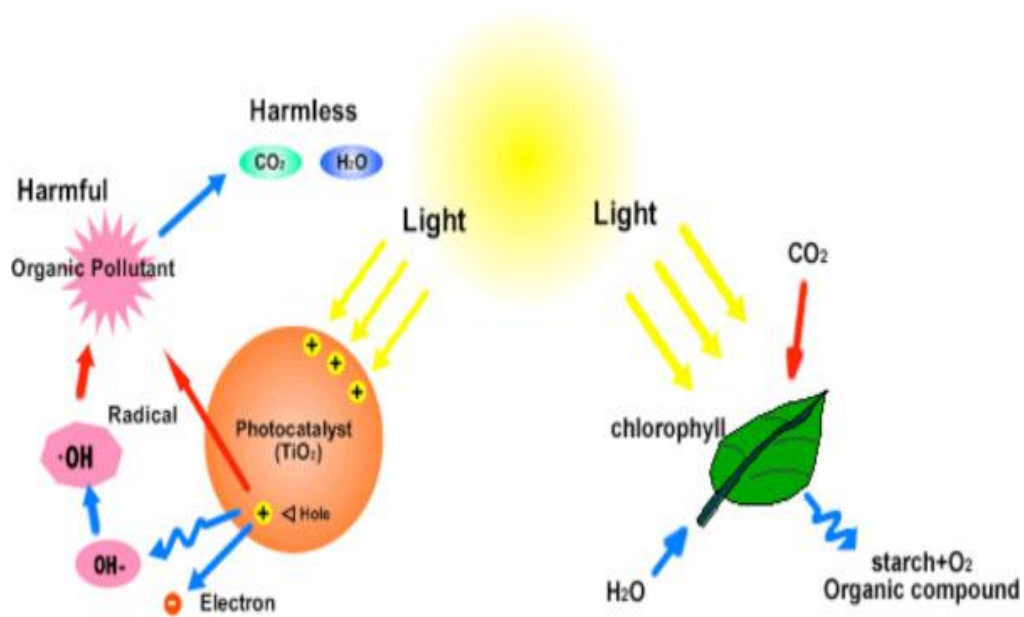


Figure 2.1 A comparison between photosynthesis and photocatalysis (Nimetoğlu, 2011).

The light source requires for photosynthesis and photocatalyst. The light shows the property of wave. Shortly, light has a wavelength and frequency. The formulas of  $\lambda=c/v$  and  $E=h.v$  help us to estimate the energy. In this formulation  $h$  is the Planck constant ( $6.63 \times 10^{-34}$  J.s) and  $c$  is the velocity of light ( $3 \times 10^8$  m/s),  $v$  is the frequency (1/s) and  $\lambda$  is the wavelength (nm). If the frequency is increased, the wavelength will be decreased and the energy will be raised. Different wavelengths have different energy level. That is why the photocatalytic activity is directly affected by the energy ( $h.v$ ) of the ray and the efficiency increases (Nimetoğlu, 2011).

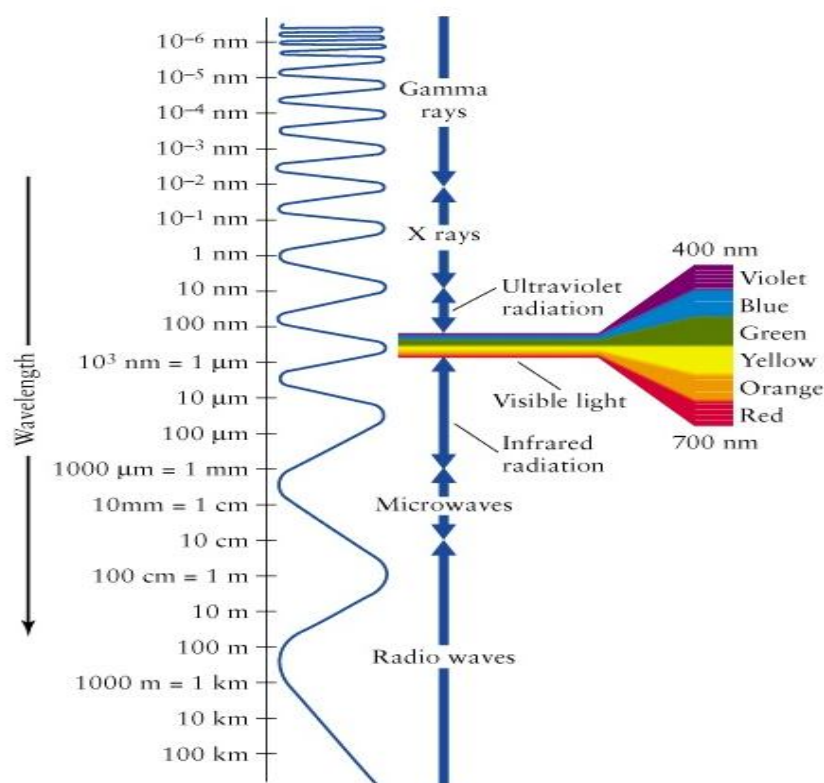


Figure 2.2 Electromagnetic spectrum (Madigan, 2011).

Sun radiation emits different wavelengths. These wavelengths are called as "Electromagnetic Spectrum". Sun radiation is arranged from by means of wavelengths. The electromagnetic spectrum is shown in Figure 2.2 and Gamma rays, X-rays, Ultraviolet Radiation, Visible light, Infrared radiation, microwaves and Radio waves are in the spectrum, respectively. Sunlight contains a small fraction of ultraviolet light (5% of solar energy), but the visible light contains 40% of solar energy (Norgard, 2007). The colors of visible light: red= ~700-635 nm, orange=~635-590 nm, yellow=~590-560 nm, green=~560-490 nm, blue=~490-450, purple=~450-400 nm. Ultraviolet light in bulk level is not feasible and economical for the huge amount of industrial wastewaters. Some countries where the sunlight is existing, photo catalysis with sunlight can be economical and suitable. For this reason, photocatalytic degradation under sunlight or visible light draws attention. This thesis is focused on the solar energy simulated light and the ability of  $K_2La_2Ti_3O_{10}$  to destroy phenol, methylene blue and cyanides. Photocatalytic degradations of phenol, methylene blue and cyanide were performed in a solar box ATLAS Suntest CPS+ simulating natural radiation and equipped with a Xenon lamp.



### 2.2.1 Photocatalytic Systems

Photocatalytic system includes water, semiconductor particles or coatings and light source for illumination. In Figure 2.3, a surface which is coated with photocatalytic material is seen. The moisture of air supplies the water which requires for the reaction, sunlight is necessary for light source and  $\text{TiO}_2$  is the photocatalyst. Photocatalytic process is started by the absorption of light with the aid of semiconductor nanoparticles. A reaction series are occurring when photocatalyst absorbs the energy from sun and as a result of the reactions, organic compounds in surface is converted to  $\text{H}_2\text{O}$  and  $\text{CO}_2$  (Kaneko & Okura, 2002).

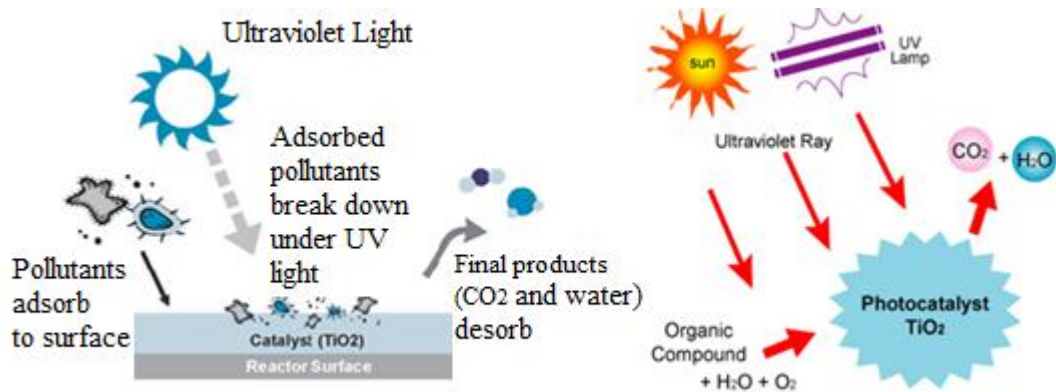


Figure 2.3 The mechanism of photocatalyst (Nimetoğlu, 2011).

The principle of the semiconductor photocatalytic reactions is simple. Photocatalyst uses a photon to excite an electron from the valence band (VB) to the conduction band (CB) and creates an excited situation. When the energy of light which is taken by irradiation is greater than the own energy in band gap, photocatalyst gives its own energy to an electron in VB and helps to electron for stepping up to conduction band (CB). This creates an excitement and electron ( $e^-$ ) – positive hole ( $h^+$ ) pair. These  $e^-$  and  $h^+$  reduce and oxidize respectively chemical species on the surface of photocatalyst. Figure 2.4 illustrates reduction and oxidation mechanisms (Kaneko & Okura, 2002).

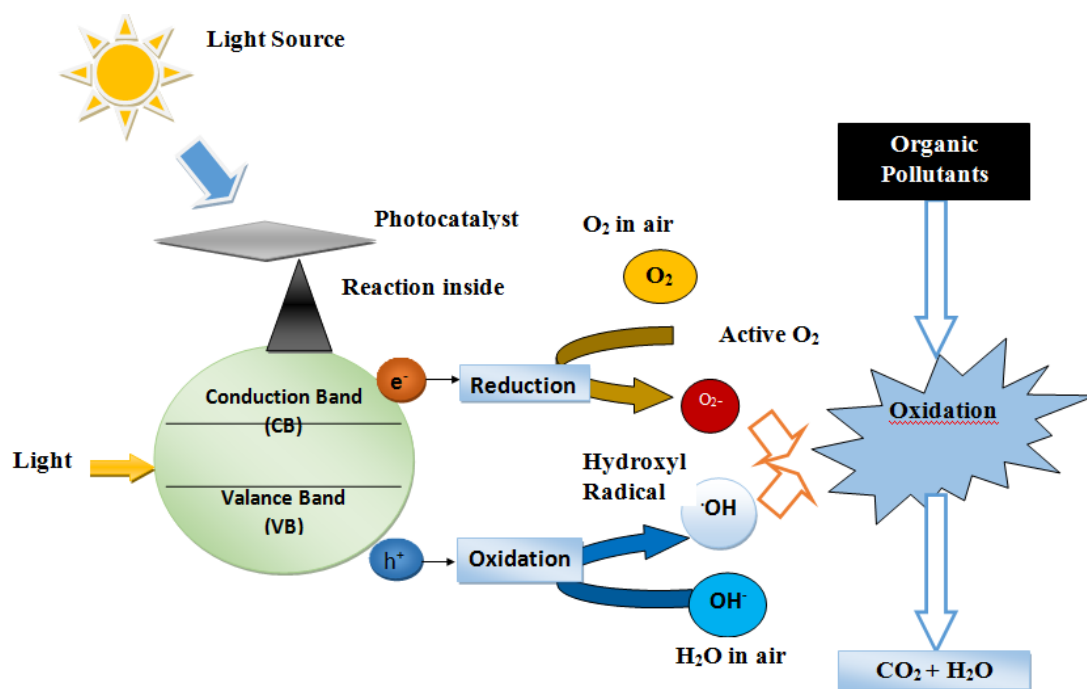


Figure 2.4 The mechanism of photocatalytic system.

### 2.3 Band Theory and Semiconductor Structure

Materials have three different types according to their electrical properties. These types are conductors, insulators and semiconductors. The purpose of our project is to produce  $K_2La_2Ti_3O_{10}$  and this material is semiconductor.

Semiconductor photocatalysts are attracting large scale research area for the treatment of hazardous chemicals. In as much as these photocatalysts have cost-effective configuration and can get complete mineralization without generation of toxic byproducts. These materials have been commercially applied as a self-cleaning coating on building and glass materials in Japan and South Korea (Krishna, Noguchi, Koopman, & Moundgil, 2006).

The most popular of them is titanium dioxide. Semiconductors can conduct due to the external effects of conductors. Normally, these materials are conductor and when heat, light, magnetic effect or electrical stress are applied, some electrons become independent and become conductor. If these external effects are removed, they return to their old type as insulator. This property provides a wide application on electronic

area. Conductor, insulator and semiconductor energy band diagram is shown in Figure 2.5 (Nimetoğlu, 2011).

The most well known conductors are metals. Metals can carry the electric flow by the reason of its free electrons which can pass from one atom to the next. These opportunities provide the electric flow to travel through the length of the metal (Nimetoğlu, 2011).

A property of metals and semiconductors are separated from non - conductive insulators for one reason. The difference between them is because of the energy orbitals. Energy orbitals are very small. Due to this reason, electrons can be excited from lower energy levels to higher energy level. These small orbital energy differences are called bands. Otherwise, these bands are so close together as energy that it takes so small amount of energy to support electrons to these higher band levels. The higher energy level that the valence electrons can be excited to is defined as the conduction band; because the electrons in this band are free to carry an electric current (Nimetoğlu, 2011).

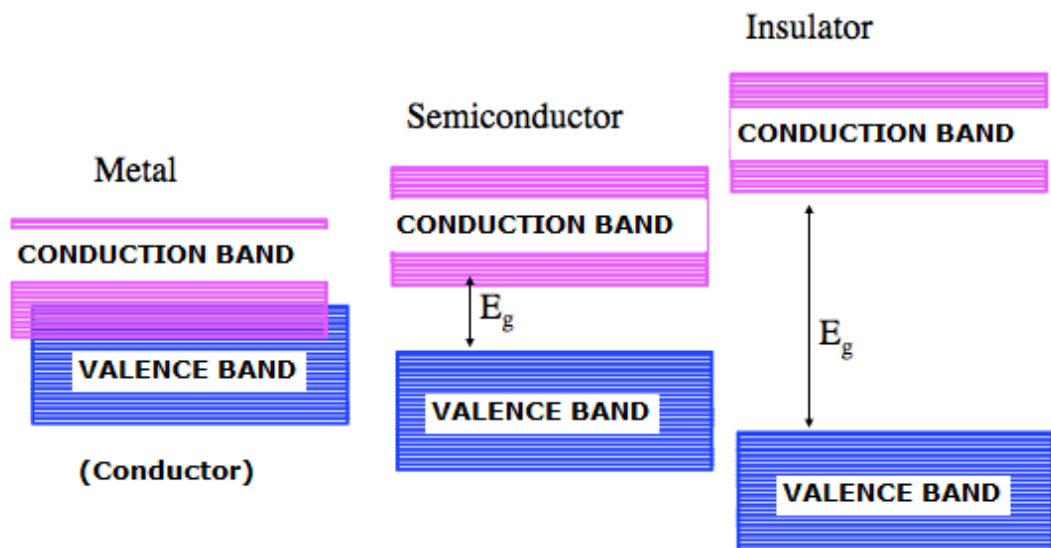


Figure 2.5 Insulator, conductor and semiconductor band energy levels (Shapley, 2012).

Insulators have large energy gap between valence and conduction bands, semiconductors have less energy gap between valence and conduction band, and the valence band and the conduction band is overlapping within the conductors.

As shown in the diagram above, the key difference between semiconductors and conductors are that the conductors have a natural overlap between their valence electrons and the conduction band, while semiconductors have a noticeable gap between the two. The result is that the electrons of conductors are able to carry a current under any condition. Meanwhile, the conductive ability of semiconductors requires energy to be put into the semiconductor material (Larsen, nd).

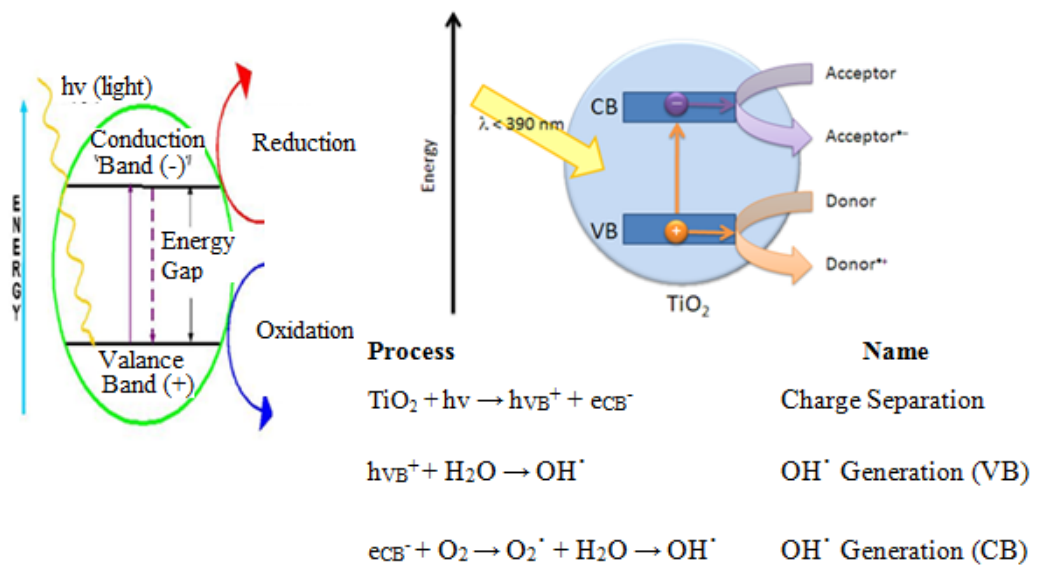


Figure 2.6 Semiconductor particle (Bahnemann, 2004).

On the top of the Figure 2.6, light of energy which is exceeding band gap is resulting with charge separation, as electron is reducing a donor (usually oxygen) and hole is oxidizing a donor (usually water). The other figure which is located on the bottom is a summary of reactions which are occurring (Bahnemann, 2004).

Between the semiconductors which is suitable for the photocatalytic reaction, titanium dioxide ( $\text{TiO}_2$ ), ( $E_g = 3.2 \text{ eV}$ ) is mostly used because this material has many advantages. The main differences between the other semiconductors are like that: it is inert and resistant to corrosion, and it requires little post-processing which makes it

inexpensive. It can react under mild-operating conditions. However, it currently needs to use ultraviolet light for photocatalysis to occur (Nimetoğlu, 2011).

When photocatalyst  $\text{TiO}_2$  absorbs ultraviolet (UV) radiation from sunlight or illuminated light source (fluorescent lamps), it will generate pairs of electrons and holes.

The electron of the valence band from  $\text{TiO}_2$  becomes excited when it is illuminated by light. The excess energy of this excited electron promoted the electron to the conduction band of  $\text{TiO}_2$ . For this reason it creates the negative-electron ( $e^-$ ) and positive-hole ( $h^+$ ) pairs. This stage is called the semiconductor's ' photo-excitation ' stage. The energy difference between the valence band and the conduction band is known the 'Band Gap'. Wavelength of the light which is necessary for this photo-excitation stage is:

$$1240 (\text{Planck's constant, } h) / 3.2 \text{ eV (band gap energy)} = 388 \text{ nm}$$

The positive - hole of  $\text{TiO}_2$  falls apart the water molecule to form hydrogen gas and hydroxyl radical. The negative - electron reacts with oxygen molecule to form super oxide anion. This cycle continues when light is available (Nimetoğlu, 2011).

Today, semiconductors are usually chosen as photocatalysts, because semiconductors have a narrow gap between the valence and conduction bands. The semiconductors need to absorb equal energy or more than its energy gap. Semiconductors use for the cleaning purposes which states on the above stages. Figure 2.7 shows an example of purification. This example is from a commercial photocatalyst. Figure 2.7.a shows old and dirty wall. The selected zone is coated with a photocatalyst. Figure 2.7.b took 3 months later.

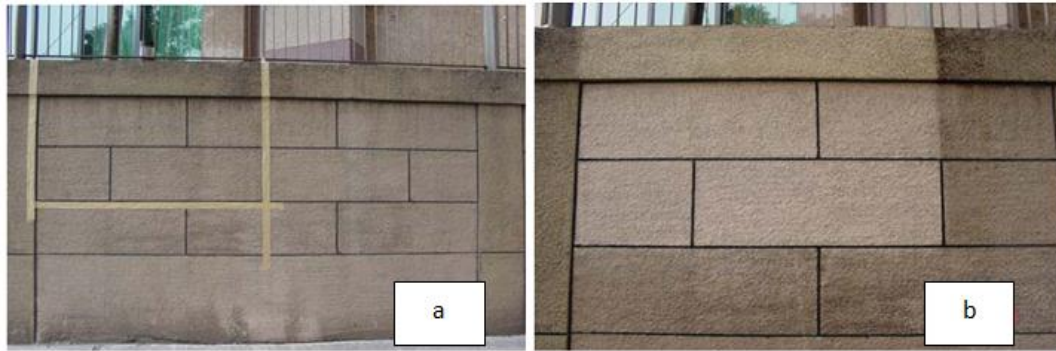


Figure 2.7 A wall, (a) without coating of photocatalyst and (b) after the coating process (TitanShield®)

Today, there are many types of material which act as a photocatalytic activity. Some of them are:  $\text{TiO}_2$ ,  $\text{SrTiO}_3$ ,  $\text{La}_2\text{TiO}_5$ ,  $\text{La}_2\text{Ti}_3\text{O}_9$ ,  $\text{La}_2\text{Ti}_2\text{O}_7$ ,  $\text{Sr}_3\text{Ti}_2\text{O}_7$ ,  $\text{PbTiO}_3$ ,  $\text{Sm}_2\text{Ti}_2\text{S}_2\text{O}_5$ ,  $\text{M}_2\text{La}_2\text{Ti}_3\text{O}_{10}$  ( $\text{M} = \text{K, Rb, Cs}$ ),  $\text{PbBi}_4\text{Ti}_4\text{O}_{15}$ ,  $\text{BaTi}_4\text{O}_9$ ,  $\text{M}_2\text{Ti}_6\text{O}_{13}$  ( $\text{M} = \text{Na, K, Rb}$ ),  $\text{La}_4\text{CaTi}_5\text{O}_{17}$ ,  $\text{M}_3(\text{PO}_4)_4$  ( $\text{M} = \text{Ti, Zr}$ ),  $\text{Ta}_2\text{O}_5$ ,  $\text{A}_4\text{Ta}_x\text{Nb}_{6-x}\text{O}_{17}$  ( $\text{A} = \text{Rb, K}$ ;  $x = 1 - 4$ ),  $\text{MTaO}_3$  ( $\text{M} = \text{Li, Na, K}$ ),  $\text{La}_{1/3}\text{TaO}_3$ ,  $\text{MTa}_2\text{O}_6$  ( $\text{M} = \text{Sr, Ba, Sn}$ ),  $\text{MTa}_2\text{O}_6$  ( $\text{M} = \text{Sr, Ba, Sn}$ ),  $\text{MTa}_2\text{O}_6$  ( $\text{M} = \text{Ni, Mn, Co}$ ),  $\text{MTaO}_4$  ( $\text{M} = \text{Cr, Fe}$ ),  $\text{Ca}_2\text{Ta}_2\text{O}_7$ ,  $\text{BiMTaO}_7$  ( $\text{M} = \text{La, Y}$ ),  $\text{Sr}_2\text{Ta}_2\text{O}_7$ ,  $\text{M}_2\text{La}_{2/3}\text{Ta}_2\text{O}_7$  ( $\text{M} = \text{K, H}$ ),  $\text{H}_2\text{SrTa}_2\text{O}_7$ ,  $\text{K}_2\text{Sr}_{15}\text{Ta}_3\text{O}_{10}$ ,  $\text{KBa}_2\text{Ta}_3\text{O}_{10}$ ,  $\text{Sr}_4\text{Ta}_2\text{O}_9$  and  $\text{M}_5\text{Ta}_4\text{O}_{15}$  ( $\text{M} = \text{Sr, Ba}$ ) (Osterloh, 2008).

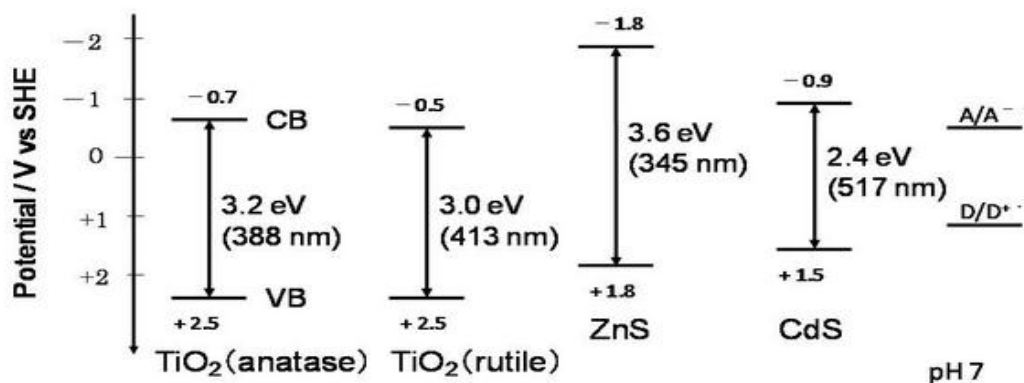


Figure 2. 8 Some metal oxides valence band energies (Osterloh, 2008).

$\text{TiO}_2$  is a white powder. It has d-electron configuration as a result of  $d^0$ , and the white color is explained by the lack of d-d. There are three types of  $\text{TiO}_2$  which are anatase, rutile and brookite phase. Light absorption effectively results in a ligand to metal charge transfer, electrons from oxygen are transferred to the vacant titanium d-orbitals. For anatase (3.2 eV) and rutile (3.0 eV) phases, the transition is in the UVA region, and results in an absorption band between 390 and 400 nm (Anonym, nd).

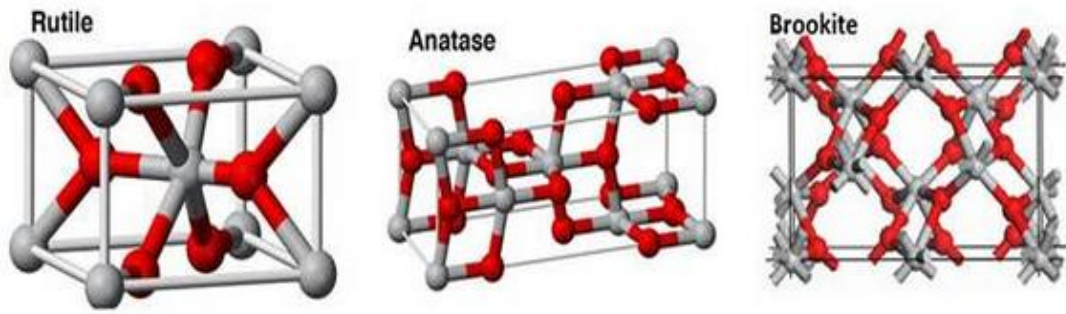


Figure 2.9 TiO<sub>2</sub> phases (a) rutile, (b) anatase, (c) brookite (Shannon, nd).

Generally, TiO<sub>2</sub> in anatase form is more photoactive than the other types. This difference of the anatase phase is thanks to the band energy difference. Anatase band gap energy is 3.2 eV thus it can absorb 338 nm or lower than this wavelength. Band gap energy of rutile phase is 3.0 eV and this type can absorb 413 nm or lower than this. Semiconductor metal oxides have a potential of positive oxidation and can oxidize every type of chemicals. OH• occurs as a result of the water oxidation, (Equation 2.1) (Şam, Ürgen and Tepehan, 2007).



The number of charge can be increased by the addition of the suitable impurity to the crystalline lattice. With the impurity addition, the dense of electron or hole can be change. In one semiconductor structure, if the electrons are the majority carriers and the gaps are the minority carriers, these types are called n-type (donor doped) semiconductor. If the total opposite of this is occurred (majority carriers are gaps and minority carriers are electrons), this is called p-type (acceptor doped) semiconductor. Undoped semiconductors are called intrinsic, while the others which are doped are extrinsic semiconductors (Kaneko & Okura, 2002).

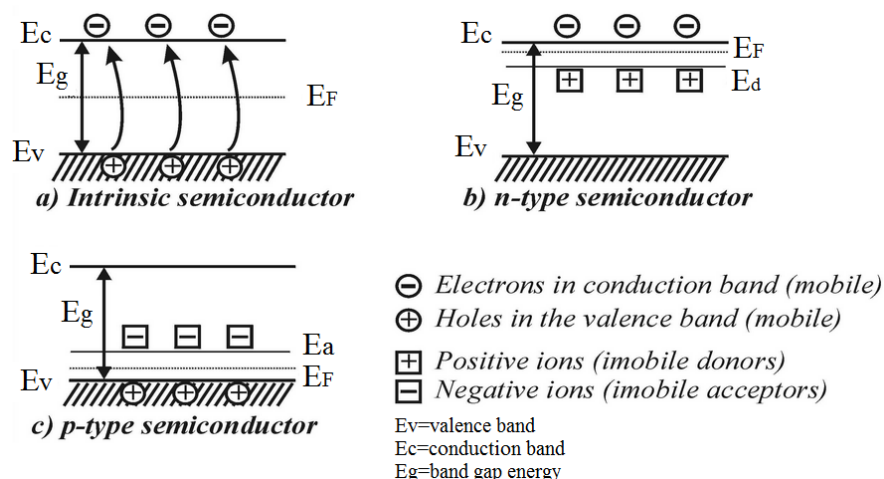


Figure 2.10 The three types of semiconductors: (a) Intrinsic semiconductors, (b) n-type semiconductors, (c) p-type semiconductors (Tiginyanu, Langa, Foell & Ursachi, 2009).

Various n-type semiconductor metal oxides like  $\text{TiO}_2$ ,  $\text{ZnO}$ ,  $\text{CdS}$ ,  $\text{SnO}_2$ , and  $\text{WO}_3$  have been tested for photocatalytic oxidation of organic pollutants in water and air (Chin, 2008). Due to the high chemical stability and the proper energy band structure, the layered perovskite photocatalyst  $\text{K}_2\text{La}_2\text{Ti}_3\text{O}_{10}$  has drawn a lot of attention for its applications in water photocatalytic splitting. The photocatalyst  $\text{K}_2\text{La}_2\text{Ti}_3\text{O}_{10}$  has one interlayer and this structure is suitable for the improvement of the photocatalytic reactivity of water treatment. Under light irradiation, the light-generated electrons move from the interlayer of  $\text{K}_2\text{La}_2\text{Ti}_3\text{O}_{10}$  to external surface and light-generated holes oxidize the water to produce  $\text{O}_2$  in the interlayer (Yang, Qui, Chen, Feng & Yin, 2007).

## 2.4 Hole Conduction

When the semiconductor is heated, electrons promoted to the conduction band leave behind an empty spot in the lattice structure where they were previously located. This electron hole is very important thing to understand the mechanism by which lattice structures are able to enhance an additional electron for conductivity. An electron hole is the conceptual opposite of an electron. It represents the lack of an electron where an electron could potentially be situated or previously was located in another full electron shell. That is to say, electron holes are resulted by electrons which are leaving their place in the lattice structure (Larsen, nd).



Electron holes can increase the conductive abilities of semiconductors. That is why electron holes are very important to increase the conductive abilities. Hole conduction first requires an electron to excite on account of to leave its valence band to the conduction band. Once the valence electron is leaving, neighboring electrons are pulled into the electron holes, filling existing electron holes while creating new neighboring ones (Larsen, nd).

## 2.5 Photocatalytic Degradation Mechanisms

The chemical reactions between the photocatalytic degradation are analyzed in three stages. In the first stage, activated particles are occurred. In this stage the photon absorption in the semiconductor surface occurs by the realization of electron-hole  $e^-/h^+$  pairs (Equation 2.2) (Yiğit, 2008).

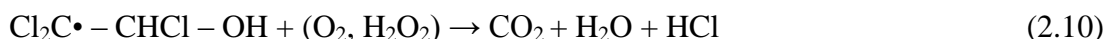


The composed  $h^+$  holes react with  $\text{H}_2\text{O}$  or  $\text{OH}^-$  ions and create the activated  $\bullet\text{OH}$  radical, at the same time the electrons are captured by  $\text{Ti}^{3+}$  and reacted with  $\text{O}_2$  molecules to create the oxygen anion radical (Yiğit, 2008).

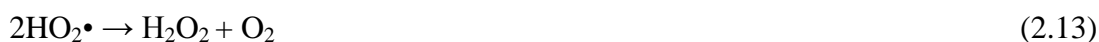


Second stage includes organic compound degradation reactions. The reactions of this stage are based on the oxidation of organic compounds to  $\text{CO}_2$  and  $\text{H}_2\text{O}$ . The organic compound of this stage ( $\text{Cl}_2\text{C} = \text{CHCl}$ ) is hydroxylated with hydroxyl radical and occur hydroxyl radical (Yiğit, 2008).





The reactions which occur in the third stage are not desired because these reactions reduce OH radical (Yiğit, 2008).



A way to increase the photoactivity is to dope photocatalyst with transition metals or noble metals. Thus, absorption band will be promoted from UV zone to visible zone. If the recombination velocity of the electron - hole pairs which is into the TiO<sub>2</sub> particles is higher, the effectiveness of the photocatalyst will decrease. Another situation which decreases the efficient is the adherence of the organic compounds on the TiO<sub>2</sub> catalyst surface (Nimetoğlu, 2011).

## 2.6 Photocatalysis of Water with Layered Compounds

For a while, researches have been done into the design and study of photosystems for the separation of water into H<sub>2</sub> and O<sub>2</sub>. The systems which are working under the visible light irradiation have a wide scale application.

Two main approaches are based on the photocatalytic studies. One of them is to imitate the natural photosynthesis with using organometalic sensitizer. The other one is to use stable inorganic materials under the photochemical situations. Inorganic photocatalysts are layered components which have low dimensionality and for this reason, electron transfer processes are matchless. Layered structures present superior properties for the ability of the ion exchange (into the interlayer gaps). Instead of using "bulk" type catalyst, using layered components have some advantages on water photolysis. Layered components have a great variety and can be modified easily with a change of cation into the intermediate layer. The most important advantage is the photocatalytic activity. Some layered components are more effective than "bulk"

catalysts. The reason can be explained like this: in the structure, electrons and gaps which produce into the every tiny inorganic layer can reach easily to the reaction area (Nimetoğlu, 2011).

### ***2.6.1 Layered Transition Metal Oxides***

Transition metal elements like Ti, Nb and Ta, which forms are  $d^0$  cations, are known to generate several oxides of layered structure displaying interlamellar activity. All of these oxides arise from titanate and/or niobate macropolyanion layers and between these layers, alkali metal cations confront the negative charges of the layers. The alkali metal cations can be replaced with several kinds of cation including protons. These oxides may be regarded as semiconductors/insulators due to their large band gap. The electronic situation of the oxide layers is excited when the photon's energy is larger than the band gap (typically in the ultraviolet area) are absorbed. This process may be considered as the excitation of electrons from the valence band (mostly consisting of oxygen 2p orbitals) to the conduction band, (mainly Ti or Nb 3d orbitals). Based on the band models of the electronic situations, the excitation process is described as the formation of electrons ( $e^-$ ) in the conduction band and positive holes ( $h^+$ ) in the valence band. If the location of the electrons and holes are determined, they may be accepted as  $Ti^{3+}$  or  $Nb^{4+}$  and  $O^{2-}$  species. As a result of the photocatalytic reactions, the behavior of photoexcited electrons and holes appears to be more or less similar to that of bulk type titanates and niobates (Kaneko & Okura, 2002).

### ***2.6.2 Layered Perovskite Oxides***

In photocatalytic studies, some perovskite layered oxides are mostly used especially for the formation of hydrogen and oxygen. These oxides demonstrate interlamellar activity and are separated on two main classes: i) Dion - Jacobson Series (DJ Series), (the general formula  $AM_{n-1}B_nO_{3m+1}$ , (e.g.  $KCa_2Nb_3O_{10}$ )) and ii) the Ruddlesden – Popper series (RP series) (general formula  $A_2M_{n-1}B_nO_{3n+1}$  (e.g.  $Na_2Gd_2Ti_3O_{10}$  and  $K_2La_2Ti_3O_{10}$ )). These structures are characterized by  $n -$  octahedral thick perovskite (Kaneko & Okura, 2002).

### 2.6.2.1 Dion – Jacobson Series

The general formula of the Dion – Jacobson series oxides is  $AM_{n-1}Nb_nO_{3n+1}$ . Band gaps were computed from diffuse reflectance spectra. Protonated compounds are better than those of their non – protonated equals (Kaneko & Okura, 2002).

Photocatalytic activity towards oxidation of higher alcohols has also been researched. For this purpose, the representative system is modeled with  $KCa_2Nb_3O_{10}$ . Also, when the chain length is lower the activity will be higher, especially for proton-exchanged forms. Through the pillaring of the layered oxides, it is possible to enhance the interlayer space to make such space available for guest molecules (Kaneko & Okura, 2002).

### 2.6.2.2 Ruddlesden – Popper Series

The general formula of the Ruddlesden - Popper series oxides is  $A_2M_{n-1}B_nO_{3n+1}$ .  $K_2La_2Ti_3O_{10}$  is a typical oxide in the Ruddlesden – Popper series which is presenting interlayer reactivity. This structure forms a hydrate with about 1 – 2  $H_2O$  molecules per formula unit under ambient conditions. Band gap of  $K_2La_2Ti_3O_{10}$  is predicted 3.6 eV (Kaneko & Okura, 2002).

## 2.7 $K_2La_2Ti_3O_{10}$

In 1972, Fujishima and Honda discovered photocatalytic generation by using semiconductor electrodes. This big invention attracted attention in the scientific community. Recently, some compounds with layered structure have displayed high photo-catalysis activity in water treatment applications. Because of the layered gap, the activity is very high, as the reaction site, and thus the efficiency of the catalysts can be enhanced. The first layered photocatalyst which was reported is  $K_4Nb_6O_{17}$  by Kudo and his coworkers. Kudo and coworkers reached that  $K_4Nb_6O_{17}$  catalyzes water decomposition reaction and generates hydrogen and oxygen after being loaded with Ni (Wenquan et al., 2005).

$K_2La_2Ti_3O_{10}$  is one of the layered perovskite type compounds with octahedral perovskite-layer ( $La_2Ti_3O_{10}^{2-}$ ), and between these layers K ions are located. Takata and coworkers studied out that  $K_2La_2Ti_3O_{10}$  presented a remarkable catalytic activity for water splitting under UV light irradiation after loading with nickel (Wenquan et al., 2005).

### 2.7.1 Crystalline Structure

$K_2La_2Ti_3O_{10}$  is a type of layered perovskite-type compound and is shown schematically in Figure 2.11. The  $K_2La_2Ti_3O_{10}$  composes with negatively charge lanthanum titanate perovskite layer and interlayer  $K^+$  ions.  $La_2Ti_3O_{10}$  which is the adjacent triple perovskite layers, are stacked with a displacement by 1/2 along the (001) direction. A lanthanum ion is in the center of the perovskite lattice. By using the X-ray diffraction data, the parameters of  $K_2La_2Ti_3O_{10}$  cell are found as  $a=b=0.387$  nm,  $c=2.98$  nm, and the thickness of the  $La_2Ti_3O_{10}$  is 1.19 nm. The inter layers are bonded by static force. The combination between inter layers are weaker, that is why it is ready to occur intercalate exchange and expand in the field of the interlayer (Huang et al, 2010).

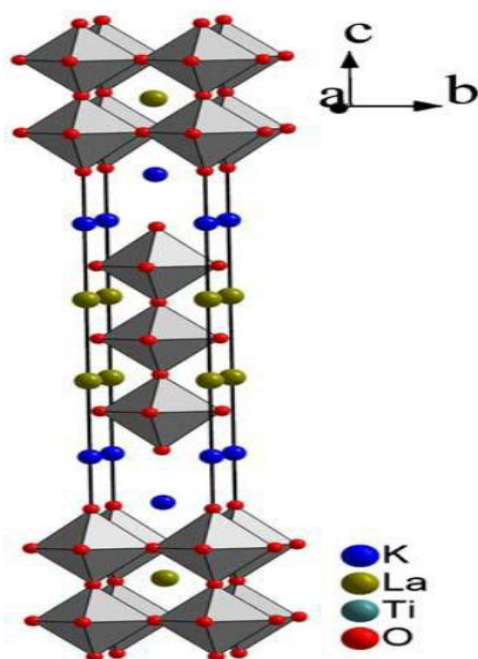


Figure 2.11  $K_2La_2Ti_3O_{10}$  crystalline structure (Huang et al, 2010).

In Figure 2.12, the band gap of  $K_2La_2Ti_3O_{10}$  is shown. The zone of the valance band in the energy between -5 and 0 eV is consisted of 2p orbitals. The conduction band in the energy range from 2–7 eV composes of  $Ti_3$  d and  $La_5$  d orbitals. The value of the band gap is approximately 2.0 eV and it is much smaller than the experimental optical band gap (3.69 eV) (Huang et al, 2010).

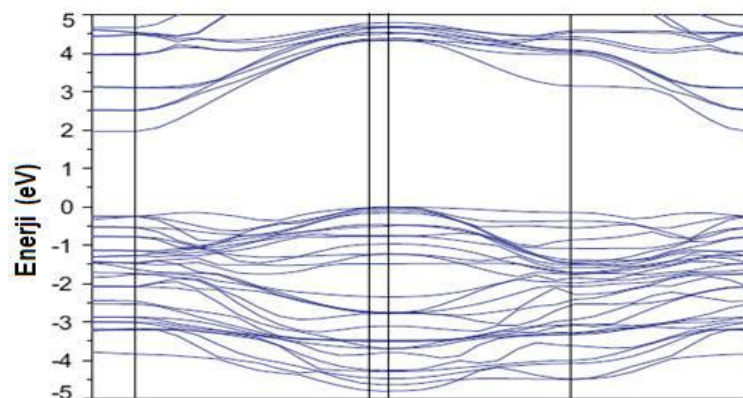


Figure 2.12  $K_2La_2Ti_3O_{10}$  energy band gap (Huang et al, 2010)

### 2.7.2 Photocatalytic Mechanisms of $K_2La_2Ti_3O_{10}$

Some of the oxide and sulfide semiconductors have sufficient band gap energy to increase the chemical reactions and to catalyze. The semiconductor property of the perovskite  $K_2La_2Ti_3O_{10}$  comes from  $TiO_2$ . According to the band theory, valance band is an energy level with full of the stimulated electrons via an external effect, and conduction band is the empty energy band gap level until the electrons will be stimulated (Cui et al, 2006).

## 2.8 The Synthesis Methods of Semiconductor Photocatalysts (Sol–Gel)

The sol-gel technique is a process to generate colloidal nanoparticles from liquid phase and the production of advanced nanomaterials and coatings are improving day by day. Two types of nanomaterial synthesising are existed. First of them is bottom-up approach and the second one is top-down approach. The top-down process includes no control of the size and morphology. The bottom-up approach can be controlled as the size and morphology. Sol-gel method is a bottom-up approach (Suneel, nd).

Sol-gel technology has a wide application range to produce ceramics, glass and composite materials. The sol-gel process, as the name implies, includes the evolution of inorganic materials (for example, metal oxide solutions, metal powders, nitrates, hydroxides and oxides) through the formation of a colloidal suspension (sol) (inorganic component is mixing with definite proportions of water and acid) and gelation of the sol in a continuous liquid phase (gel). Sol is the suspension of the colloidal solid particles at liquid phase. These particles should have more dispersion forces than the gravity. In as much as colloids are smaller than 500 nm, these particles cannot be seen in normal optical microscope due to their maximum magnitude is equal to the wavelength. Gel is composing from the precipitation of the colloidal particles. Gel is a phase between solid and liquid. The precursors for synthesizing these colloids generally comprise of a metal or metalloid element. The starting materials are due to the form of dispersible oxide and forms of sol in contact with water or dilute acid (Suneel, nd).

The steps of the sol-gel process below mentioned.

**Step 1:** Alkoxide Hydrolysis. Alkoxides are the precursor for the formation of different stable solutions (the sol). The general formula is  $M(OR)_n$ . M is the metal compound which will be covered and R is the alkyl group. The factors which influence the hydrolysis rate are the amount of water, catalyst, solvent concentration and temperature (Evcin, nd).

**Step 2:** Polymerization. This step is the dispersion of the sediment by solvent. A sol is prepared for the dispersion of the sediment. Gelation is resulting from the formation of an oxide- or alcohol- by a polycondensation or polyesterification reaction. For this reason, the viscosity of the solution increases (Suneel, nd).

**Step 3:** Aging of the gel (Syneresis), during the polycondensation reactions continue until the gel transforms into a solid mass, expulsion of solvent from gel pores is occurring. The effective factors in this step are pH, temperature, reaction time,

concentration, aging temperature and aging duration. Gel is a form which constitute liquid phase more than solid phase and between these two phases (Suneel, nd).

**Step 4:** Drying of the gel. An important step to create gel form is the drying of the gel without creates any cracks. The drying of the gel is to remove the excess of the solvent (alcohol, water). The gel is shrinking and the solid resultant contains high amount of pore. This solid is called xerogel (Suneel, nd).

**Step 5:** Dehydration. This is reached by calcinations of the monolith at temperatures up to  $800^{\circ}\text{C}$  (Suneel, nd).

**Step 6:** Densification and decomposition of the gels at high temperatures ( $T > 800^{\circ}\text{C}$ ). The remaining organic materials are volatilized. The typical steps for sol-gel method are shown in the schematic diagram below (Suneel, nd).

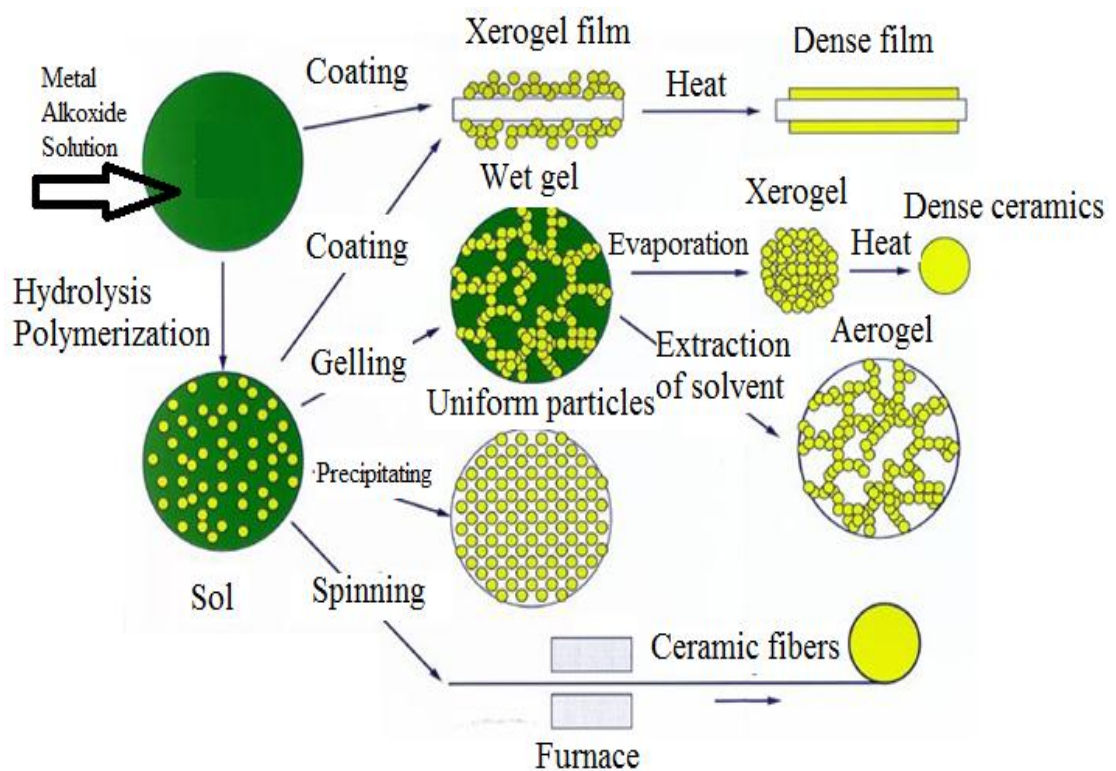


Figure 2.13 Sol-gel technologies and their products (Sariyusriati, 2008).



The advantage of this system appears due to the possibility of synthesizing nonmetallic inorganic materials like glasses, glass ceramics or ceramic materials at very low temperatures. High surface area and free energy provide sintering processes with low temperature (Suneel, nd).

The major disadvantage is the unwanted reactant such as residual hydroxide or carbon. And also processing time of nano powders are very long (Suneel, nd).

## 2.9 The Coating Techniques for Producing Thin Films

Sol – gel processes include dip, spray and spin coating techniques. Through these techniques,  $K_2La_2Ti_3O_{10}$  films of high photocatalytic activity can be produced. It is necessary to choose adequate conditions to yield highly active photocatalytic coatings (Smail et al, 2009).

### 2.9.1 Dip Coating Techniques

Dip coating techniques is defined as a process which is immersed in a liquid and then draws back with a well-defined withdrawal speed under controlled temperature and atmospheric conditions. The straight and uniform coating thickness is mainly based on the withdrawal speed, the solid content and the viscosity of the liquid (Schimidti & Mennig, 2000).

The coating thickness can be between 50  $\mu\text{m}$  and 20 nm with maintaining high optical quality. The schematic figure of a dip coating process is shown in Figure 2.14 (Schimidti & Mennig, 2000).

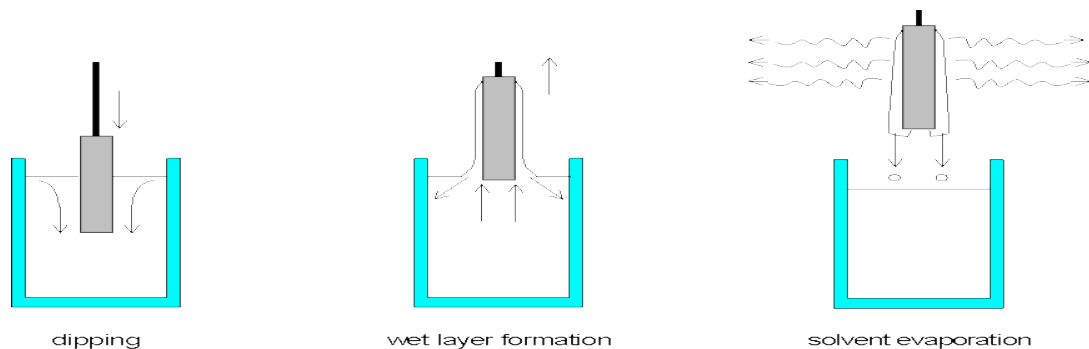


Figure 2.14 Stages of the dip coating process (Schimidti & Mennig, 2000).

### 2.9.2 Spray Coating Techniques

Spray coating techniques have a large scale application in organic lacquers industry. The solution is sprayed by a nozzle and thin droplets are produced. The droplets are sprayed through the substrate. The thin film is formed due to the high reactivity of the droplets. Spray coating processing speed is 1 m/min and it is 10 times faster than dip coating systems. High production speed, facility of the coating shape, cheap equipment cost is the advantages of this coating technique. The thickness cannot be always homogeny and the thickness problems are the constraint of the process (Schimidti & Mennig, 2000).

### 2.9.3 Spin Coating Techniques

Spin coating is a cheap and faster method to produce homogeneous layers. It is used rather for the coating of thin substrates. Spin coating has 4 main steps. At first, an excess amount of the solvent (fluid) is placed on the substrate. Secondly, the rotation is occurred at high speed in order to spread the fluid by centrifugal force. The film thickness can be adjusted by changing the rotation speed, the rotation time, and the concentration of the solution which is used. Thirdly, the fluid is slowly becoming thin. And finally, solvent evaporation is occurring and the coating become thin.

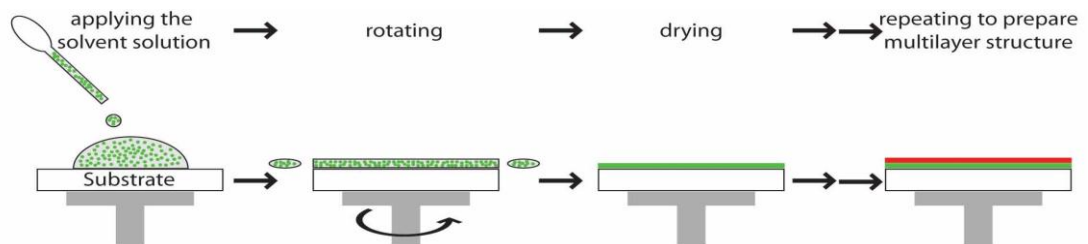


Figure 2.15 A schematic demonstration of spin coating technique (Anonym, nd).

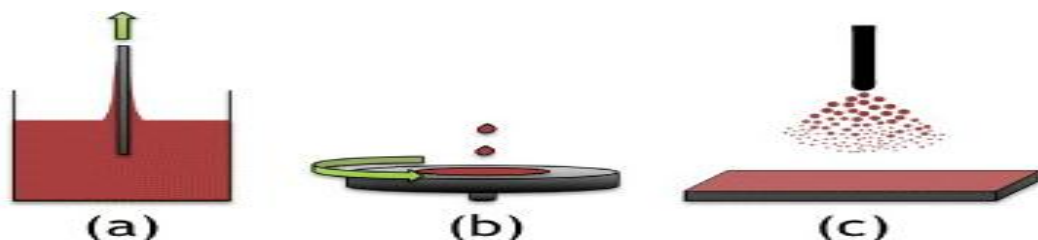


Figure 2.16 The three sol gel method: (a) dip coating, (b) spin coating and (c) spray coating (Faure et al, 2013).

## CHAPTER THREE

### MATERIAL AND METHOD

#### 3.1 The Aim of the Study

Layered perovskite structured potassium lanthanum titanate  $K_2La_2Ti_3O_{10}$  is a photocatalytic material and it was prepared by using sol – gel method. For this reason K, La and Ti based precursor materials and methanol, ethanol and glacial acetic acid solutions are used. pH, turbidity and rheological characteristics were examined for the solutions which were prepared.

Thermogravimetry-Differential Thermal Analyzer (DTA – TG) and Fourier Transform Infrared (FTIR) machines were used to optimize the coatings as part of the phase analysis and the fabrication regime. Prior to the transformation of the chemical bonds into crystalline state and the organic compounds intrinsic in their composition in varying temperatures, chemical bonds of the fabricated gels were determined by using a FTIR device. In addition, with DTA-TG device and in the presence of oxygen, the gels were heated in specific velocities for determining their endothermic and exothermic reactions and were examined in terms of thermodynamics. After these steps, powders and coatings were produced. The crystalline structure of  $K_2La_2Ti_3O_{10}$  powder and coating was analyzed by X-Ray Diffraction (XRD) device. The micro structure and surface properties of the coatings were analyzed by Scanning Electron Microscopy (SEM) device. The optical properties were determined by the help of a spectrophotometer. The suitable micro structure and optical characteristic of the coated material were identified. The photocatalytic degradation processes were realized to treat phenol, methylene blue and cyanide. Photocatalytic degradation experiments were carried out in a solar box ATLAS SUNTEST CPS+ which is simulating natural radiation (Figure 3.1). The light source has a vapor xenon lamp ( $300\text{ nm} < \lambda < 800\text{ nm}$ ) and the power can change between 250 and 765  $W/m^2$ .

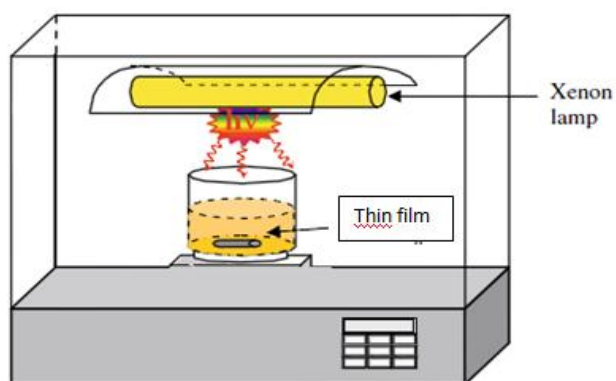


Figure 3.1 A schematic representation of the Photoreactor (Smail et al, 2009).

To determine the order of the reactions for the photocatalytic effectiveness of phenol, methylene blue and cyanide, kinetic studies were carried out according to the treatment rates.

### 3.2 Materials

Potassium 2,4 pentanedionate hydrate, lanthanum (III) 2,4 pentanedionate hydrate, titanium (IV) isopropoxide, glacial acetic acid, propionic acid, triethanolamine are used in the sol – gel process as the starting material, chelating agent, solvent and modifying liquid. The powder raw materials, chelating agent, solvent and modifying liquid which are used to produce  $K_2La_2Ti_3O_{10}$  are given in Table 3.1.

Table 3.1 Raw materials and its properties

Chemical Type	Chemical Name	Chemical Formula	Purity	Molecular Weight (gram)
Precursors	Lanthanum (III) 2,4 pentanedionate hydrate	$C_5H_{21}LaO_6 \cdot xH_2O$	-	436.24
	Potassium 2,4 pentanedionate hydrate	$C_5H_7KO_2 \cdot xH_2O$	97 %	138.21
	Titanium (IV) isopropoxide	$C_{12}H_{28}O_4Ti$	95 %	284.23
Solvent	Propionic acid	$C_3H_6O_2$	99 %	74.08
Chelating agent	Glacial acetic acid (GAA)	$CH_3COOH$	99.9 %	60.05
Surface activator material	Triethanolamine (TEA)	$C_6H_{15}NO_3$	-	149.19

### 3.3 Production Process

In this stage potassium lanthanum titanate powders and films were produced. As shown in the block flow diagram, to prepare the La solution, La compound was mixed with solvent and chelating agent till the La is dissolved. To reduce the surface tension, triethanolamine was added to the La solution. After this process, K compound was putted in the beaker, and the mixing process continues as far as K is dissolved. The temperature of sublimation of the potassium is low. That is why, the nimiety of K compound was added according the literature. Ti solution titanium (IV) isopropoxide was prepared and added. The solution was mixed with ultrasonic mixer at 45–50°C until they became transparent approximately 30 minutes. The following step was the coating of the thin films. Before the coating application, substrates were cleaned with acetone bath by ultrasonic bath. The substrates stayed here nearly 15 minutes. Thin films were generated by spin coating technique.

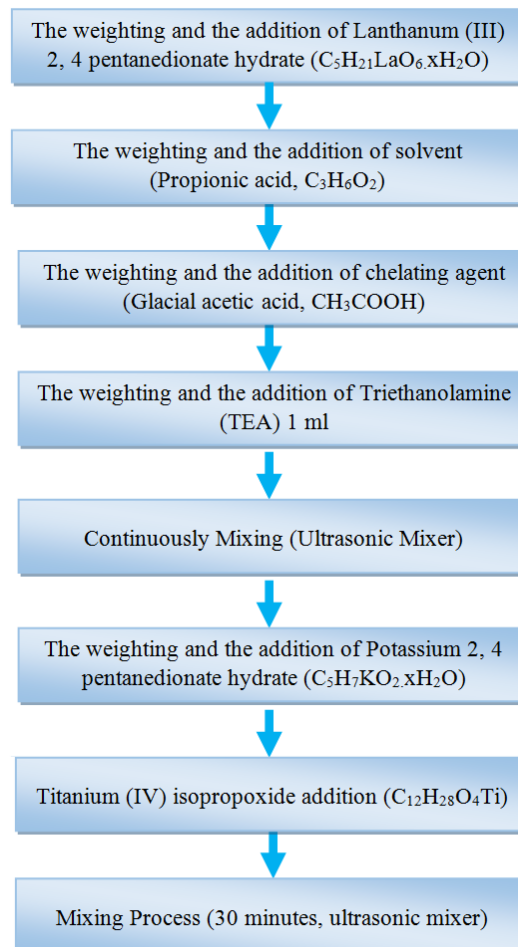


Figure 3.2 Production flow chart.

According to the tests, the results were not as well as planned. Because of not achieving the optimum outcomes with typical spin coating technique, the production process was changed. For this reason, buffer layer application was approved. To increase the crystallographic harmony, buffer layer application was applied. CeO<sub>2</sub> was selected for a buffer layer. Figure 3.4 illustrates the schematic display of buffer layer application.

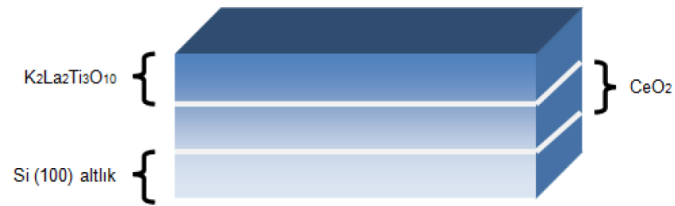


Figure 3.3 A schematic figure of buffer layer technique.

Table 3.2 Materials used in the production of CeO<sub>2</sub>

	<b>Cerium(III) Acetyl-acetone hydrate</b>	<b>Methanol</b>	<b>GAA</b>
<b>CeO<sub>2</sub></b>	0.375 g	10 ml	1 ml

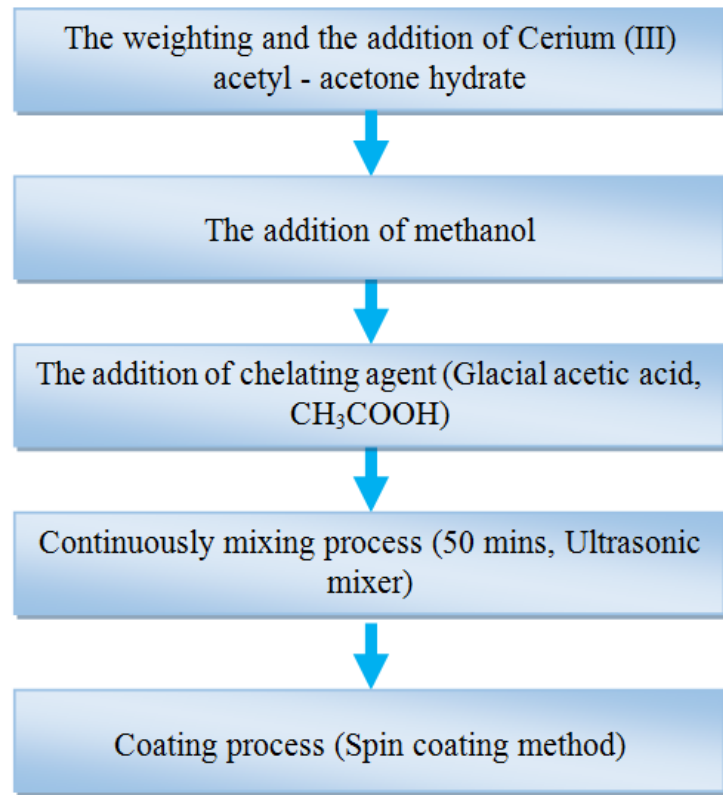


Figure 3.4 The flow chart of the production of CeO<sub>2</sub>.

CeO<sub>2</sub> was prepared by the information given in Table 3.2 and the flow chart was given in Figure 3.4. CeO<sub>2</sub> compound was prepared with using Ce, methanol and chelating agent. The ultrasonic mixer was used till the solution was dissolved. After the solution production, next step was the coating process. Firstly, buffer layer (CeO<sub>2</sub>) was coated. Before the coating operation, glass substrates were kept for 15 minutes at room temperature in air by waiting in ultrasonic bath with acetone solution for cleaning purposes. After drying process of substrates, spin coating method was used to produce thin films. Spin coating is a cheap and fast method to produce homogeneous layers. An excess amount of the solvent was placed on the substrate, which was rotated at high speed in order to spread the fluid by centrifugal force. The film thickness can be adjusted by changing the rotation speed, the rotation time, and the concentration of the used solution. Coating times and speeds were given in Table 3.3. For the multilayer coating production, after the gel the samples were dried at 300°C for 10 minutes and 500°C for 5 minutes in air. After that, obtained multilayer coatings were heat treated at 500°C for 30 minutes. As a last stage of this procedure, the samples were annealed at 700°C for 30 minutes in air as shown in Figure 3.5.

Table 3.3 Spin coating parameters

Step	Time (s)	Rotational Speed (rpm)
1	5	100
2	10	500
3	15	4000
4	10	0

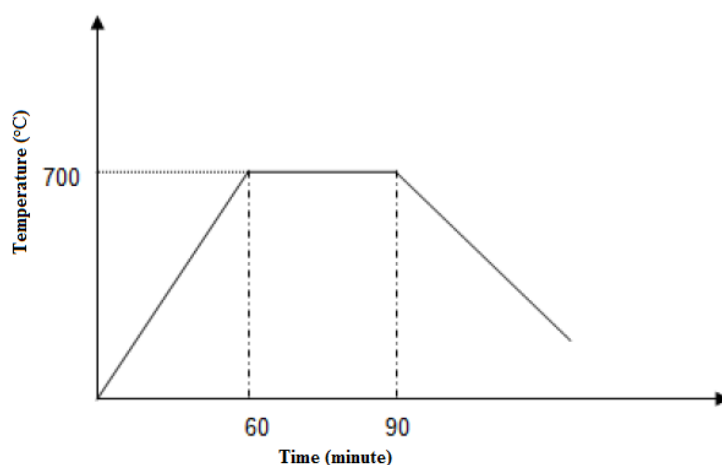


Figure 3.5 CeO<sub>2</sub> heat treatment process.

To find the ceramic phase, temperature related to this phase was determined. For this reason, thermal behaviors were determined by using DTA/TG equipment. These data were required for the heat treatment of the films. A display of KLTO thin film is given in Figure 3.6.



Figure 3.6 KLTO Film.

### **3.4 Characterization**

#### ***3.4.1 The Aim of Characterization***

Thus far, the main issue which is focused was the structure of semiconductors and its applications. The determination of the structure and composition of materials were not mentioned. For this reason, to identify if the method was successful when a material is fabricated in the laboratory condition, some techniques were utilized to investigate the structure and properties. In this stage the main subject was the effective techniques which are available to characterize KLTO compounds.

#### ***3.4.2 Solution Characterization***

The sol-gel process is an advanced process to generate gel, polymeric crystalline or glass phase in wide range from liquid form. The characterization is directly influence the ultimate film stoichiometry. The important goal is to produce the liquid form carefully. Therefore for the characterization of the solutions many tests are applied.

##### ***3.4.2.1 Turbidity Tests***

Before the coating, turbidity tests were performed to understand the solubility of the powder which is added to the solution. Turbidity tests were made by standard



VELP TB1 Model Turbidity Meter. Test range is 0 – 1000 ntu. If the turbidity is approached to 0, the solution is fully dissolved. If the turbidity is near to 1000 ntu, particles will suspend. To find transparent solutions, turbidity value should be near to 0 ntu.

#### *3.4.2.2 pH Values of Solutions*

The pH values of the prepared solutions are measured with the help of Hanna HI - 1230 electrode pH meter to understand the solution condition including, basic or acidic characteristics. The pH is an important factor of gelling and gel polymeric structure.

#### *3.4.2.3 Rheological Tests*

The viscosity, gel point, shear stress and modulus of elasticity were determined by using CVO 100 Digital Rheometer. Viscosity is the main controller of the film thickness. Because of this, the solutions which will be used in thin films should be in low viscosity, in other words it should be diluted. The viscosity and shear values are important for the coating process. Low viscosity is preferable for the coating of the material.

#### *3.4.2.4 Contact Angle Measurement*

The contact angle is created between a solid surface and a liquid surface which is in touch. It quantifies the wettability of a solid surface by a liquid via the Young equation. Contact angle reflects the relative strength of the affinity between the own molecules of liquid (cohesion force) and the affinity between liquid and solid (adhesion force). If the cohesion forces are bigger than adhesive forces, the angle between solid and liquid will be increase. Another way, a big contact angle means that the affinity between liquid and solid is less and the contrary of this is exist. If contact angle is less than  $90^{\circ}$ , liquid soaks the cape, if it is bigger than  $90^{\circ}$ , wetting does not exist. To summaries, contact angle which is used in coating process is important to make a good coating. The measurement of contact angle is done by

contact angle measurement device. To find the wettability between solution and substrate, contact angle was measured.

### ***3.4.3 Process Optimization***

For the producing of the targeted material and to decide optimum thermal heat condition, these tests are applied. For this reason, all specimens' DTA – TG and FTIR analysis were done.

#### *3.4.3.1 Differential Thermal Analysis/Thermogravimetry (DTA/TG)*

This method is used to determine the thermal properties of a bulk material as thermogravimetric analysis (TGA). This method provides detailed information about the thermal stability, reactions type, and suitable heat treatment. The operating principle of TGA is very simple – the solid is placed in a tiny microbalance pan and heated according to preset conditions. SHIMADZU DTA/TG device is used.

#### *3.4.3.2 Fourier Transform Infrared (FTIR)*

For the directive of process optimization; chemical bonds of the fabricated gels before the transformation (from solution to crystalline state (powder)) in varying temperatures (100, 200, 300, 400, 600, 800 and 1000°C and 15 minutes) were determined by a FTIR (Thermo Scientific Nicolet iS10) device.

### ***3.4.4 Material Characterization***

#### *3.4.4.1 X – Ray Diffraction (XRD)*

To identify existing phase of the coated material obtained with sol – gel method, X – ray diffraction analyze method were performed with using ThermoScientific ARL X'tra diffractometer. The measurements were realized in Cu tubes at 30 kV tension and 20 mA intensity by using CuK $\alpha$  radiation ( $\lambda = 0.15405$  nm). This ray beam diffracted the three dimensional crystal lattice of the material and the

diffraction patterns are obtained. The crystal structure occurred by analyzing and the comparison with standard patterns.

#### *3.4.4.2 Scanning Electron Microscopy – Energy Dispersive Spectrophotometer (SEM - EDS)*

To analyze and determine surface morphology of the coatings JEOL JSM – 6060 Scanning Electron Microscope (SEM) was used. This study was done by using accelerated electrons under high voltage on the specimen. And the interaction between electrons and specimen atoms was the principle of this process.

#### *3.4.4.3 Elemental Analysis - X-Ray Photoelectron Spectrophotometer (XPS)*

To do the elemental analysis, ThermoScientific K - Alpha X-ray photoelectron spectrophotometer was used. The principal of XPS is to send X rays to the material and to measure surface kinetic energy and electron number which break away from surface.

#### *3.4.4.4 Surface Roughness - Atomic Force Microscope (AFM)*

This microscope provides 3 D display of the surface. To determine the roughness and to obtain two and three dimension image, the Nanosurf easyScan2 was used.

### **3.5 The Pollutants and the Properties**

#### ***3.5.1 Phenol***

Phenolic compounds have a widespread using area in most of the industries and daily life and it is a common pollutant in waste water bodies. Phenol is very dangerous owing to the stability; high toxicity and it have a carcinogenic character. This compound causes a great deal of damage and the ecosystem of the water sources and human health is threaded by phenolic pollutants. The treatment of the phenol is a very big question. The studies have been focused on the modification of

the catalyst with using the photocatalytic principles and the factors which influence the photocatalytic rate and the reaction kinetics.

Phenol is known as the monohydroxy derivative of benzene (Sawyer N.C. et. al., 1994). It is classified in organic substances class. At first, phenol was recovered from coal tar. The other areas of usage are coal gasification, coke production, pharmaceuticals, pesticides, fertilizers (Tay et al., 2001, Veeresh et al., 2005), construction, automotive, and to produce synthetic resins, dyes, biocides (Sá & Boaventura, 2001, Fang et al., 2004). In addition, it becomes a disinfectant, slime-killing agent, and an additive in medicines. Production of biphenol A is another usage area of phenol. (Metcalf & Eddy, 2003).

Phenol is soluble in liquid sulphur dioxide, acetic acid, carbon tetrachloride, alcohol, chloroform, ether, glycerol, petrolatum, carbon disulphide, volatile and fixed oils, aqueous alkali hydroxides, and acetone. It is not very soluble in mineral oil. It is nearly insoluble in petroleum ether. Theoretically, 1 gram of phenol is dissolving in 15 ml of water and 12 ml of benzene. If phenol comes into contact with heat, flame or oxidizers, it is combustible. When it is heated, it discharges toxic fumes.

Phenol is the derivative of benzene. Instead of the hydrogen, hydroxyl ( $\text{OH}$ ) groups are replaced. When hydrogen is removed from benzene molecule, the root residue is called phenyl ( $\text{C}_6\text{H}_5$ ). Phenyl is acidifier group contrary to the alkyl group. Phenyl improves the acidic condition of the material. Phenols are very toxic and when it is in liquid or vapor form, it has a special odor. Due to the higher toxicity and higher oxygen demand (theoretically, 2.4 kg  $\text{O}_2$ /kg phenol), US Environmental Protection Agency (EPA) and World Health Organization (WHO) accept phenol in the first pollutant group. For drinking water, the World Health Organization prescribed a guideline and the concentration is accepted 0.001 mg/l (WHO, 1994). The problem is occurring under 1  $\mu\text{g/l}$  concentrations and it changes the taste and creates odor problem in drinkable water (Chen et al., 2009).

Phenol is colorless or white solid and when it is exposed to air or light, the mass is turning to red or pink. It has a sour odor. The chemical formula is  $C_6H_5OH$  and the molecular weight is 94.11 g /mol. It is very soluble in water and quite flammable. Chemical structure of phenol is shown in Figure 3.7 (Molva, 2004).

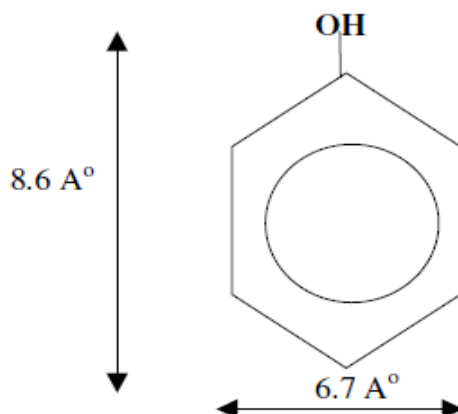


Figure 3.7 Dimensions of phenol (Molva, 2004).

Phenol irritates the skin, eyes, and mucous membranes in humans after acute (short-term) inhalation or dermal exposures. The symptoms of the long - term exposure are anorexia, progressive weight loss, diarrhea, vertigo, and salivation, a dark coloration of the urine, and blood and liver. According to the animal studies, animals which exposed to phenol by oral way have some findings as the reduction of fetal body weights, growth retardation, and abnormal development in the offspring of animals (U.S. EPA 63FR).

The phenolic compounds are quite stable and remain in the environment for longer periods. Due to the toxicity and carcinogenic character, they are dangerous for the aquatic life in water bodies and human health. According to the Water Pollution Control Regulations in Turkey (2004) the discharge limit of phenols in inland water is approximately 1 mg/L.

Table 3.4 Water pollution control regulations - phenol limits

Parameter	Water Quality Classes			
	I	II	III	IV
Phenolic Substances (volatile) (mg/L)	0.002	0.01	0.1	> 0.1

The table below shows a comparison of chemical, biological and photocatalytic methods and the effectiveness of these processes.

Table 3.5 Chemical and biological treatment methods for phenol according to the literature

Parameter	Initial Concentration	Treatment Process	Efficiency %	pH	References
Phenol (C <sub>6</sub> H <sub>5</sub> OH)	10 mg/l	Adsorption– flocculation using organobentonite	90	7	Shen, (2001)
	20 mg/l				
Phenol (20°C)	2 mg/l	Adsorption	58		Lin, Pan, Chen, Cheng, & Xu, (2008)
	6 mg/l		36.67		
	10 mg/l		35.60		
	20 mg/l		33.60		
	30 mg/l		29.87		
	100 mg/l		25.88		
	200 mg/l		19.86		
	300 mg/l		13.34		
	400 mg/l		10.18		
Phenol (40°C)	2 mg/l		62.40		
	6 mg/l		39.33		
	10 mg/l		35.60		
	20 mg/l		34.40		
	30 mg/l		30.67		
	100 mg/l		27.36		
	200 mg/l		20.44		
	300 mg/l		13.71		
	400 mg/l		10.27		
Phenol (60°C)	2 mg/l		69.40		
	6 mg/l		41.67		
	10 mg/l		36.40		
	20 mg/l		35.40		
	30 mg/l		31.47		
	100 mg/l		28.32		
	200 mg/l		20.52		
	300 mg/l		13.75		
	400 mg/l		10.33		
Phenol	30 mg/l	Electrochemical removal (2 hours)	97	7	Abdelwahab, Amin, & El - Astoukhy, (2008)
Phenol	50 mg/l	Ozone=2 g/l.hour	94.34		Turhan, & Uzman, (2007)
		Ozone=4g/l.hour	96.34		
		Ozone=6 g/l.hour	98.36		
	75 mg/l	Ozone=2 g/l.hour	99.94		
		Ozone=4g/l.hour	94.86		
		Ozone=6 g/l.hour	90.95		
Phenol	100	Aerobic granular SBR	100		Moussavi, Barikbin, & Mahmoudi, (2010)
	225		100		
	450		100		
	1000		100		
	1500		100		
	1700		99.6		
	2000		98.6		

Table 3.6 A summary table for the photocatalytic treatment methods of phenol according to the literature

Parameter	Initial Concentration	The catalyst used	Efficiency %	Time (hour)	pH	Device	References					
Phenol (C <sub>6</sub> H <sub>5</sub> OH)	75 ppm	Aqueous zinc oxide suspension using solar energy	47	9	5.61	1000 W Xenon Lamp	Pardeshi, & Patil, (2008)					
Phenol	100 mg/l	TiO <sub>2</sub> + UV	76	12		253.7 nm UV lamp	Guo, Ma, & Li, (2006)					
P - clorophenol	50 mg/l	TiO <sub>2</sub> Degusa P -25	85 - 90	4			Kirilov, Koumanova, & Petrov, (2006)					
Phenol	0.5 * 10 <sup>-4</sup> mol/l	TiO <sub>2</sub>	30	3		180W medium pressure mercury lamp	Sobczynski, Duczmal, & Zmudzinski, (2004)					
	0.75 * 10 <sup>-4</sup> mol/l		25									
	1 * 10 <sup>-4</sup> mol/l											
	1.5 * 10 <sup>-4</sup> mol/l											
	2 * 10 <sup>-4</sup> mol/l											
2,4,6 - trimethylphenol	0.1 mM	TiO <sub>2</sub> + UV	100	1	3.00 ± 0.05	Pressure Mercury Lamp	Kusvuran, Samil, Atabur, & Erbatur, (2005)					
	0.5 mM		56									
2,4,6 - trichlorophenol	0.1 mM		70									
	0.5 mM		44									
2,4,6-tribromophenol	0.1 mM		60									
	0.5 mM		22									
2 clorophenol	12.5 mg/l		Co doped TiO <sub>2</sub>					93.4	3	9	100 W high-pressure mercury lamp	Barakat, Schaeffer, Hayes, & Ismat - Shah, (2005)
	25 mg/l							85.1				
	50 mg/l	77.8										
	75 mg/l	76.6										
Phenol	0.13 mM	TiO <sub>2</sub> + UV	90	3		400 W high-pressure mercury lamp	Chiou, Wu, & Juang, (2008)					
	0.71 mM		42									
m - nitrophenol	0.13 mM	TiO <sub>2</sub> + UV	83	3	4.1 - 12.7	400 W high-pressure mercury lamp	Chiou, Wu, & Juang, (2008)					
	0.71 mM		43									
Phenol	100 mg/L (1.06*10 <sup>-3</sup> M)	UV/H <sub>2</sub> O <sub>2</sub>	97.1	5	7	16 W Mercury Lamp	Çatalkaya, Bali, & Şengül, (2004)					
Phenol	100 mg/l	UV/H <sub>2</sub> O <sub>2</sub> + Fe <sup>2+</sup>	100	5		16 W Mercury Lamp	Çatalkaya, Bali, & Şengül, (2004)					
Phenol	200 mg/l	Fenton	57	1		8 W Pressure Mercury Lamp	Babuponnu sami, & Muthukumar, (2012)					
		Electro Fenton	89.5									
		Sono - electro - Fenton	100									
		Foto - electro - Fenton	100									

Both type of the lamps (Xenon and Mercury-vapor) are a specialized type of gas discharge lamp by passing current through a gas under pressure. The current which flows between the lamp's electrodes is an arc and it ignites the gas. At xenon lamp technology, an electric light is produced a light by passing electricity through ionized xenon gas at high pressure. It uses Xenon gas. A bright light is producing and it imitates natural sunlight. On the other hand, mercury-vapor lamp, as is evident from its name, an electric arc produces light by using vaporized mercury. Mercury-vapor lamp uses mercury with other gases to improve the performance and reliability. The main difference between the lamp types is the light spectrum. Xenon lamp emits all wavelengths through the visible zone (400 nm to 700 nm). This zone is approximately corresponding to the natural daylight. On the other side, mercury-vapor lamp shows strong peaks through the visible zone with the strongest peak in the yellow region (560-590 nm). Xenon lamp is used in this study.

### ***3.5.2 Methylene Blue***

Methylene blue (MB) is a type of thiazine dye and azo dye. and it has large scale utilization in industries. The chemical compound of Methylene Blue is a type of heterocyclic aromatic and its chemical formula is formed as  $C_{16}H_{18}ClN_3S \cdot 3H_2O$  (3,7-bis(dimethylamino)-fenazotionium chloride). The areas of usage are coloring the papers, hair dye, fabric dying and wool dying. The applications of methylene blue are mostly from textile industries. It is commonly used in dyestuff applications and as a redox indicator. For this reason, it is the major pollutant of textile industry wastewaters (Yao & Wang, 2010).

Methylene blue is a cationic dye. It consists of dark green color and odorless. At ambient temperature, it demonstrates a solid condition. The chemical structure can be seen by Figure 3.8 (Yao & Wang, 2010).



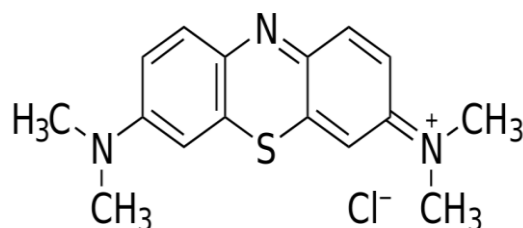


Figure 3.8 The chemical structure of methylene blue (Yao & Wang, 2010).

Methylene blue is not very toxic, but it can cause some damages. If it is inhaled, the complication of breathing appears in short - term. If it is given orally, some symptoms appear as a combustibile sense, a heartbeats increase, going into shock, sickness, vomiting, diarrhea, gastritis, cyanosis, jaundice, and quadriplegia and cell necrosis.

When the methylene blue dissolves in water, three absorbances can be seen in the UV - visible beam zone. The first absorbance band is 264 nm, and the two others are 291 nm and 664 nm, respectively. The absorbance 291 nm and 664 nm are mostly used for removing the methylene blue. Within the experiments, 664 nm wavelengths is chosen to make the analysis in visible radiation (Yao & Wang, 2010).

The solubility at ambient condition is 40 g/l and the solubility in methanol is 15 g/l. In practice, generally  $10^{-5}$  M is preferable. The band in 664 nm cannot pass 0.8 absorbance. According to Water Pollution Control Regulations (2004) the discharge limit of methylene blue can be seen in Table 3.7.

Table 3.7 Water pollution control regulations - methylene blue limits

Parameter	Water Quality Classes			
	I	II	III	IV
The surfactants which react with methylene blue (MBAS) (mg/l)	0.05	0.2	1	>1.5
Marine Water Quality General Criteria				
Parameter	Criteria			
The surfactants which react with methylene blue (MBAS) (mg/l)	10 (As principle, Turkish Standards Institute is forbidden to release the materials which cannot degrade biologically)			

The table below shows a comparison of chemical, biological and photocatalytic methods and the effectiveness of these processes.

Table 3.8 A summary table for the photocatalytic treatment methods of methylene blue according to the literature

Parameter	Initial Concentration	Treatment Process	Efficiency %	pH	References
Methylene Blue	260 mg/l	Removal with adsorbent	93.10	9	Li, Chang, Jiang, Jean, & Hong, (2011)
Methylene Blue	10 mg/l	Activated carbon	80	7.5	Sandoval, Cooper, Aymar, Jain, & Hristovski, (2011)
Methylene Blue	100 mg/l	Photocatalytic reactor	80	9	Rizzo, Koch, Belgiorno, & Anderson, (2006)
Methylene Blue	100 mg/l	Membrane System	89.90	9	Madaeni, Jamali, & Islami, (2011)
Methylene Blue	100 mg/l	Sequencing Batch Reactor	56		MA, Wang, Song, Wang, Fan, & Li, (2011)

### 3.5.3 Cyanide

Cyanide is an inorganic toxic material. (-1) valence form of carbon and nitrogen (CN) is an important group in inorganic carbon chemistry. Cyanide is weaker than air. The specific weight is 0.687 g/ml. That is why, the half - life of cyanide in the air is very long. But it can disperse in the air and becomes non toxic. It is using for varying purposes. The little doses have lethal effect. The lethal effect in liquid phase is estimated 1 - 3 mg (Gümüş, 2001). Cyanide is come into existence from industries as electrolysis coating (NaCN), gold and silver mining (NaCN), metal working (alkali and metal cyanide), pesticides, oil refinery, coal gasification and electroplating processes. Cyanide exposure can be by cutaneously, oral or respiratory. Low doses can be transformed to thiocyanide (SCN) (between 20 minutes and 1 hour) by an enzyme in liver and released by urinary tract. But the high doses have lethal effect. The lethal dose for HCN is 50 mg, for sodium and potassium salts is 200 - 300 mg. If 0.2 - 0.3 mg/l cyanide is inhaled by air, it kills immediately. If 0.13 mg/l is inhaled, the lethal effect reveals after 1 hour. 0.02 - 0.03 mg are harmless (Pilato, 2010).



Figure 3.9 The chemical structure of cyanide

According to the Water Pollution Control Regulations in Turkey (2004), the discharge limit of cyanide can be seen in Table 3.9.

Table 3.9 Water pollution control regulations - cyanide limits

Parameter	Water Quality Classes			
	I	II	III	IV
Total Cyanide ( $\mu\text{g CN/L}$ )	10	50	100	> 100

The table below shows a comparison of chemical, biological and photocatalytic methods and the effectiveness of these processes.

Table 3.10 A summary table for the photocatalytic treatment methods of cyanide according to the literature

Parameter	Initial Concentration	Treatment Process	Efficiency %	pH	References
Cyanide	260 mg/l	Oxidation of activated carbon saturated copper and hydrogen peroxide	90	7	Yeddou et al. (2011)
Cyanide	260 mg/l	Oxidation with activated carbon and hydrogen peroxide	80	11	Yeddou et al. (2011)
Cyanide	100 mg/l	Adsorption	93.20	10	Zhu, Ren, Wei, Duan, Yao, & Zhao, (2011)
Cyanide	100 ppm	Degussa P25 $\text{TiO}_2$ (0.5 g/l) photooxidation	96	11.5	Aguado et al. (2002)

Due to the comparison tables of phenol, methylene blue and cyanide, the optimum conditions were chosen to make the experimental analysis. The variables were obtained and selected, according to the literature studies.

## 3.6 Method

### 3.6.1 Photocatalytic Method

The photocatalytic degradation processes were realized to treat phenol, methylene blue and cyanide. Photocatalytic degradation experiments were carried out in a solar box ATLAS SUNTEST CPS+ which is simulating natural radiation. The light source has a vapor xenon lamp ( $300 \text{ nm} < \lambda < 800 \text{ nm}$ ) and the power can change between 250 and  $765 \text{ W/m}^2$ .

To prepare an industrial wastewater:

- To produce 10 mg/l phenol (Merck, 99-100.5%) solution, 10 mg of phenol was weighting out with using analytic balance. This 10 mg/l phenol was completed with 1 liter of pure water. For providing the homogeny mix, 15 minutes of stirring was done with using magnetic mixer.
- The same method was obtained to produce 100 mg/l phenol (Merck, 99-100.5%) solution.
- $10^{-5}$  M methylene blue (Sigma-Aldrich, 97%) solution was prepared by measuring 0.03199 g of metylene blue powder. The absorbance of the degradation experiments were measured by using Shimadzu UVmini-1240 spectrophotometer.
- To produce 100 mg/l cyanide (Merck, 97%) solution, 100 mg of cyanide was weighting out. This 100 mg cyanide poured over 1 liter of pure water. For providing the homogeny mix, 15 minutes of stirring was done with using magnetic mixer.
- The same method was obtained to produce 300 mg/l cyanide solution.

To see the effectiveness of KLTO, an arbitration specimen was examined as a reference without any photocatalyst. And to make a comparison,  $\text{TiO}_2$  catalyst also examined to see the differences between them. 0.01 g  $\text{TiO}_2$  nanopowder (Sigma-Aldrich) was used as catalyst. The testing sets were planned as 1, 2, 3, 4 and 5 hours.

Some experiments below were given in detail. The replications for the performance tests were designed as 5 hours.

### ***3.6.2 Statistical Method - Factorial Experimental Design***

Statistical methods support the understanding and the description of the variability. The variability is everywhere in a routine life and statistical thinking helps to take a decision. Some factors represent potential sources of variability in the system. This observed variability in our treatment system depends on many factors, such as pH, initial pollutant concentration and irradiance ranges. These variables are chosen according to the literature reviews. Statistics gives a framework to describe which potential sources of variables are the most important or which have the greatest impact on the efficiency (Montgomery & Runger, 2010).

In a designed experiment the engineer can change the controllable variables of the system or process, observes the output data, and makes an inference or decision about the variables which are responsible in output performance. Every designed experiment involves some activities (Montgomery & Runger, 2010):

1. Conjecture (guess) – the original hypothesis that motivates the experiment.
2. Experiment – the test performed to investigate the conjecture.
3. Analysis – the statistical analysis of the data from the experiment.
4. Conclusion – what has been learned about the original conjecture from the experiment?

Phenol, methylene blue and cyanide photocatalytic experiments were performed and pH, initial concentration and irradiance ranges are chosen as variable. The observation of the design parameters and the performance is made an inference or decision about the variables which are responsible in output performance. For phenol and cyanide, three factors two replicates factorial design and for methylene blue, two factors two replicates factorial design were set up. Each experiment was tested 2

times and 16 experiments are done for each one. The goal of the research problem which identified was to reach effective treatment result with our selected variables.

Every experiment is tested twice. If  $H_0$ 's are true, the variances are equal.

$\tau_i$  = effect of  $i^{\text{th}}$  level of factor A;

$H_{01}$ :  $\tau_1 = \tau_2 = \tau_3$ , pH has no effect on the removal,

$H_{11}$ :  $\tau_1 \neq \tau_2 \neq \tau_3$ , pH has an effect on the removal.

$B_j$  = effect of  $j^{\text{th}}$  level of factor B;

$H_{02}$ :  $B_1 = B_2$ , Initial concentration ( $C_0$ ) has no effect on the removal,

$H_{12}$ :  $B_1 \neq B_2$ , Initial concentration has an effect on the removal.

$\alpha_k$  = effect of  $k^{\text{th}}$  level of factor C;

$H_{03}$ :  $\alpha_1 = \alpha_2$ , Light intensity has no effect on the removal,

$H_{13}$ :  $\alpha_1 \neq \alpha_2$ , Light intensity has an effect on the removal.

$(\tau B)_{ij} = (B\alpha)_{jk} = (\tau\alpha)_{ik}$  = interactions ,

$H_{04}$ :  $(\tau B)_{ij} = 0$ , pH and  $C_0$  interaction have no effect on the performance,

$H_{14}$ :  $(\tau B)_{ij} \neq 0$ , There are pH and  $C_0$  interaction effects on the performance,

$H_{05}$ :  $(B\alpha)_{jk} = 0$ ,  $C_0$  and light intensity interaction have no effect on the performance,

$H_{15}$ :  $(B\alpha)_{jk} \neq 0$ , There are  $C_0$  and light intensity effects on the performance,

$H_{06}$ :  $(\tau\alpha)_{ik} = 0$  pH and light intensity have no effect on the performance,

$H_{16}$ :  $(\tau\alpha)_{ik} \neq 0$ , There are pH and light intensity effects on the performance.

$H_{07}$ :  $(\tau B\alpha)_{ijk} = 0$  pH, initial concentration and light intensity have no effect on the performance,

$H_{17}$ :  $(\tau B\alpha)_{ijk} \neq 0$ , There are pH, initial concentration and light intensity effects on the performance.

### 3.6.3 Reaction Kinetic Method

To determine the order of the reaction for photodegradation of phenol, methylene blue and cyanide in the SUNTEST CPS+ reactor, kinetic studies were performed according to the treatment results. The degradation curves were taken out and zero, first and second order reaction kinetics were tested.

$C_0$  is the initial concentration,  $C$  is the concentration after the reaction time,  $t$  is reaction time (h) and  $k_0, k_1, k_2$  and  $k_n$  (mg/l.min) are rate constants for zero, first, second and nth order kinetics, respectively (Baycan, 2005). Kinetics are obtained from the equations below:

#### Zero order kinetics:

$$\text{Reaction order:} \quad k_0 = -\frac{dC}{dt} \quad (4.1)$$

$$\text{After integration:} \quad C = C_0 - k_0 t \quad (4.2)$$

$$\text{Conversion degree:} \quad x = \frac{k_0}{C_0} t = \frac{C_0 - C}{C_0} \quad (4.3)$$

$$\text{Half - life:} \quad t_{1/2} = \frac{C_0}{2k_0} \quad (4.4)$$

#### First order kinetics:

$$\text{Reaction order:} \quad k_1 C = -\frac{dC}{dt} \quad (4.5)$$

$$\text{After integration:} \quad C = C_0 e^{-k_1 t} \quad (4.6)$$

$$\text{Conversion degree:} \quad -\ln(1 - x) = k_1 t \quad (4.7)$$

$$\text{Half - life:} \quad t_{1/2} = \frac{\ln 2}{k_1} \quad (4.8)$$

#### Second order kinetics:

$$\text{Reaction order:} \quad k_2 C^2 = -\frac{dC}{dt} \quad (4.9)$$

$$\text{After integration:} \quad \frac{1}{C} = \frac{1}{C_0} + k_2 t \quad (4.10)$$

Conversion degree:  $\frac{x}{1-x} = 1 + k_2 C_0 t$  (4.11)

Half - life:  $t_{1/2} = \frac{1}{k_3 C_0}$  (4.12)

**n<sup>th</sup> order kinetics:**

Reaction order:  $k_n C^n = -\frac{dC}{dt}$  (4.13)

After integration:  $C^{1-n} = C_0^{1-n} - (1 - n)k_n t$  (4.14)

**3.7 Atlas Suntest CPS+**

In this study Atlas Suntest CPS+ is used as a light source. This xenon test instrument is with 560 cm<sup>2</sup> of exposure area. It is equipped with a flat specimen tray. Some information about this device:

Table 3.11 Properties of SUNTEST CPS+

SUNTEST Features	CPS+	
Air – cooled Xenon lamps	1500 W	
Minimum Guaranteed Lamp Life (at one sun level)	1500 Hours	
Physical Dimension (WxDxH)	78 cm x 35 cm x 35 cm	
Direct Setting and Control of Irradiance in the wavelength range	300 - 800 nm/Lux; or 300-400 nm/340 nm	
Footprint	100 cm x 95 cm	
Floor Weight	29 kg (64 lb)	
Specimen rack capacity	560 cm <sup>2</sup>	
Specimen tray size in cm x cm	28 x 20	
SUNSENSIV sensor for controlling irradiance at 300-800nm / Lux	Daylight Filter	Window Glass Filter
	250-765 W/m <sup>2</sup>	250-765 W/m <sup>2</sup>



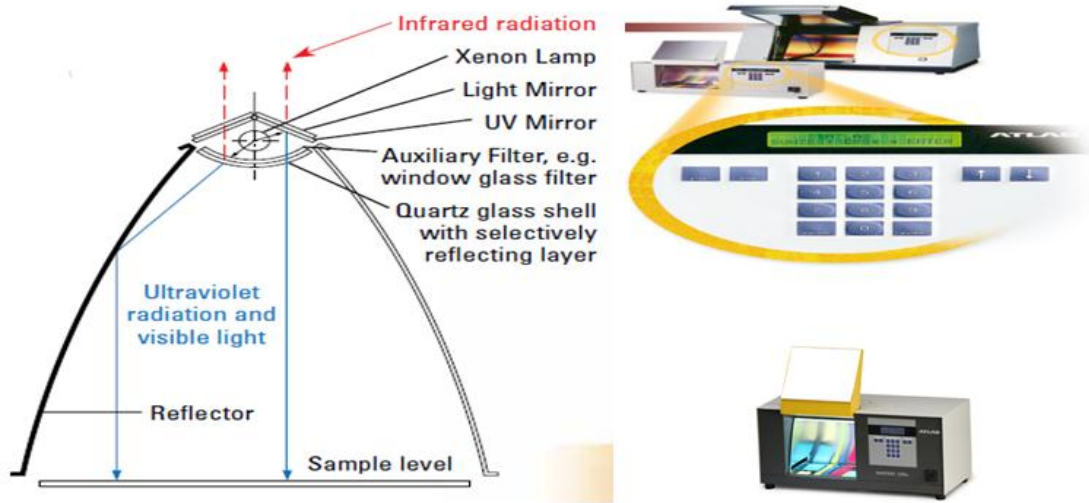


Figure 3.10 ATLAS Suntest CPS+ images (Suntest CPS/CPS+ Operating Manual).

Table 3.12 Sunlight measurements of ATLAS SUNTEST CPS+

Sun light Measurements		Irradiance Range W/m <sup>2</sup>			
		300 - 400 nm	340 nm	420 nm	300 - 800 nm
Average Optimum Natural Daylight	Measured 45°C South Cloudless Miami, FL	28	0.30	0.67	287
Peak Natural Daylight	Measured solar noon on Vernal Equinox at normal incidence Miami, FL	66	0.70	1.53	617

## CHAPTER FOUR RESULTS AND DISCUSSION

### 4.1 Solution Properties

#### 4.1.1 Turbidity Values

Before the coating, turbidity tests are carried out to understand the solubility of the precursors which are added to the solution. Turbidity tests are made by standard VELP TB1 Model Turbidity Meter. The solutions prepared after the calibration process and putted in glass tube (25 mm diameter and 50 mm length).

The solution turbidity values are shown in Table 4.1. To estimate the turbidity, 5 measurements were done for each solution and the arithmetic mean of them was calculated. It was found that the prepared solutions were homogenizes and transparent.

Table 4.1. Solutions turbidity value

<b>Solution</b>	<b>Turbidity (ntu) *</b>
CeO <sub>2</sub>	53.56
KLTO	77.06

\* The mean of value

#### 4.1.2 pH Values

Table 4.2 gives data about pH values of the Ce based solutions and Table 4.3 mentioned data about pH values of K, La and Ti - based solutions. To estimate the solutions pH's, 5 measurements was done for each solution and their arithmetic mean was calculated.

Table 4.2 pH values of Ce based solutions

<b>Measurement Order</b>	<b>pH</b>
1	4.40
2	4.42
3	4.44
4	4.47
5	4.48

Table 4.3 pH values of K, La, Ti - based solutions

Measurement Order	pH
1	3.51
2	3.48
3	3.48
4	3.53
5	3.55

It is clear from Tables 4.2 and 4.3 that the arithmetic means of the pH values for Ce - based and K, La, Ti - based solutions are 4.44 and 3.51, respectively. The solutions exhibit acidic characteristic. This acidic condition is the consequence of the solvent and chelating agent.

#### 4.1.3 Rheological Properties

Viscosity is the key factor to control the film thickness. So, solution's viscosities must be diluted. Viscosity is measured as time dependent. The angular velocity is found 300 Hz, the ambient temperature is 25°C and 60°C and the time is determined 2500 seconds and 1000 seconds as test parameters for solutions viscosity. To investigate the gelling temperature with respect to different temperature, modulus of elasticity and viscose were measured. At 25°C, the modulus of viscose was found  $2.5 \times 10^2$  Pa. Figure 4.1 illustrates module - time graphs.

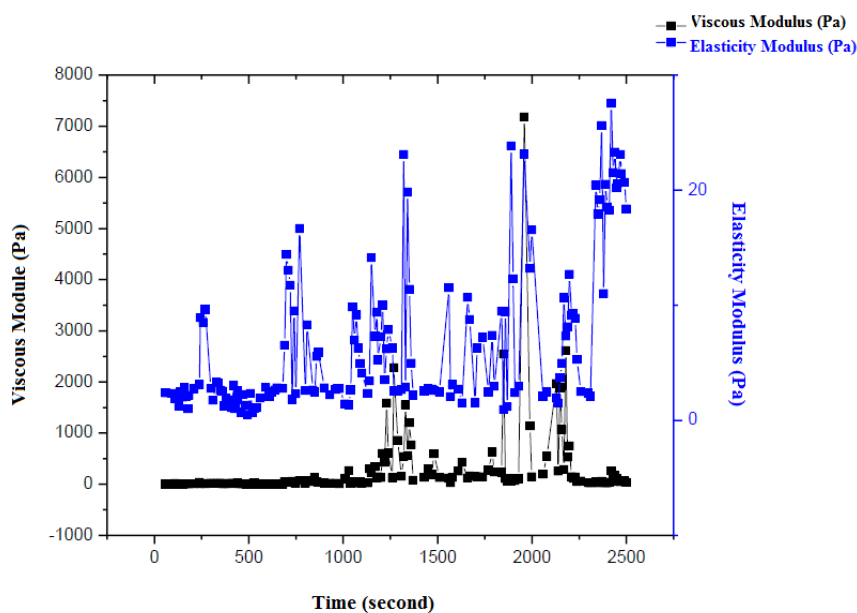


Figure 4.1 The change of the modulus of elasticity and viscous (25°C).

#### ***4.1.4 Contact Angle Measurement***

Measurements showed that the contact angle values of Ce - based and K, La, Ti - based are 4° and 3°, respectively. The results are less than 90°. That is why; there is no inconsistency about wettability between substrates and solution.

#### **4.2 Process Optimization**

For the producing of the targeted material and to decide optimum thermal heat condition these tests are applied. For this reason to all specimens DTA – TG and FTIR analysis were done.

##### ***4.2.1 Differential Thermal Analysis/Thermogravimetry (DTA/TG) Analysis***

The solutions were dried at 500°C in 2 hours and powder was produced. The prepared xerogels were heated between 25°C and 1200°C with a 10 °C/min heat change and in an oxygen atmosphere. The prepared KLTO based powders were heated in specific velocities in the presence of oxygen to determine the endothermic and exothermic reactions.

Figure 4.2 shows the KLTO xerogel thermal behavior at 500°C and 30 minutes. The curve mentions that endothermic and exothermic reactions occur on the chosen temperatures, between 25°C and 1200°C. Firstly, the endothermic reaction of the volatile organic compounds was occurred. In second step, the carbon which exists in alcoxide materials, solvent (propionic acid) and chelator (GAA) was burning and created exothermic reaction. Finally, endothermic phase conversion reactions of KLTO phase composed.

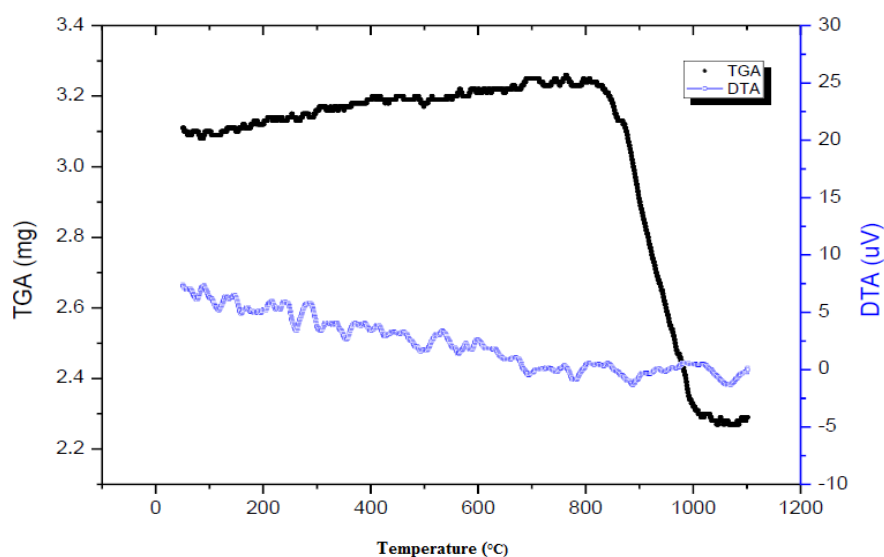


Figure 4.2 DTA/TG curves of KLTO powder xerogel.

Beginning temperature, ending temperature of the reactions, reaction energy and reaction type were found by DTA/TG curves. According to these informations, the optimum temperature and detention period were determined between a specific temperature ranges. With respect to these data's thermal treatment phase were given in Table 4.4. As a result, the optimum annealing temperature for the phase transformation is determined in 850 °C and 1200 °C.

Table 4.4 Thermal treatment analysis phase

	<b>Reaction Temperature Range (°C)</b>	<b>Reaction Type</b>	<b>Optimum Temperature Value (°C)</b>	<b>Foreseen Detention Time</b>
Drying - Burning of organics	27.29 - 500.08	Endothermic Exothermic	500	30 minutes
Phase conversion	850.08 - 1200.07	Exothermic	850/1200	180 minutes

#### 4.2.2 Fourier Transform Infrared (FTIR)

The absorbance spectrum of specimens was found at 25 °C and between the wavelengths 600-4000 cm<sup>-1</sup>. Figure 4.3 gives information about the pure KLTO spectrums at specified temperatures such as 25, 100, 200, 300, 400, 600, 800 and 1000°C for 15 minutes in air. FTIR data were regularly conformed to DTA - TG results. O-H, C=O and M-OCOO-M bond frequencies are decreased and vanished

around 600 °C. Chen et al. indicated that signals demonstrated O-Ti-O formation characteristics between the ranges of 400 - 1200 °C. At 800 °C, any signal of O-H, C=O and M-OCOO-M bonds could not be found. As a result of these signals, organic structures and hydroxyls are completely vanished. The peaks which are appeared by a decrease with increasing temperature band between the ranges of 850 - 950  $\text{cm}^{-1}$  are thought to be K, La, Ti ions of oxygen bond. In this case, process is selected according to the heat temperature profile.

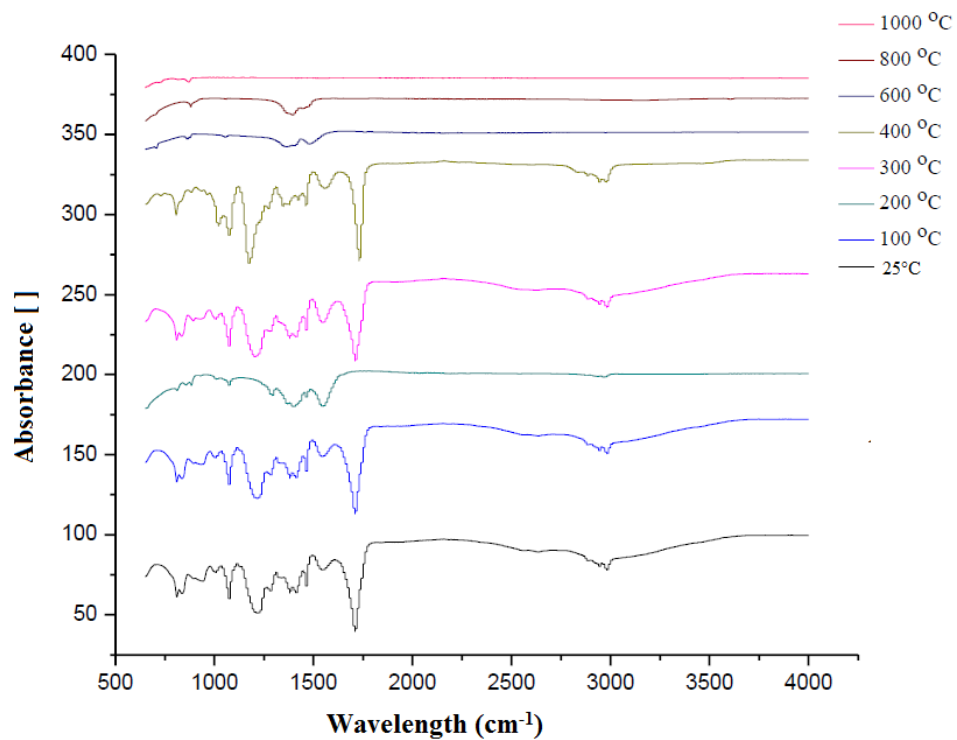


Figure 4.3 FTIR spectrums of the KLTO xerogels.

## 4.3 Film Characterization

### 4.3.1 XRD Analysis

These properties were related with temperature, time and the amount of potassium.  $\text{CeO}_2$  and KLTO were coated 5 and 7 times on the glass substrates, respectively. These codes were given according to heat treatment properties.

Table 4.5 Thin film codes

Specimen Code	Temperature ( $^{\circ}\text{C}$ )	Time (h)	K* (g)
1	850	3	0.8
2	950	3	0.8
3	1000	8	0.8
4	1100	3	0.8
5	1100	3	-
6	1100	8	0.2
7	1300	5	0.2
8	1300	8	0.2
9	1300	8	0.1

\* The initial amount of potassium in furnace

Phase analysis was performed with the comparison of the available reference pattern which is situated in library. 9 different specimens were examined. In every specimen steps, a property increased or decreased to reach the optimum phase. These properties were the temperature, time and the amount of K precursor. It was found that the phase of KLTO is achieved. The condition of the phase obtained were  $1300^{\circ}\text{C}$ , 8 hours and 0.1 gram K precursor. The XRD pattern of  $\text{K}_2\text{La}_2\text{Ti}_3\text{O}_{10}$  is given in Figure 4.4. According to the result, sharp peaks show that the crystalline structure is obtained. XRD patterns showed different angle peaks. Different additives and concentrations are thought to result this situation.

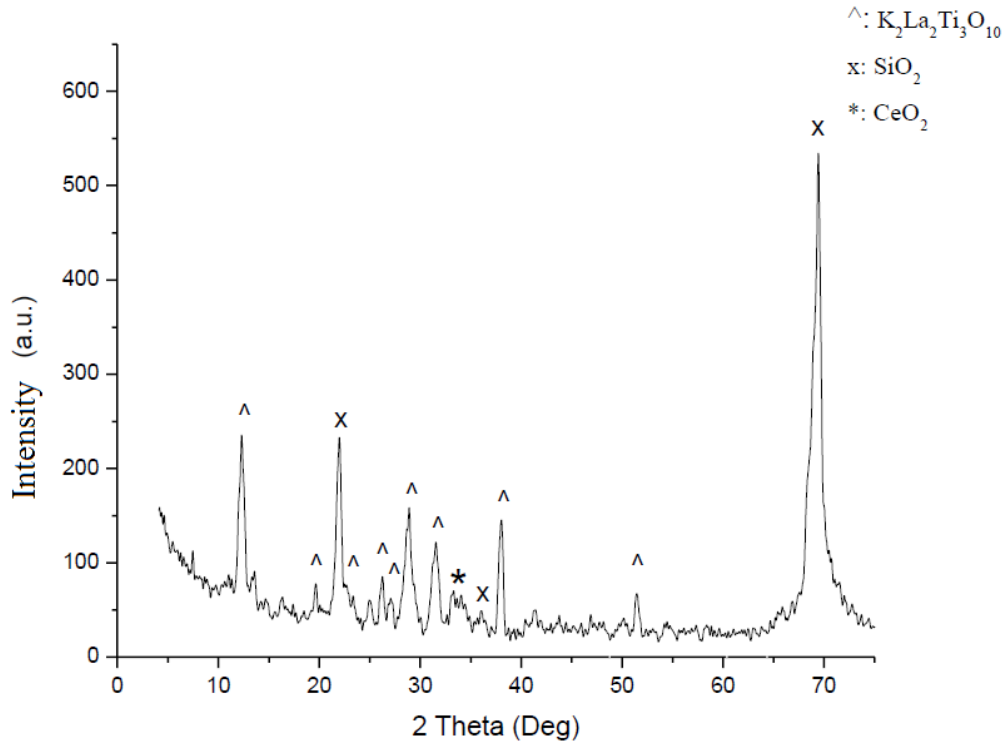
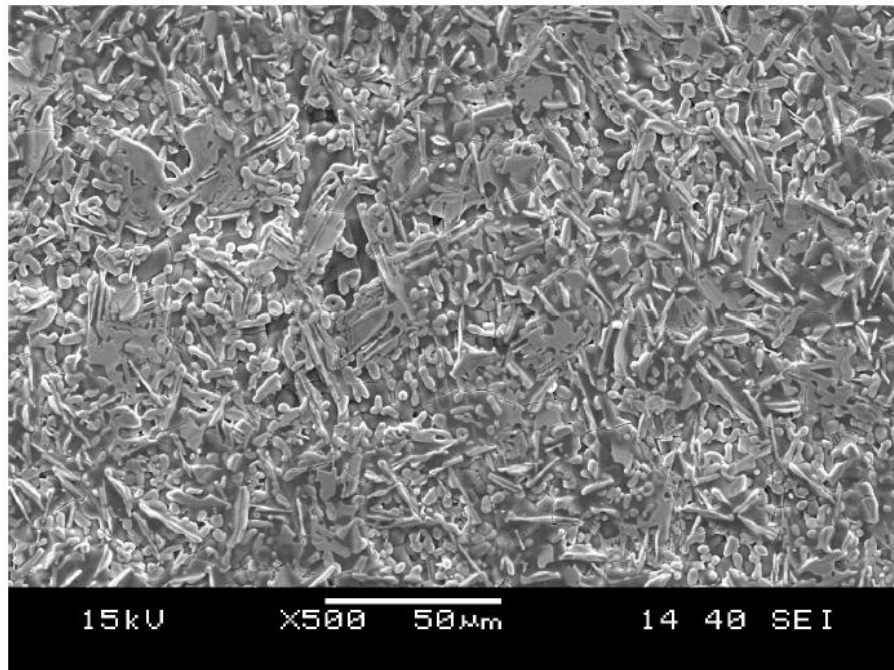


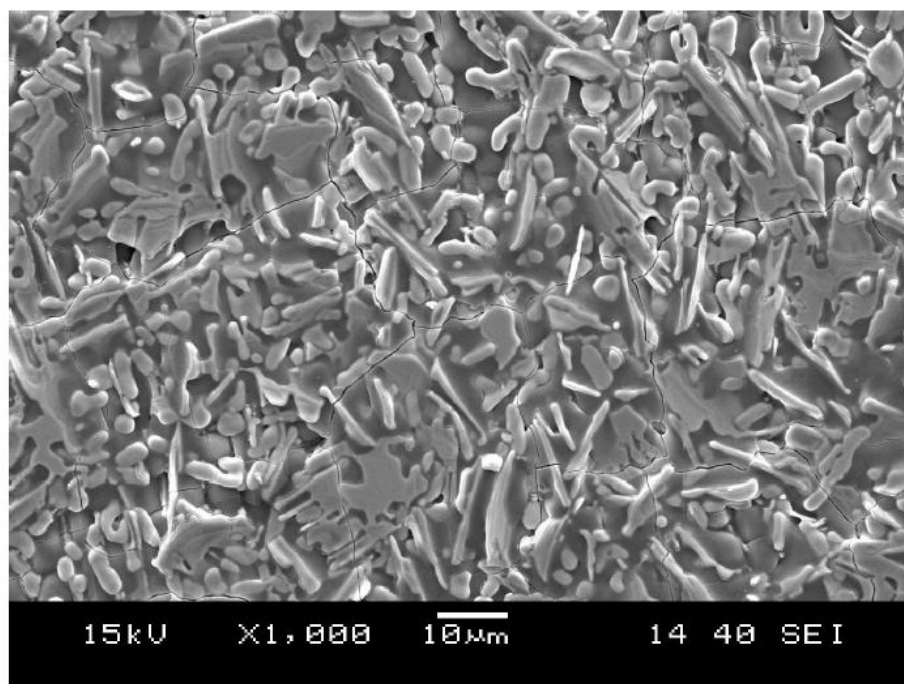
Figure 4.4 XRD pattern of the optimum phase (specimen 9).

### 4.3.2 SEM - EDS Analysis

To analyze and determine the coating surface morphology JEOL JSM – 6060 Scanning Electron Microscope (SEM) was used. The surface area was covered by the needless dense coating particle.

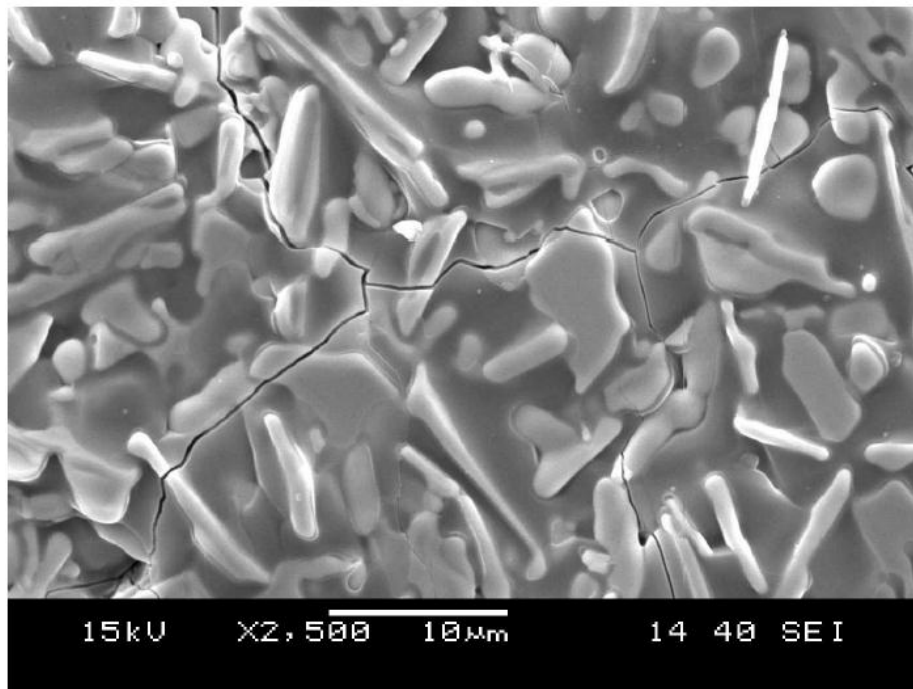


(a)

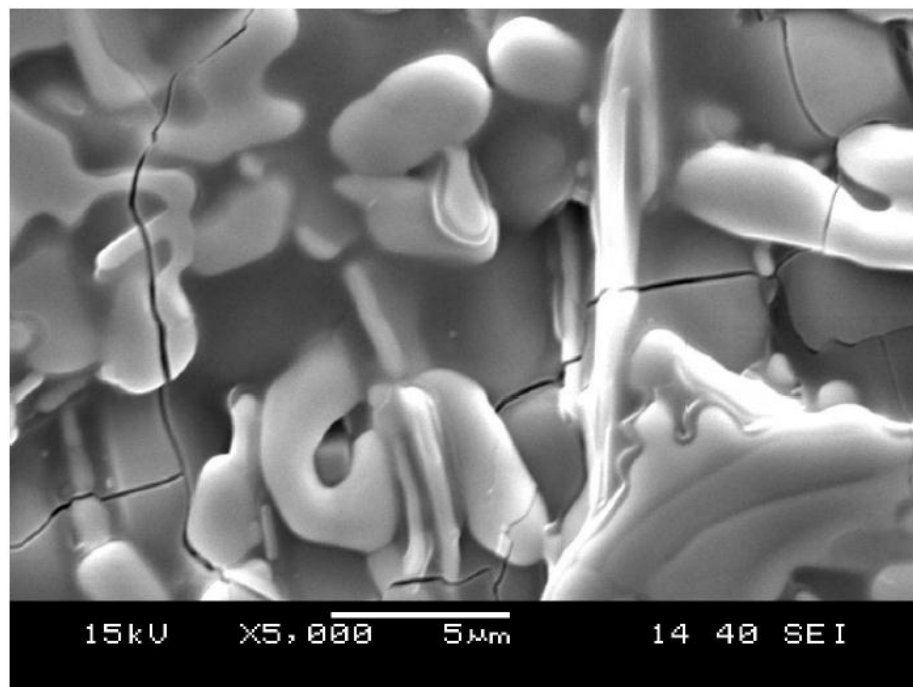


(b)

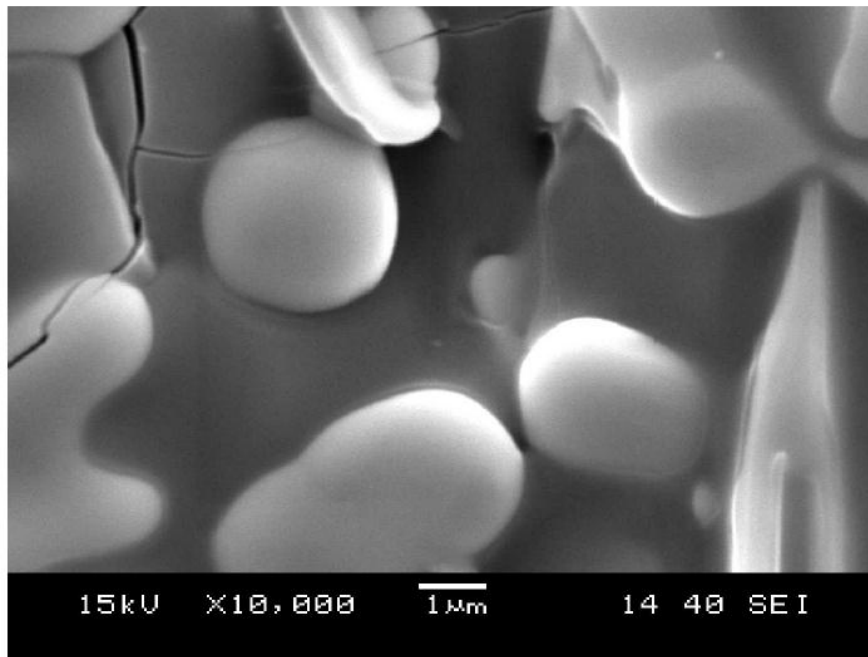




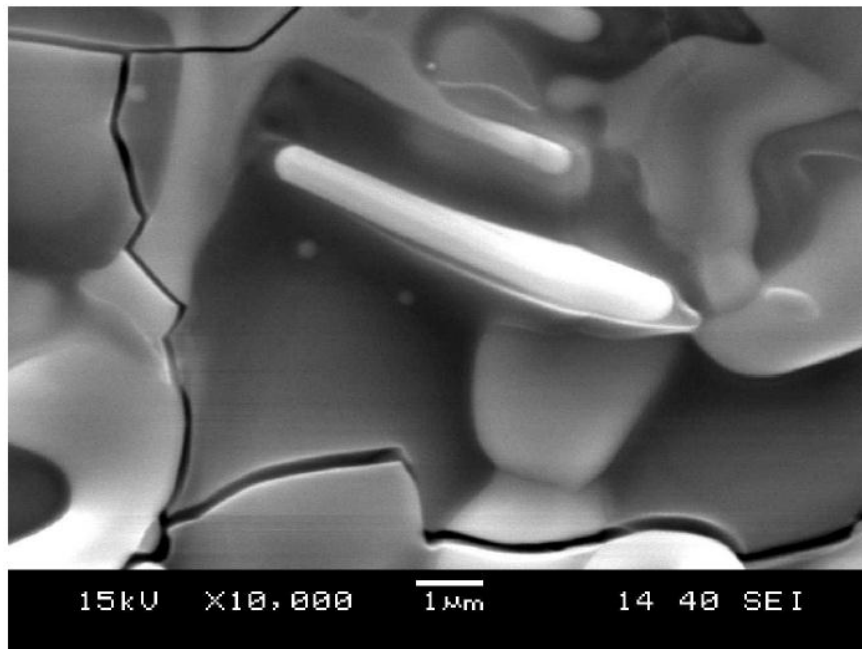
(c)



(d)



(e)



(f)

Figure 4.5 SEM micrographs of  $K_2La_2Ti_3O_{10}$  thin films at different magnifications.

### 4.3.3 Elemental Analysis and XPS Results

The result of the elemental analysis solutions showed in Figure 4.6. According to the results, K, La, Ti, O elements, substrate material (Si) and buffer layer (Ce) were determined. The elemental analysis results and XRD were consentaneously.

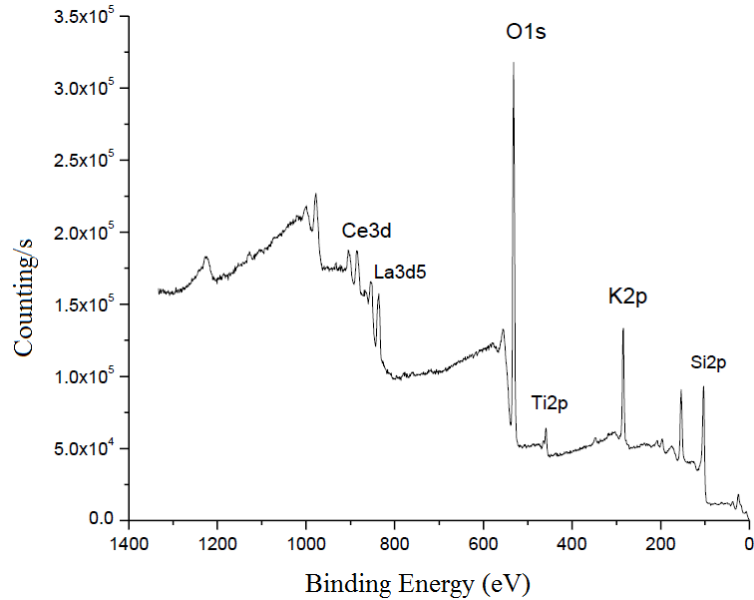


Figure 4.6 The spectrum of  $K_2La_2Ti_3O_{10}$  from XPS.

### 4.3.4 Surface Roughness - AFM Analysis

The surfaces are granular. The average roughness of the 2 specimens was found 445.69 and 900.27 nm, respectively. When the roughness is increased, films become a good photocatalyst.

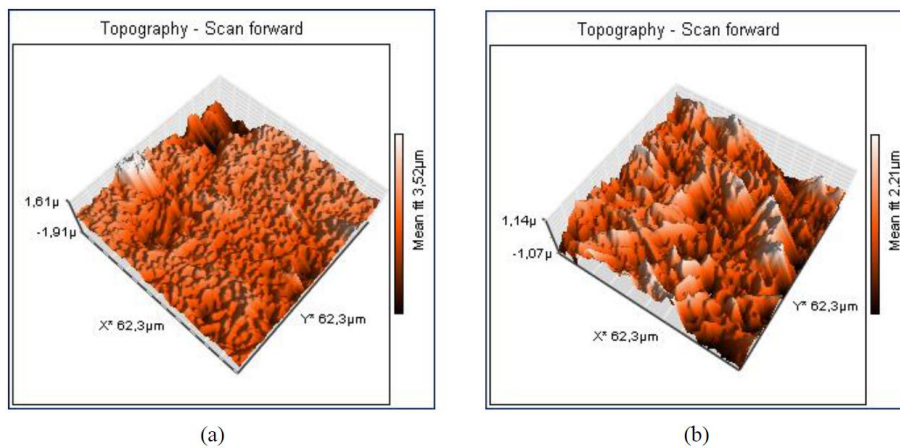


Figure 4.7 AFM images of KLTO films from different areas.

#### 4.4 Photocatalytic Degradation Results

For every catalyst, the beakers were filled till 25 ml and it was placed on the testing apparatus as shown in Figure 4.8. All photocatalytic experiments were examined by ATLAS SUNTEST CPS+.

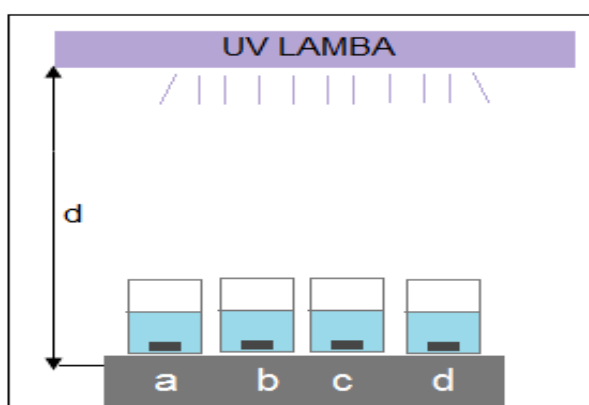


Figure 4.8 Schematic experiment apparatus (Nimetoğlu, 2011).

To determine effective pH of the process, different pH values were carried out: acidic (pH = 3), neutral (pH = 7) and alkali (pH = 10) conditions at different initial pollutant concentrations. In cyanide studies, pH was examined at alkali conditions because of the toxic effect at low pH values.

The effect of different pH values and concentrations on removal efficiencies for phenol, cyanide and methylene blue are given in tables below as a function of light intensity. The experiments were done with KLTO thin film, and 0.01 g TiO<sub>2</sub> nanopowder (Sigma-Aldrich). To see the difference and to make a deduction, an arbitration specimen was carried out for every experiment. The testing sets were planned as 1, 2, 3, 4 and 5 hours. Some experiments below were given in detail. The replications for the performance tests were designed as 5 hours.

##### 4.4.1 Photodegradation Results of Phenol

In this step, some experiments were given in detail. Last table of this stage gave a summary of all experiments. Experiments were given with KLTO and TiO<sub>2</sub>. To find out the efficiency of thin films, a reference experiment was done to each pollutant

and in each step.  $\text{TiO}_2$  is a commercial and bought from Sigma - Aldrich. The full product name is Titanium (IV) oxide. The size of nano particle is 21 nm. KLTO was not treating phenol as well as  $\text{TiO}_2$ .

Table 4.6 gives details about phenol degradation efficiencies under 10 mg/l initial concentration,  $250 \text{ W/m}^2$  light intensity and pH at 7 conditions. Figure 4.9 and 4.10 illustrate graphically the variation of the concentration vs. time and efficiency vs. time of phenol.

Table 4.6 The efficiencies of phenol experiment (10 mg/l,  $250 \text{ W/m}^2$  and pH = 7)

	<b>Time</b>	<b>Initial Concentration (mg/l)</b>	<b>Output Concentration (mg/l)</b>	<b>Efficiency (%)</b>
<b>KLTO</b>	1 h	10	8.43	15.70
	2 h	10	7.61	23.90
	3 h	10	7.79	22.10
	4 h	10	8.04	19.60
	5 h	10	8.24	17.60
	15 h	10	7.02	29.80
<b>Reference</b>	1 h	10	9.97	0.30
	2 h	10	9.6	4.00
	3 h	10	9.62	3.80
	4 h	10	9.61	3.90
	5 h	10	9.64	3.60
	15 h	10	9.47	5.30
<b><math>\text{TiO}_2</math></b>	1 h	10	1.64	83.60
	2 h	10	<0.14	98.60
	3 h	10	<0.14	98.60
	4 h	10	<0.14	98.60
	5 h	10	<0.14	98.60
	15 h	10	<0.14	98.60

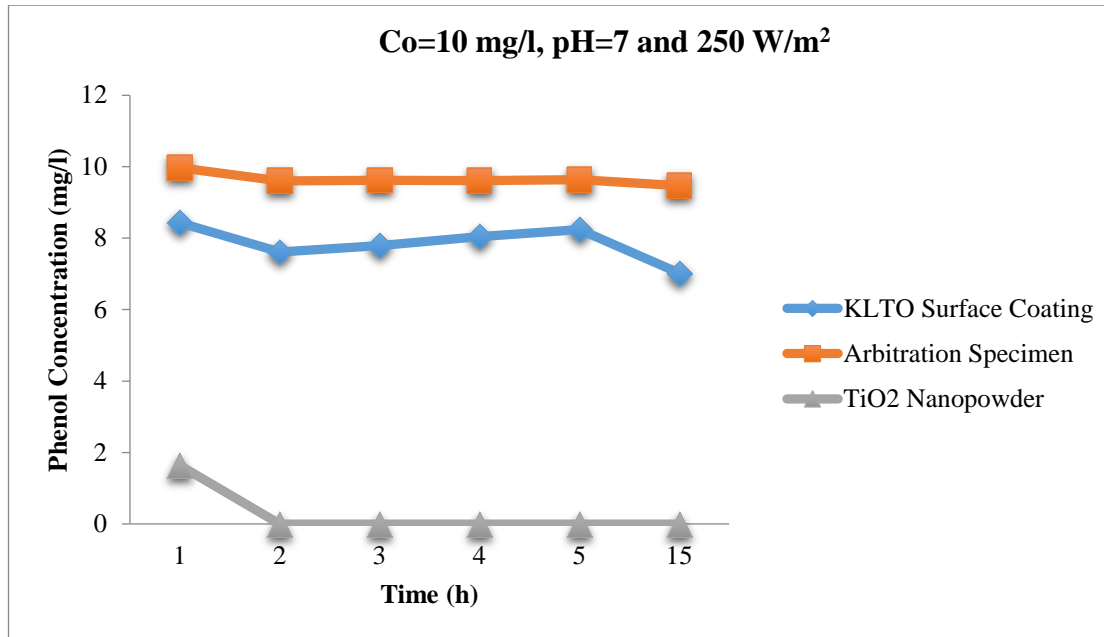


Figure 4.9 Phenol concentration vs. time results ( $C_o=10$  mg/l,  $250$  W/m<sup>2</sup> and pH = 7).

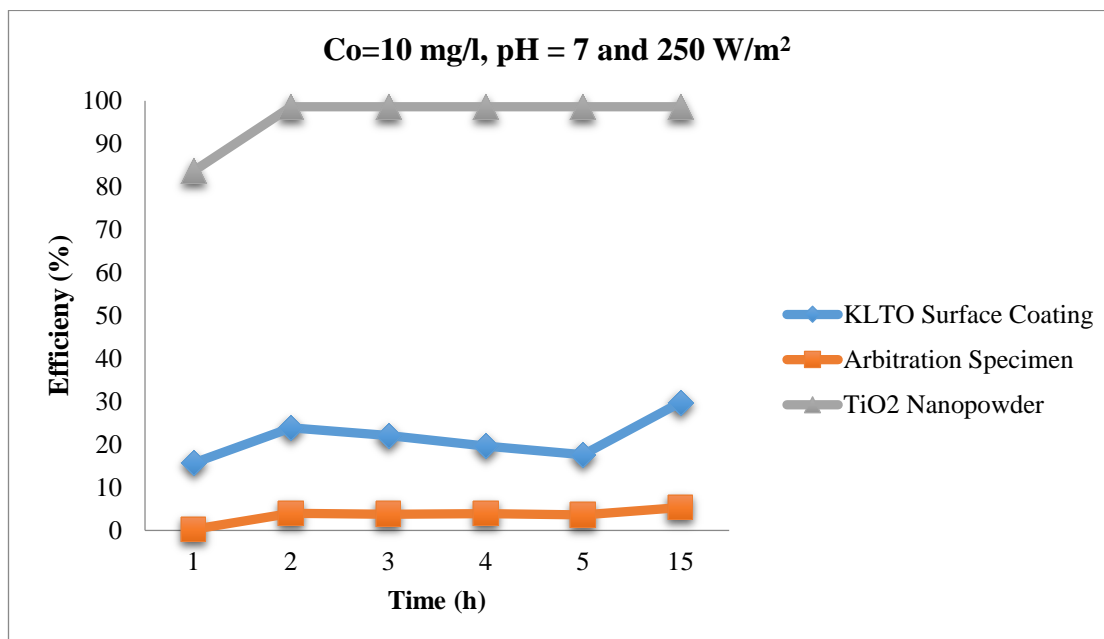


Figure 4.10 Phenol removal efficiencies (%) ( $C_o = 10$  mg/l,  $250$  W/m<sup>2</sup> and pH = 7).

Table 4.7 informs phenol degradation efficiencies under 100 mg/l initial concentration, 250 W/m<sup>2</sup> light intensity and pH at 7 conditions. Figure 4.11 and 4.12 demonstrate the alteration of the concentration vs. time and efficiency vs. time of phenol. A slight change can be seen at reference (arbitration) specimen (without catalyst) during the test. That is why; 5 - hour test results have been observed for it.

Table 4.7 The efficiencies of phenol experiment (100 mg/l, 250 W/m<sup>2</sup> and pH = 7)

	<b>Time</b>	<b>Initial Concentration (mg/l)</b>	<b>Output Concentration (mg/l)</b>	<b>Efficiency (%)</b>
<b>KLTO</b>	1 h	100	94.97	5.03
	2 h	100	94.99	5.01
	3 h	100	89.23	10.77
	4 h	100	87.74	12.26
	5 h	100	71.16	28.84
<b>Reference</b>	5 h	100	85.45	14.55
<b>TiO<sub>2</sub></b>	1 h	100	19.75	80.25
	2 h	100	6.44	93
	3 h	100	0	56
	4 h	100	0	100
	5 h	100	0	100

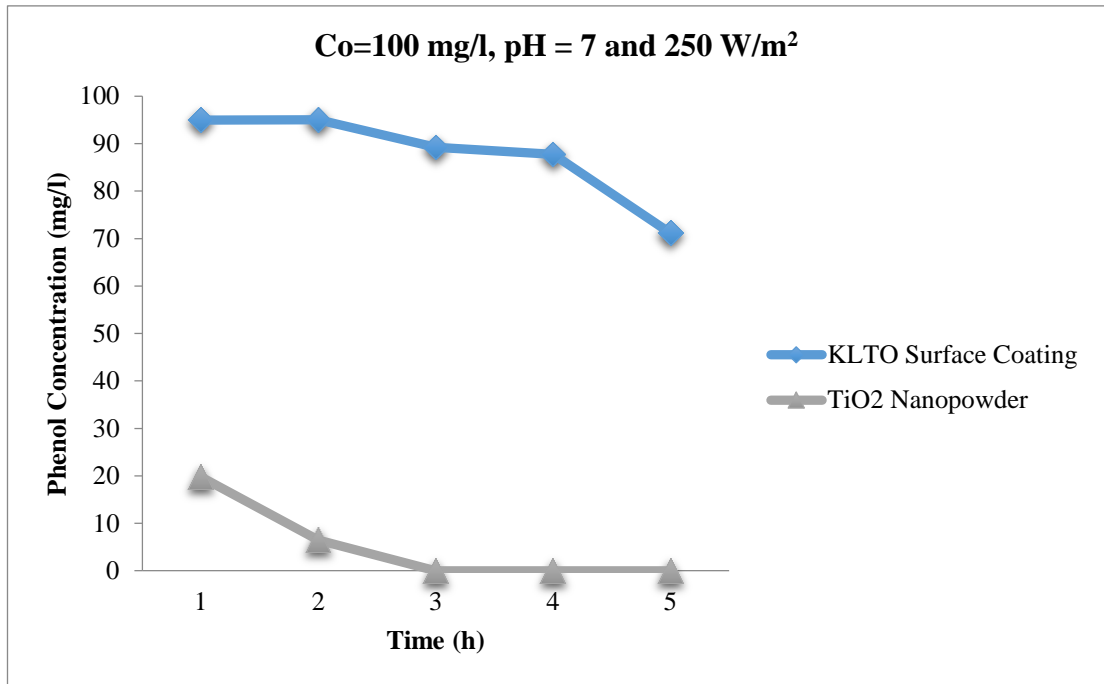


Figure 4.11 Phenol concentration vs. time results (Co=100 mg/l, 250 W/m<sup>2</sup>, pH=7).

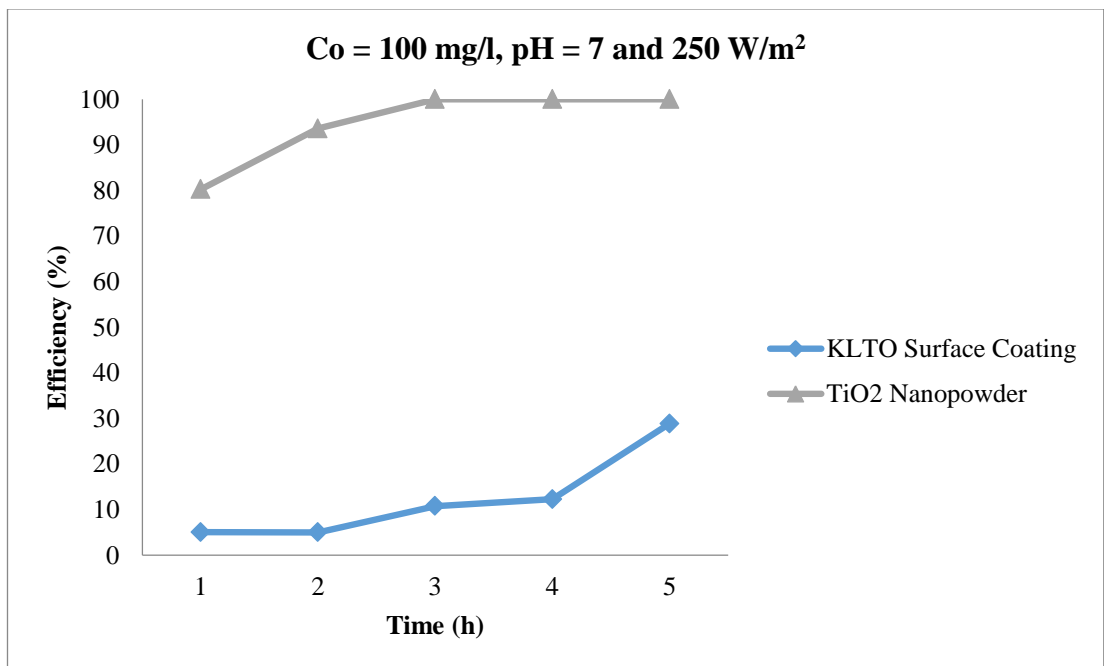


Figure 4.12 Phenol removal efficiencies (%) (Co = 100 mg/l, 250 W/m<sup>2</sup> and pH = 7).



Table 4.8 gives information about phenol degradation efficiencies under 10 mg/l initial concentration, 750 W/m<sup>2</sup> light intensity and pH at 7 conditions. Figure 4.13 and 4.14 mention data about the change of the concentration vs. time and efficiency vs. time of phenol. To see the change owing to the light intensity, 750 W/m<sup>2</sup> is performed.

Table 4.8 The efficiencies of phenol experiment (10 mg/l, 750 W/m<sup>2</sup> and pH = 7)

	<b>Time</b>	<b>Initial Concentration (mg/l)</b>	<b>Output Concentration (mg/l)</b>	<b>Efficiency (%)</b>
<b>KLTO</b>	1 h	10	8.99	10.10
	2 h	10	8.74	12.60
	3 h	10	8.1	19.00
	4 h	10	7.83	21.70
	5 h	10	7.09	29.10
<b>Reference</b>	1 h	10	9.1	9.00
	2 h	10	9.76	2.40
	3 h	10	8.72	12.80
	4 h	10	9.49	5.10
	5 h	10	8.94	10.60
<b>TiO<sub>2</sub></b>	1 h	10	6.00	40.00
	2 h	10	5.17	48.30
	3 h	10	4.11	58.90
	4 h	10	<0.14	98.60
	5 h	10	<0.14	98.60

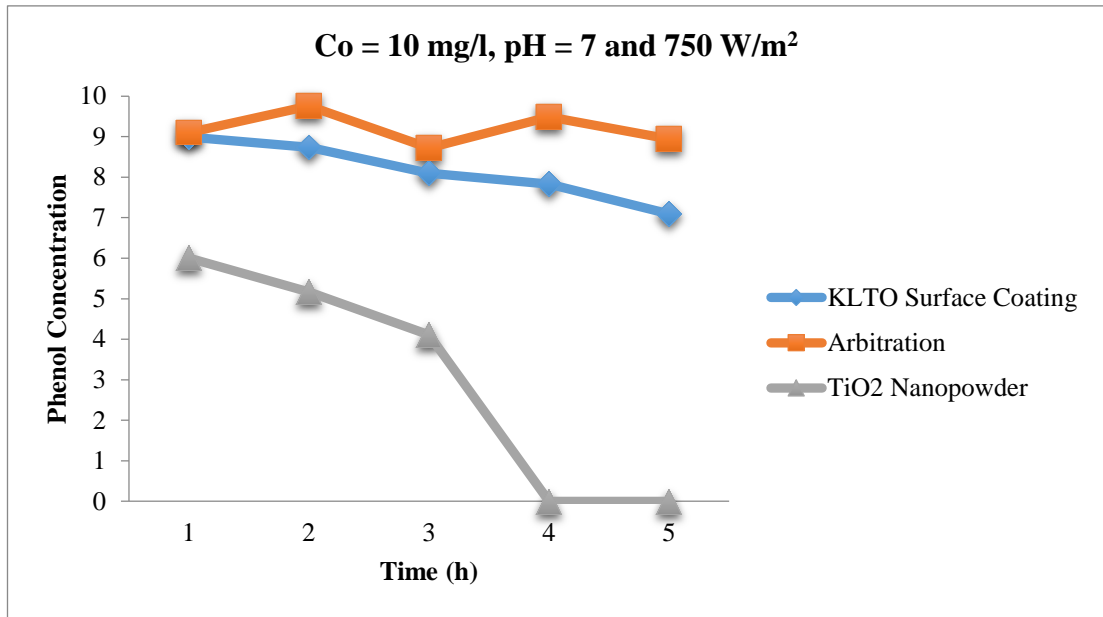


Figure 4.13 Phenol concentration vs. time results (Co=10 mg/l, 750 W/m<sup>2</sup> and pH = 7).

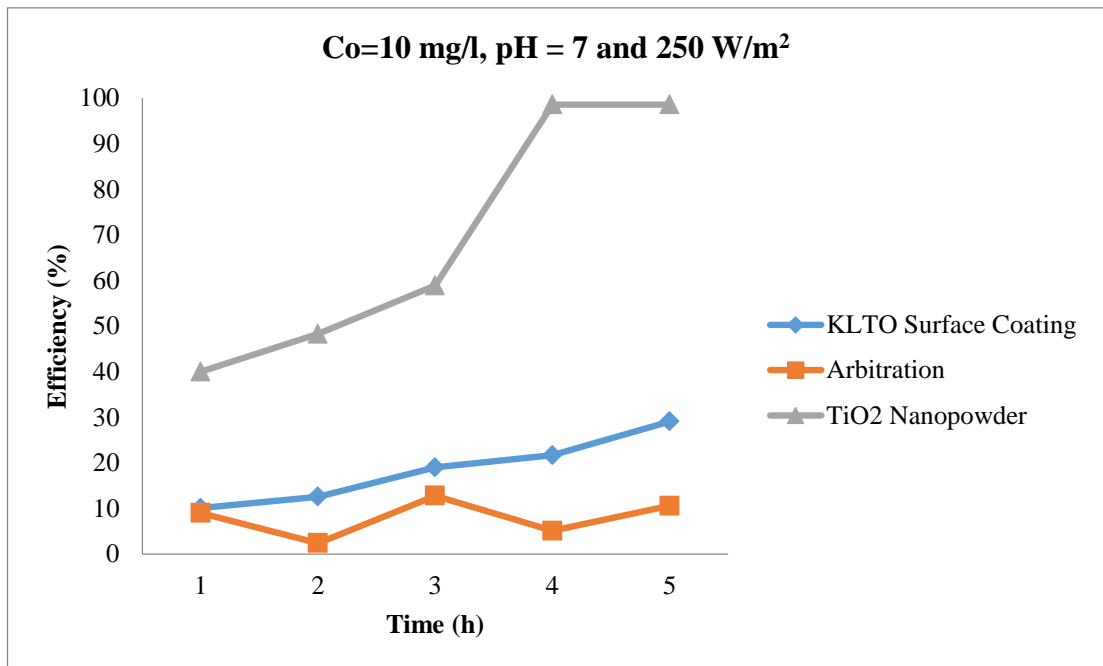


Figure 4.14 Phenol removal efficiencies (%) (Co = 10 mg/l, 750 W/m<sup>2</sup> and pH = 7).

Table 4.9 shows different conditions about phenol degradation efficiencies under 100 mg/l initial concentration, 750 W/m<sup>2</sup> light intensity and pH at 7 conditions. Figure 4.15 and 4.16 mention data about the change of the concentration vs. time and efficiency vs. time of phenol. Now, it is aimed to see the differences of the efficiency by the modification of the initial concentration.

Table 4.9 The efficiencies of phenol experiment (100 mg/l, 750 W/m<sup>2</sup> and pH = 7)

	<b>Time</b>	<b>Initial Concentration (mg/l)</b>	<b>Output Concentration (mg/l)</b>	<b>Efficiency (%)</b>
<b>KLTO</b>	1 h	100	98.97	1.03
	2 h	100	96.88	3.12
	3 h	100	97.23	2.77
	4 h	100	93.27	6.73
	5 h	100	88.16	11.84
<b>Reference</b>	5 h	100	94.45	5.55
<b>TiO<sub>2</sub></b>	1 h	100	14.84	85.16
	2 h	100	7.64	92.36
	3 h	100	1.13	98.87
	4 h	100	0	100
	5 h	100	0	100

During the phenol experiments, the color of the water changed from colorless or light pink. The light effect creates these color changes. Phenol is a white crystalline mass and if it exposes to light, it turns red or pink.

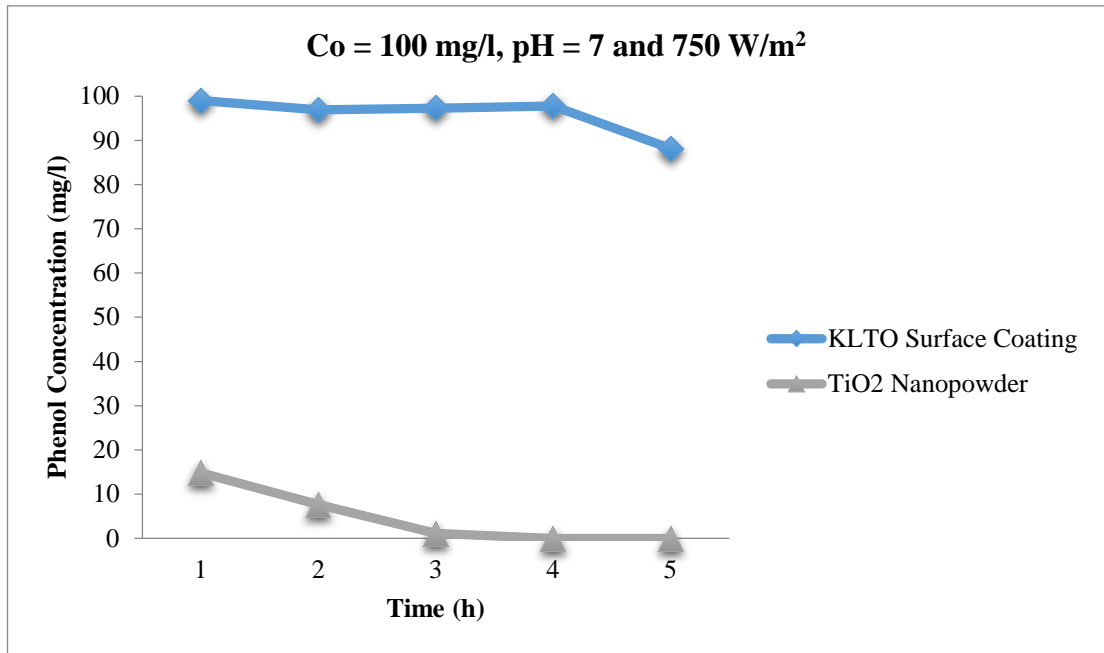


Figure 4.15 Phenol concentration vs. time results (Co=100 mg/l, 750 W/m<sup>2</sup> and pH = 7).

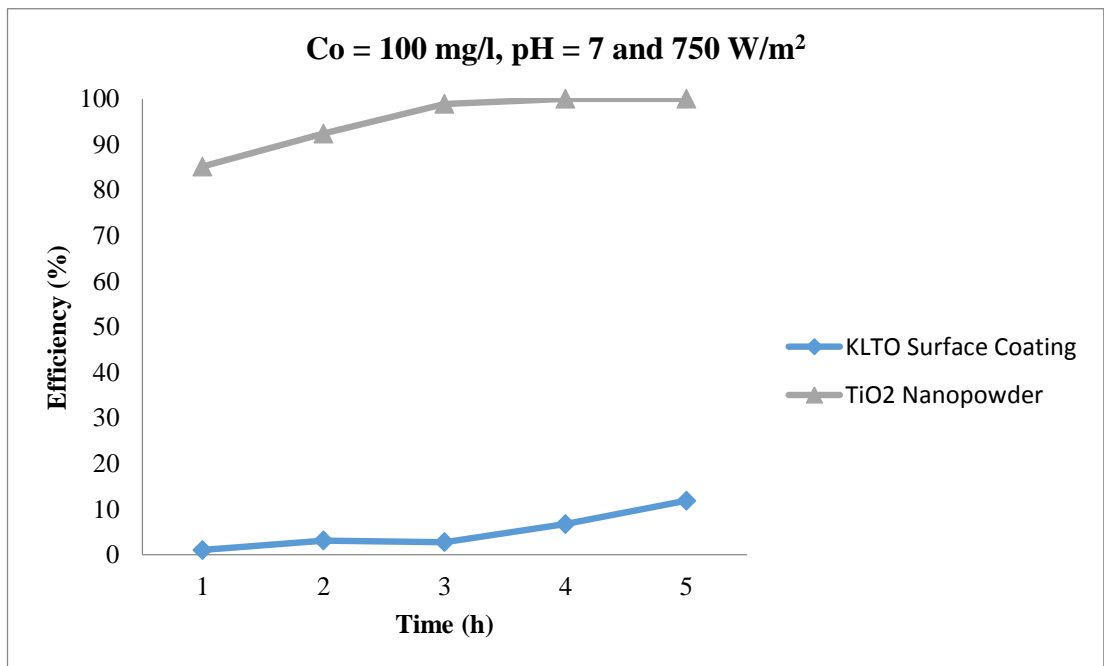


Figure 4.16 Phenol removal efficiencies (%) (Co = 100 mg/l, 750 W/m<sup>2</sup> and pH = 7).

Table 4.10 Summary of phenol experiments

Time (h)	Photocatalytic degradation results (mg/l)																							
	pH = 7												pH = 7											
	10 mg/l phenol						100 mg/l phenol						10 mg/l phenol						100 mg/l phenol					
	KLTO		Arbit.		TiO <sub>2</sub>		KLTO		Arbit.		TiO <sub>2</sub>		KLTO		Arbit.		TiO <sub>2</sub>		KLTO		Arbit.		TiO <sub>2</sub>	
	1 <sup>st</sup>	2 <sup>nd</sup>	1 <sup>st</sup>	2 <sup>nd</sup>	1 <sup>st</sup>	2 <sup>nd</sup>	1 <sup>st</sup>	2 <sup>nd</sup>	1 <sup>st</sup>	2 <sup>nd</sup>	1 <sup>st</sup>	2 <sup>nd</sup>	1 <sup>st</sup>	2 <sup>nd</sup>	1 <sup>st</sup>	2 <sup>nd</sup>	1 <sup>st</sup>	2 <sup>nd</sup>	1 <sup>st</sup>	2 <sup>nd</sup>	1 <sup>st</sup>	2 <sup>nd</sup>	1 <sup>st</sup>	2 <sup>nd</sup>
1	8.43		9.97		1.64		94.97				19.75		8.99		9.1		6.00		98.97				14.84	
2	7.61		9.6		<0.14		94.99				6.44		8.74		9.76		5.17		96.88				7.64	
3	7.79		9.62		<0.14		89.23				0		8.1		8.72		4.11		97.23				1.13	
4	8.04		9.61		<0.14		87.74				0		7.83		9.49		<0.14		93.27				0	
5	8.24	8,22	9.64	8,15	<0.14	0,32	71.16	74.76	85.45	81.16	0	3.87	7.09	6,69	8.94	6,22	<0.14	0,12	88.16	59.96	94.45	63.37	0	0
15	7.02		9.47		<0.14																			
	250 W/m <sup>2</sup>												750 W/m <sup>2</sup>											
	pH = 10												pH = 10											
	10 mg/l phenol						100 mg/l phenol						10 mg/l phenol						100 mg/l phenol					
	KLTO		Arbit.		TiO <sub>2</sub>		KLTO		Arbit.		TiO <sub>2</sub>		KLTO		Arbit.		TiO <sub>2</sub>		KLTO		Arbit.		TiO <sub>2</sub>	
	1 <sup>st</sup>	2 <sup>nd</sup>	1 <sup>st</sup>	2 <sup>nd</sup>	1 <sup>st</sup>	2 <sup>nd</sup>	1 <sup>st</sup>	2 <sup>nd</sup>	1 <sup>st</sup>	2 <sup>nd</sup>	1 <sup>st</sup>	2 <sup>nd</sup>	1 <sup>st</sup>	2 <sup>nd</sup>	1 <sup>st</sup>	2 <sup>nd</sup>	1 <sup>st</sup>	2 <sup>nd</sup>	1 <sup>st</sup>	2 <sup>nd</sup>	1 <sup>st</sup>	2 <sup>nd</sup>	1 <sup>st</sup>	2 <sup>nd</sup>
1							94.97				19.75								98.97				14.84	
2							94.99				6.44								96.88				7.64	
3							89.23				0								87.23				1.13	
4							87.74				0								74.75				0	
5	7.61	7.82	7.38	7.42	0.17	0.19	85.45	80.39	71.16	80.17	0	5.1	7.65	6.39	6.9	6.68	0.14	0.15	65.58	60.14	67.23	63.38	0	0.1
	250 W/m <sup>2</sup>												750 W/m <sup>2</sup>											

Table 4.11 Summary of phenol degradation efficiencies (%)

Time (h)		Photocatalytic degradation efficiencies (%)																							
		pH = 7												pH = 7											
		10 mg/l phenol						100 mg/l phenol						10 mg/l phenol						100 mg/l phenol					
		KLTO		Arbit.		TiO <sub>2</sub>		KLTO		Arbit.		TiO <sub>2</sub>		KLTO		Arbit.		TiO <sub>2</sub>		KLTO		Arbit.		TiO <sub>2</sub>	
1 <sup>st</sup>	2 <sup>nd</sup>	1 <sup>st</sup>	2 <sup>nd</sup>	1 <sup>st</sup>	2 <sup>nd</sup>	1 <sup>st</sup>	2 <sup>nd</sup>	1 <sup>st</sup>	2 <sup>nd</sup>	1 <sup>st</sup>	2 <sup>nd</sup>	1 <sup>st</sup>	2 <sup>nd</sup>	1 <sup>st</sup>	2 <sup>nd</sup>	1 <sup>st</sup>	2 <sup>nd</sup>	1 <sup>st</sup>	2 <sup>nd</sup>	1 <sup>st</sup>	2 <sup>nd</sup>	1 <sup>st</sup>	2 <sup>nd</sup>		
5	17.6	17.8	3.6	18.5	99.2	96.8	28.84	18.84	14.55	25.24	100	96.13	29.1	37.8	10.6	33.1	99	98.8	11.84	40.04	5.55	36.63	100	99.86	
250 W/m <sup>2</sup>												750 W/m <sup>2</sup>													
Time (h)		Photocatalytic degradation efficiencies (%)																							
		pH = 10												pH = 10											
		10 mg/l phenol						100 mg/l phenol						10 mg/l phenol						100 mg/l phenol					
		KLTO		Arbit.		TiO <sub>2</sub>		KLTO		Arbit.		TiO <sub>2</sub>		KLTO		Arbit.		TiO <sub>2</sub>		KLTO		Arbit.		TiO <sub>2</sub>	
1 <sup>st</sup>	2 <sup>nd</sup>	1 <sup>st</sup>	2 <sup>nd</sup>	1 <sup>st</sup>	2 <sup>nd</sup>	1 <sup>st</sup>	2 <sup>nd</sup>	1 <sup>st</sup>	2 <sup>nd</sup>	1 <sup>st</sup>	2 <sup>nd</sup>	1 <sup>st</sup>	2 <sup>nd</sup>	1 <sup>st</sup>	2 <sup>nd</sup>	1 <sup>st</sup>	2 <sup>nd</sup>	1 <sup>st</sup>	2 <sup>nd</sup>	1 <sup>st</sup>	2 <sup>nd</sup>	1 <sup>st</sup>	2 <sup>nd</sup>		
5	23.9	21.8	26.2	25.8	98.3	98.1	14.55	19.61	28.84	19.83	100	94.9	23.5	36.1	31	33.2	98.8	98.5	34.42	39.86	11.84	36.62	100	99.9	
250 W/m <sup>2</sup>												750 W/m <sup>2</sup>													

#### 4.4.2 Photodegradation Results of Methylene Blue

In this step, one of the methylene blue experiments which pH is 3 was given in detail. Last table of this stage gave a summary of all experiments. Table 4.12 and Table 4.13 demonstrate methylene blue degradation efficiencies in the light of  $10^{-5}$  M initial concentration, pH at 3 and 250 or 750 W/m<sup>2</sup> light intensity. Figure 4.17 and 4.18 give information about the change of the absorbance vs. time and efficiency vs. time of methylene blue.

Table 4.12 The efficiencies of methylene blue experiment ( $10^{-5}$  M, 250 W/m<sup>2</sup> and pH = 3)

	<b>Time</b>	<b>Initial Absorbance</b>	<b>Output Absorbance</b>	<b>Efficiency (%)</b>
<b>KLTO</b>	1 h	0.765	0.594	22.35
	2 h	0.765	0.510	33.33
	3 h	0.765	0.440	42.48
	4 h	0.765	0.330	56.86
	5 h	0.765	0.290	62.09
	15 h	0.765	0.170	77.78
<b>Reference</b>	1 h	0.765	0.650	15.03
	2 h	0.765	0.540	29.41
	3 h	0.765	0.490	35.95
	4 h	0.765	0.448	41.44
	5 h	0.765	0.418	45.36
	15 h	0.765	0.375	50.98
<b>TiO<sub>2</sub></b>	1 h	0.765	0 (in 16 min.)	100
	2 h	0.765	0	100
	3 h	0.765	0	100
	4 h	0.765	0	100
	5 h	0.765	0	100
	15 h	0.765	0	100

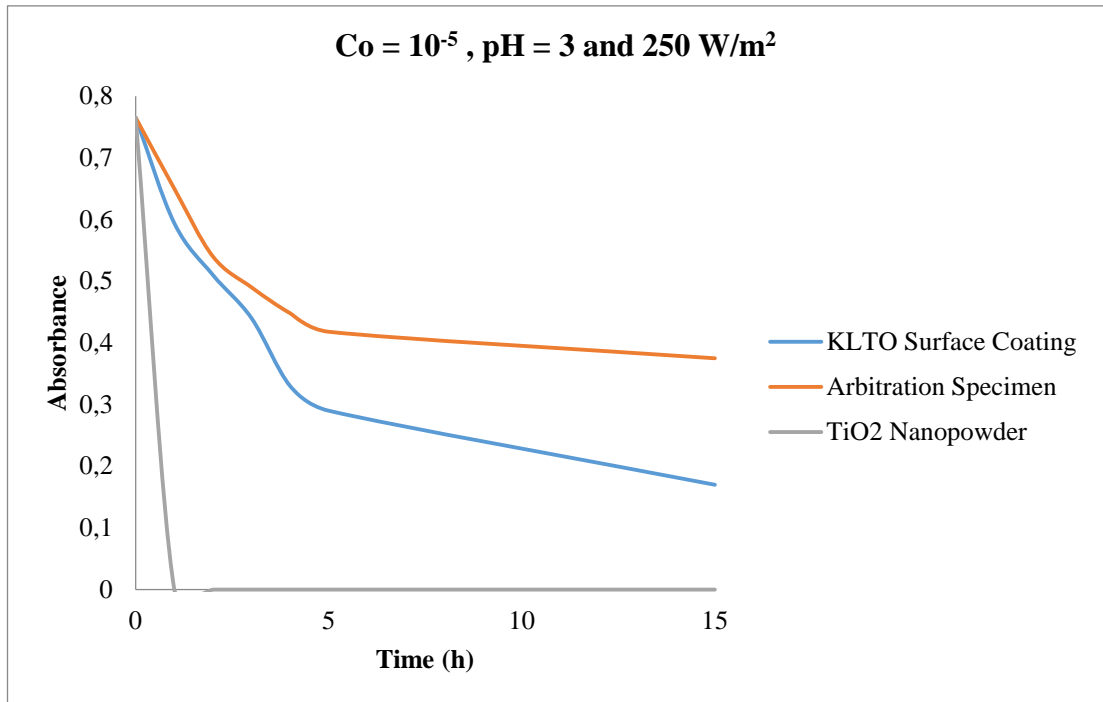


Figure 4.17 Methylene blue removal absorbance vs. time ( $Co = 10^{-5}$  M,  $250 \text{ W/m}^2$  and  $\text{pH} = 3$ ).

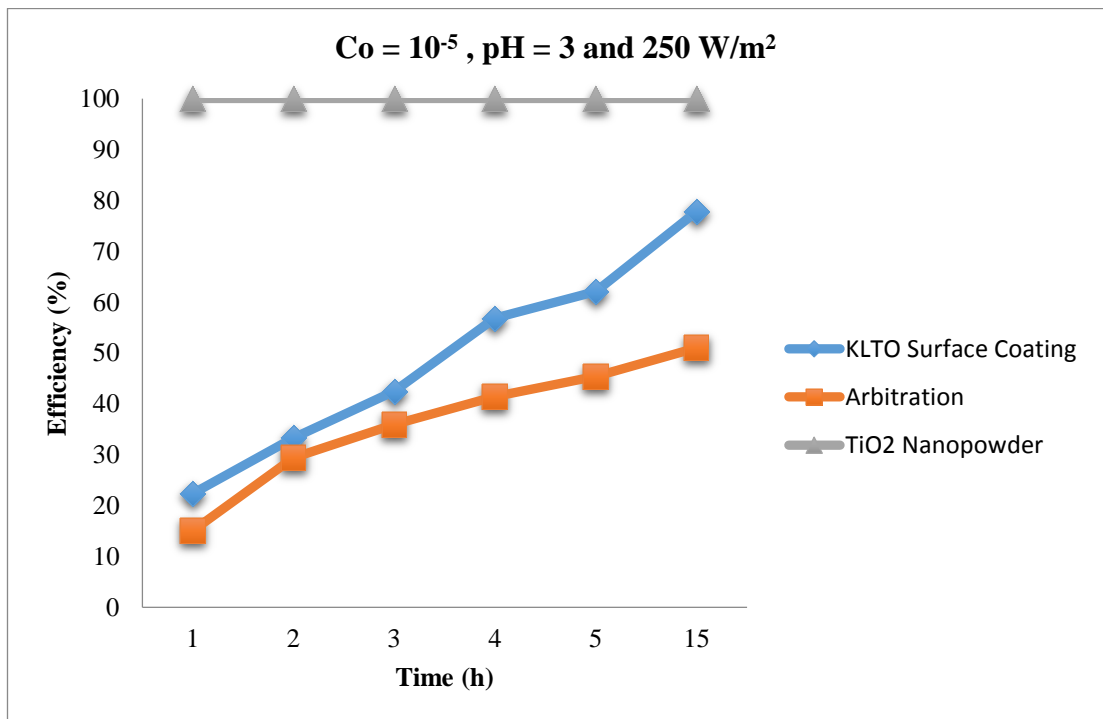


Figure 4.18 Methylene blue removal efficiencies (%) ( $Co = 10^{-5}$  M,  $250 \text{ W/m}^2$  and  $\text{pH} = 3$ ).



Table 4.13 shows methylene blue degradation efficiencies at 750 W/m<sup>2</sup> light intensity.

Table 4.13 The efficiencies of methylene blue experiment (10<sup>-5</sup> M, 750 W/m<sup>2</sup> and pH = 5)

	<b>Time</b>	<b>Initial Absorbance</b>	<b>Output Absorbance</b>	<b>Efficiency (%)</b>
<b>KLTO</b>	1 h	0.765	0.431	43.66
	2 h	0.765	0.033	95.69
<b>Reference</b>	1 h	0.765	0.603	21.18
	2 h	0.765	0.357	53.33
<b>TiO<sub>2</sub></b>	1 h	0.765	0	100
	2 h	0.765	0	100

Table 4.14 Summary of methylene blue experiments

Time (h)	Photocatalytic degradation results (as absorbance)																	
	pH = 3						pH = 3						pH = 7					
	10 <sup>-5</sup> M methylene blue																	
	KLTO		Arbit.		TiO <sub>2</sub>		KLTO		Arbit.		TiO <sub>2</sub>		KLTO		Arbit.		TiO <sub>2</sub>	
	1 <sup>st</sup>	2 <sup>nd</sup>	1 <sup>st</sup>	2 <sup>nd</sup>	1 <sup>st</sup>	2 <sup>nd</sup>	1 <sup>st</sup>	2 <sup>nd</sup>	1 <sup>st</sup>	2 <sup>nd</sup>	1 <sup>st</sup>	2 <sup>nd</sup>	1 <sup>st</sup>	2 <sup>nd</sup>	1 <sup>st</sup>	2 <sup>nd</sup>	1 <sup>st</sup>	2 <sup>nd</sup>
0	0.765	0.765	0.765	0.765	0.765	0.765	0.765	0.765	0.765	0.765	0.765	0.765	0.765	0.765	0.765	0.765	0.765	0.765
1	0.594		0.65		0	0	0.431		0.603		0							
2	0.51		0.54		0	0												
3	0.44		0.49		0	0												
4	0.33		0.448		0	0												
5	0.290	0.261	0.418	0.243	0	0	0.033	0.031	0.357	0.281	0	0	0.265	0.269	0.433	0.411	0	0
15	0.17		0.375		0	0												
	250 W/m <sup>2</sup>						750 W/m <sup>2</sup>						250 W/m <sup>2</sup>					
Time (h)	Photocatalytic degradation results (as absorbance)																	
	pH = 7						pH = 10						pH = 10					
	10 <sup>-5</sup> M methylene blue																	
	KLTO		Arbit.		TiO <sub>2</sub>		KLTO		Arbit.		TiO <sub>2</sub>		KLTO		Arbit.		TiO <sub>2</sub>	
	1 <sup>st</sup>	2 <sup>nd</sup>	1 <sup>st</sup>	2 <sup>nd</sup>	1 <sup>st</sup>	2 <sup>nd</sup>	1 <sup>st</sup>	2 <sup>nd</sup>	1 <sup>st</sup>	2 <sup>nd</sup>	1 <sup>st</sup>	2 <sup>nd</sup>	1 <sup>st</sup>	2 <sup>nd</sup>	1 <sup>st</sup>	2 <sup>nd</sup>	1 <sup>st</sup>	2 <sup>nd</sup>
0	0.765	0.765	0.765	0.765	0.765	0.765	0.765	0.765	0.765	0.765	0.765	0.765	0.765	0.765	0.765	0.765	0.765	0.765
5	0.04	0.033	0.203	0.197	0	0	0.067	0.055	0.154	0.213	0	0	0.001	0.012	0.161	0.162	0	0
	750 W/m <sup>2</sup>						250 W/m <sup>2</sup>						750 W/m <sup>2</sup>					

Table 4.15 Summary of methylene blue degradation efficiencies (%)

Time (h)	Photocatalytic degradation efficiencies (%)																	
	pH = 3						pH = 3						pH = 7					
	10 <sup>-5</sup> M methylene blue																	
	KLTO		Arbit.		TiO <sub>2</sub>		KLTO		Arbit.		TiO <sub>2</sub>		KLTO		Arbit.		TiO <sub>2</sub>	
1 <sup>st</sup>	2 <sup>nd</sup>	1 <sup>st</sup>	2 <sup>nd</sup>	1 <sup>st</sup>	2 <sup>nd</sup>	1 <sup>st</sup>	2 <sup>nd</sup>	1 <sup>st</sup>	2 <sup>nd</sup>	1 <sup>st</sup>	2 <sup>nd</sup>	1 <sup>st</sup>	2 <sup>nd</sup>	1 <sup>st</sup>	2 <sup>nd</sup>	1 <sup>st</sup>	2 <sup>nd</sup>	
5	62.09	65.88	45.36	68.24	100	100	95.69	96.08	53.33	63.33	100	100	65.36	64.84	43.40	46.27	100	100
	250 W/m <sup>2</sup>						750 W/m <sup>2</sup>						250 W/m <sup>2</sup>					
Time (h)	Photocatalytic degradation efficiencies (%)																	
	pH = 7						pH = 10						pH = 10					
	10 <sup>-5</sup> M methylene blue																	
	KLTO		Arbit.		TiO <sub>2</sub>		KLTO		Arbit.		TiO <sub>2</sub>		KLTO		Arbit.		TiO <sub>2</sub>	
1 <sup>st</sup>	2 <sup>nd</sup>	1 <sup>st</sup>	2 <sup>nd</sup>	1 <sup>st</sup>	2 <sup>nd</sup>	1 <sup>st</sup>	2 <sup>nd</sup>	1 <sup>st</sup>	2 <sup>nd</sup>	1 <sup>st</sup>	2 <sup>nd</sup>	1 <sup>st</sup>	2 <sup>nd</sup>	1 <sup>st</sup>	2 <sup>nd</sup>	1 <sup>st</sup>	2 <sup>nd</sup>	
5	94.77	95.69	73.46	74.25	100	100	91.24	92.81	79.93	72.16	100	100	99.87	98.43	78.95	78.82	100	100
	750 W/m <sup>2</sup>						250 W/m <sup>2</sup>						750 W/m <sup>2</sup>					

#### 4.4.3 Photodegradation Results of Cyanide

In this step, two cyanide experiments were given in detail. Last table of this stage gave a summary of all experiments. Table 4.16 and Table 4.17 give information about cyanide degradation efficiencies at 100 mg/l initial concentration, pH at 10 and 250 or 750 W/m<sup>2</sup> light intensity. Figure 4.19 and 4.20 illustrate the initial concentration vs. time and efficiency vs. time of cyanide at 250 W/m<sup>2</sup>.

Table 4.16 The efficiencies of cyanide experiments (100 mg/l, 250 W/m<sup>2</sup> and pH = 10)

	<b>Time</b>	<b>Initial Concentration (mg/l)</b>	<b>Output Concentration (mg/l)</b>	<b>Efficiency (%)</b>
<b>KLTO</b>	1 h	100	42	58.00
	2 h	100	33.6	66.40
	3 h	100	20.4	79.60
	4 h	100	18.8	81.20
	5 h	100	9.6	90.40
<b>Reference</b>	1 h	100	42.8	57.20
	2 h	100	41.2	58.80
	3 h	100	32	68.00
	4 h	100	32.8	67.20
	5 h	100	27.6	72.40
<b>TiO<sub>2</sub></b>	1 h	100	31.2	68.80
	2 h	100	16.12	83.88
	3 h	100	9.2	90.80
	4 h	100	0.468	99.53
	5 h	100	0.68	99.32

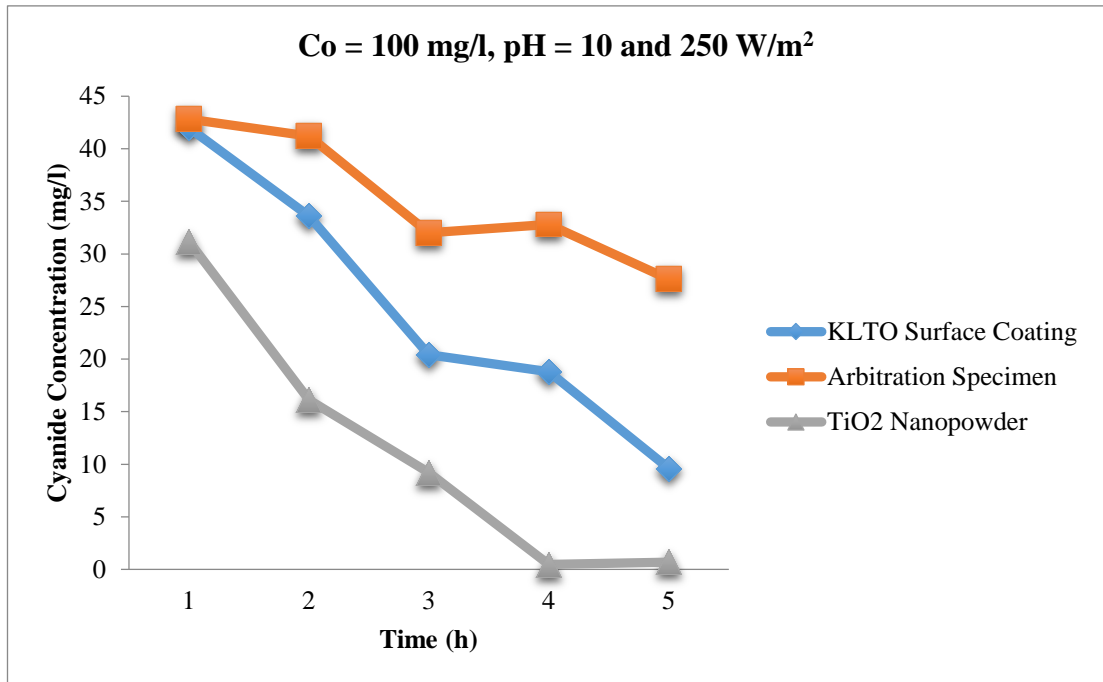


Figure 4.19 Cyanide concentration vs. time results ( $C_o=100$  mg/l,  $250$  W/m<sup>2</sup> and pH = 10).

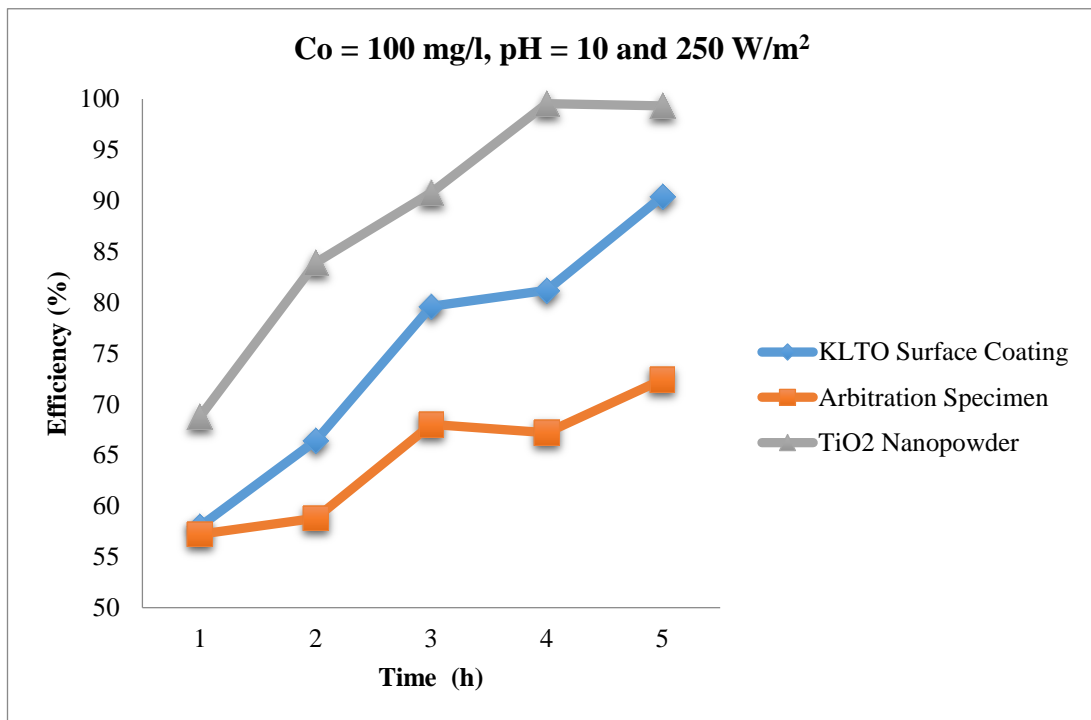


Figure 4.20 Cyanide removal efficiencies (%) ( $C_o = 100$  mg/l,  $250$  W/m<sup>2</sup> and pH = 10).

Cyanide removal efficiencies are given in Table 4.17. Figure 4.21 and 4.22 give detail about the change of the initial concentration vs. time and efficiency vs. time of cyanide at 750 W/m<sup>2</sup>.

Table 4.17 The efficiencies of cyanide experiments (100 mg/l, 750 W/m<sup>2</sup> and pH = 10)

	<b>Time</b>	<b>Initial Concentration (mg/l)</b>	<b>Output Concentration (mg/l)</b>	<b>Efficiency (%)</b>
<b>KLTO</b>	1 h	100	37.2	62.80
	2 h	100	29.2	70.80
	3 h	100	26.4	73.60
	4 h	100	8	92.00
	5 h	100	0.128	99.87
<b>Reference</b>	1 h	100	53.2	46.80
	2 h	100	46.8	53.20
	3 h	100	36	64.00
	4 h	100	14.80	85.20
	5 h	100	12.40	87.60
<b>TiO<sub>2</sub></b>	1 h	100	19.6	80.40
	2 h	100	18	82.00
	3 h	100	0.112	99.89
	4 h	100	0.016	99.98
	5 h	100	0.24	99.76

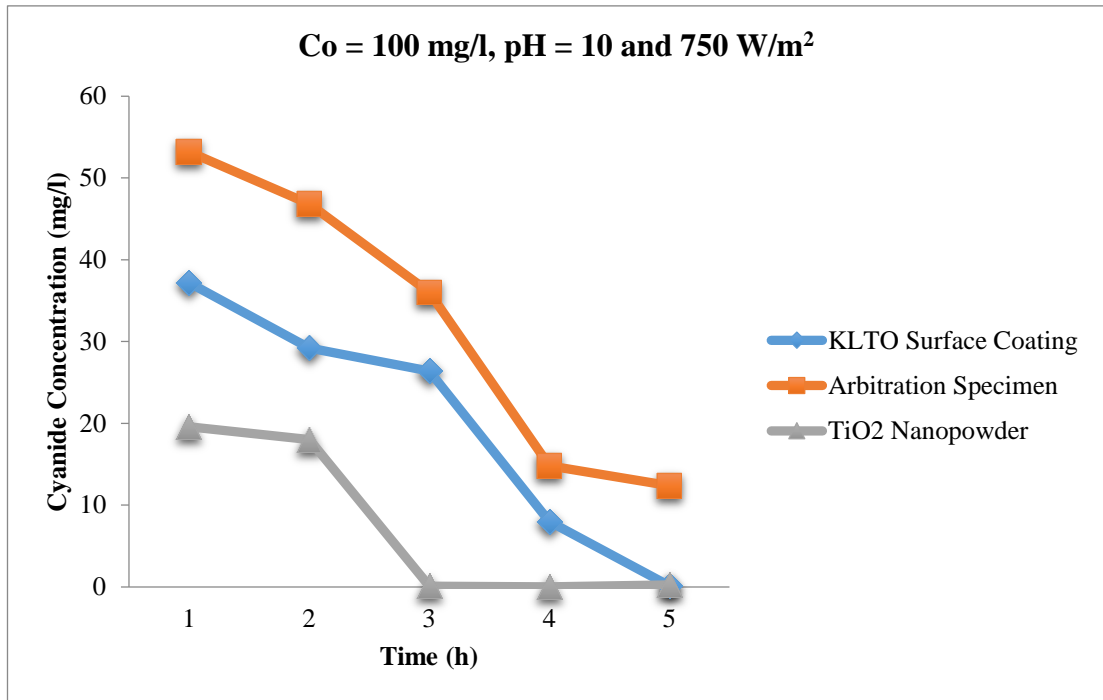


Figure 4.21 Cyanide concentration vs. time results (100 mg/l, 750 W/m<sup>2</sup> and pH = 10).

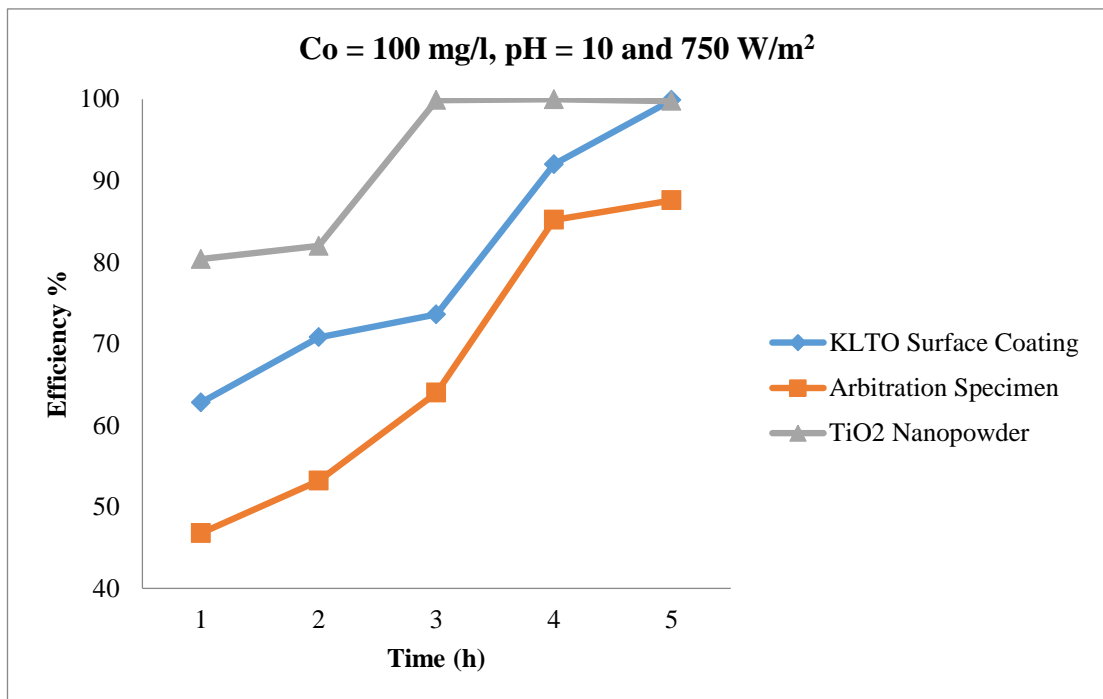


Figure 4.22 Cyanide removal efficiencies (%) (Co = 100 mg/l, 750 W/m<sup>2</sup> and pH = 10).

Table 4.18 Summary of cyanide experiments

Time (h)	Photocatalytic degradation results (mg/l)																							
	pH = 10												pH = 10											
	100 mg/l cyanide						300 mg/l cyanide						100 mg/l cyanide						300 mg/l cyanide					
	KLTO		Arbit.		TiO <sub>2</sub>		KLTO		Arbit.		TiO <sub>2</sub>		KLTO		Arbit.		TiO <sub>2</sub>		KLTO		Arbit.		TiO <sub>2</sub>	
1 <sup>st</sup>	2 <sup>nd</sup>	1 <sup>st</sup>	2 <sup>nd</sup>	1 <sup>st</sup>	2 <sup>nd</sup>	1 <sup>st</sup>	2 <sup>nd</sup>	1 <sup>st</sup>	2 <sup>nd</sup>	1 <sup>st</sup>	2 <sup>nd</sup>	1 <sup>st</sup>	2 <sup>nd</sup>	1 <sup>st</sup>	2 <sup>nd</sup>	1 <sup>st</sup>	2 <sup>nd</sup>	1 <sup>st</sup>	2 <sup>nd</sup>	1 <sup>st</sup>	2 <sup>nd</sup>	1 <sup>st</sup>	2 <sup>nd</sup>	
5	9.6	10.3	27.6	27.9	0.68	0.75	53.98	67.15	87.6	69.23	3.39	3.01	0.128	0.233	12.40	10.1	0.24	0.219	3.38	5.57	65.55	66.39	0.039	0.26
	250 W/m <sup>2</sup>												750 W/m <sup>2</sup>											
Time (h)	pH = 12												pH = 12											
	100 mg/l cyanide						300 mg/l cyanide						100 mg/l cyanide						300 mg/l cyanide					
	KLTO		Arbit.		TiO <sub>2</sub>		KLTO		Arbit.		TiO <sub>2</sub>		KLTO		Arbit.		TiO <sub>2</sub>		KLTO		Arbit.		TiO <sub>2</sub>	
	1 <sup>st</sup>	2 <sup>nd</sup>	1 <sup>st</sup>	2 <sup>nd</sup>	1 <sup>st</sup>	2 <sup>nd</sup>	1 <sup>st</sup>	2 <sup>nd</sup>	1 <sup>st</sup>	2 <sup>nd</sup>	1 <sup>st</sup>	2 <sup>nd</sup>	1 <sup>st</sup>	2 <sup>nd</sup>	1 <sup>st</sup>	2 <sup>nd</sup>	1 <sup>st</sup>	2 <sup>nd</sup>	1 <sup>st</sup>	2 <sup>nd</sup>	1 <sup>st</sup>	2 <sup>nd</sup>	1 <sup>st</sup>	2 <sup>nd</sup>
5	13.1	14.95	22.5	24.8	0.194	1.0	53.98	59.70	87.6	81.6	2.38	9.0	0.25	2	19.2	21	0.79	1.0	4.48	7.5	34.68	37.86	0.057	0.1
	250 W/m <sup>2</sup>												750 W/m <sup>2</sup>											



Table 4.19 Summary of cyanide degradation efficiencies (%)

Time (h)	Photocatalytic degradation efficiencies (%)																							
	pH = 10												pH = 10											
	100 mg/l cyanide						300 mg/l cyanide						100 mg/l cyanide						300 mg/l cyanide					
	KLTO		Arbit.		TiO <sub>2</sub>		KLTO		Arbit.		TiO <sub>2</sub>		KLTO		Arbit.		TiO <sub>2</sub>		KLTO		Arbit.		TiO <sub>2</sub>	
1 <sup>st</sup>	2 <sup>nd</sup>	1 <sup>st</sup>	2 <sup>nd</sup>	1 <sup>st</sup>	2 <sup>nd</sup>	1 <sup>st</sup>	2 <sup>nd</sup>	1 <sup>st</sup>	2 <sup>nd</sup>	1 <sup>st</sup>	2 <sup>nd</sup>	1 <sup>st</sup>	2 <sup>nd</sup>	1 <sup>st</sup>	2 <sup>nd</sup>	1 <sup>st</sup>	2 <sup>nd</sup>	1 <sup>st</sup>	2 <sup>nd</sup>	1 <sup>st</sup>	2 <sup>nd</sup>	1 <sup>st</sup>	2 <sup>nd</sup>	
5	90.4	89.7	72.4	72.1	99.32	99.25	82.01	77.62	70.80	76.92	98.87	99	99.87	99.77	87.60	89.89	99.76	99.78	98.87	98.14	78.15	77.87	99.99	99.91
	250 W/m <sup>2</sup>												750 W/m <sup>2</sup>											
Time (h)	Photocatalytic degradation efficiencies (%)																							
	pH = 12												pH = 12											
	100 mg/l cyanide						300 mg/l cyanide						100 mg/l cyanide						300 mg/l cyanide					
	KLTO		Arbit.		TiO <sub>2</sub>		KLTO		Arbit.		TiO <sub>2</sub>		KLTO		Arbit.		TiO <sub>2</sub>		KLTO		Arbit.		TiO <sub>2</sub>	
1 <sup>st</sup>	2 <sup>nd</sup>	1 <sup>st</sup>	2 <sup>nd</sup>	1 <sup>st</sup>	2 <sup>nd</sup>	1 <sup>st</sup>	2 <sup>nd</sup>	1 <sup>st</sup>	2 <sup>nd</sup>	1 <sup>st</sup>	2 <sup>nd</sup>	1 <sup>st</sup>	2 <sup>nd</sup>	1 <sup>st</sup>	2 <sup>nd</sup>	1 <sup>st</sup>	2 <sup>nd</sup>	1 <sup>st</sup>	2 <sup>nd</sup>	1 <sup>st</sup>	2 <sup>nd</sup>	1 <sup>st</sup>	2 <sup>nd</sup>	
5	86.9	85.05	77.5	75.2	99.81	99	82.01	70.10	70.80	72.80	99.21	97	99.75	98	80.80	79	99.21	99	98.51	97.50	88.44	87.38	99.98	99.9
	250 W/m <sup>2</sup>												750 W/m <sup>2</sup>											

#### 4.5 Kinetic Studies of Photodegradation Results with Synthetic Wastewaters

To determine the order of the reactions for photodegradation of phenol, methylene blue and cyanide in the SUNTEST CPS+ reactor, kinetic studies were performed according to the treatment results. The degradation curves were taken out and zero, first and second order reaction kinetics were tested.  $k_0, k_1, k_2$  and  $k_n$  (mg/l.min) are the rate constants for zero, first, second and nth order kinetics, respectively.

As a result of the kinetic studies, all experiment was fitted to different reaction order. That is why, only the suitable order graphs were given, and the other order constants were given in tables below.

Kinetic studies of phenol solution were examined for 4 different conditions.

Condition 1:10 mg/l initial concentration, 250 W/m<sup>2</sup> and pH at 7.

Condition 2:100 mg/l initial concentration, 250 W/m<sup>2</sup> and pH at 7.

Condition 1:10 mg/l initial concentration, 750 W/m<sup>2</sup> and pH at 7.

Condition 1:100 mg/l initial concentration, 750 W/m<sup>2</sup> and pH at 7.

To obtain cyanide kinetic, 2 different conditions were performed.

Condition 1:100 mg/l initial concentration, 250 W/m<sup>2</sup> and pH at 10.

Condition 2:100 mg/l initial concentration, 750 W/m<sup>2</sup> and pH at 10.

As a result of the studies methylene blue also examined with 2 different conditions.

Condition 1:10<sup>-5</sup> M initial concentration, 250 W/m<sup>2</sup> and pH at 3.

Condition 2: 10<sup>-5</sup> M initial concentration, 750 W/m<sup>2</sup> and pH at 3.

The bold characters at the tables 4.20, 4.21, 4.22, 4.23, 4.24, 4.25, 4.26 and 4.27 are the maximum correlation constants.

Under photocatalytic degradation experiments for phenol ( $C_0 = 10 \text{ mg/l}$ ,  $250 \text{ W/m}^2$  and  $\text{pH} = 7$ ),  $\text{TiO}_2$  nanopowder studies can be fitted to a second order reaction law. The results of the phenol test were shown in Table 4.20 which lists the order rate constants calculated and correlation ( $R^2$ ) constants for each order. If the correlation constants are higher, the model is adequate to treat the pollutants. KLTO surface coating cannot be fitted to a reaction order. The maximum second order reaction rate constant was obtained with  $\text{TiO}_2$  nanopowder degradation experiment as can be seen from Table 4.20. The curve was given in Figure 4.23.

Table 4.20 The reaction order types of phenol ( $10 \text{ mg/l}$ ,  $250 \text{ W/m}^2$ ,  $\text{pH} = 7$ )

	0 <sup>th</sup> order		1 <sup>st</sup> order		2 <sup>nd</sup> order	
	$k_0$ ( $\text{mg/l}\cdot\text{min}$ )	$R^2$	$k_1$ ( $\text{min}^{-1}$ )	$R^2$	$k_2$ ( $\text{Lmg}^{-1}\text{min}^{-1}$ )	$R^2$
<b>KLTO Surface Coating</b>	$3.31 \cdot 10^{-3}$	0.4647	$3.93 \cdot 10^{-4}$	0.5095	$4.72 \cdot 10^{-5}$	<b>0.5550</b>
<b>Ref.</b>	$5.89 \cdot 10^{-4}$	0.5059	$6.05 \cdot 10^{-5}$	0.5118	$6.218 \cdot 10^{-6}$	<b>0.5176</b>
<b><math>\text{TiO}_2</math> Nanopowder</b>	0.0111	0.1904	$6.905 \cdot 10^{-3}$	0.50098	0.055	<b>0.9827</b>

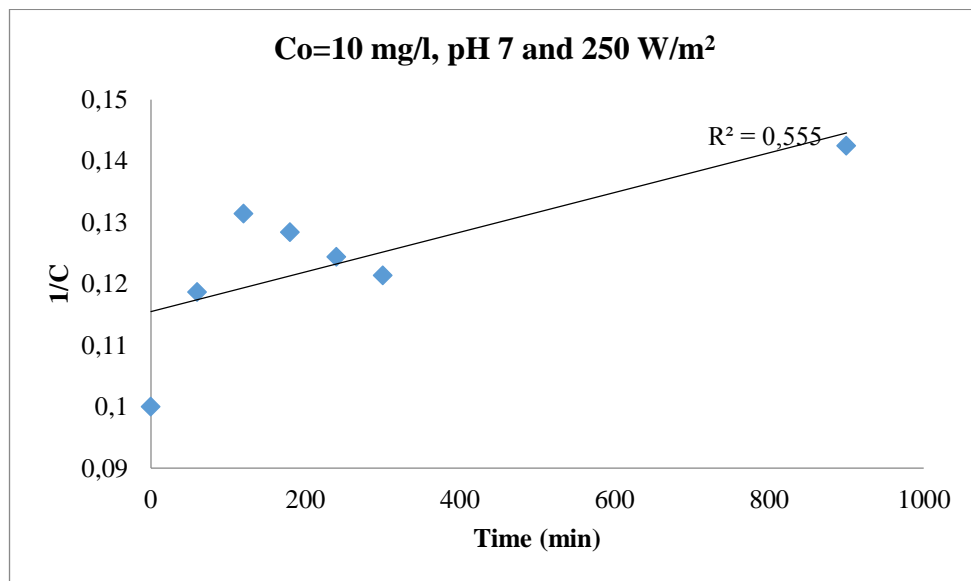


Figure 4.23 Concentration vs. time for second order degradation of phenol (KLTO Surface Coating).

The most suitable degradation curve of phenol (100 mg/l, 250 W/m<sup>2</sup>, pH 7) can be fitted to a zero order reaction rate with KLTO surface coating experiments which can be seen in Table 4.21 and the curve is in Figure 4.24.

Table 4.21 The reaction order types of phenol (100 mg/l, 250 W/m<sup>2</sup>, pH = 7)

	0 <sup>th</sup> order		1 <sup>st</sup> order		2 <sup>nd</sup> order	
	k <sub>0</sub> (mg/l.min)	R <sup>2</sup>	k <sub>1</sub> (min <sup>-1</sup> )	R <sup>2</sup>	k <sub>2</sub> (Lmg <sup>-1</sup> min <sup>-1</sup> )	R <sup>2</sup>
<b>KLTO Surface Coating</b>	0.0961	<b>0.8259</b>	0.00113	0.7917	1.351*10 <sup>-5</sup>	0.7561
<b>TiO<sub>2</sub> Nanopowder</b>	0.333	0.5878	0.046	<b>0.9244</b>	0.066	0.4302

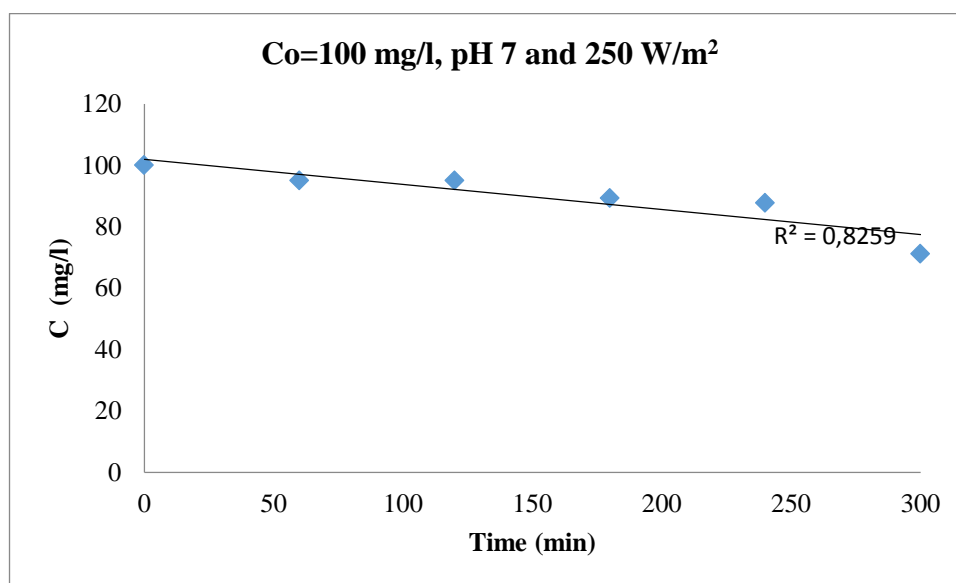


Figure 4.24 Concentration vs. time for zero order degradation of phenol (KLTO Surface Coating).

As can be seen from Table 4.20 and 4.21, the phenol initial concentration increase from 10 mg/l to 100 mg/l has changed the reaction order by using KLTO surface coating. The rise of the phenol initial concentration affects positively the reaction rate and correlation constants. The reaction rate constants increased at pH 7.

It was found that the oxidation of phenol (10 mg/l, 750 W/m<sup>2</sup>, pH 7) can be fitted to a first order reaction rate by using KLTO surface coating which can be seen in Table 4.22 and the curve is in Figure 4.25. KLTO surface coating samples showed the bigger R<sup>2</sup> value, 0.9747. And TiO<sub>2</sub> curve also was high with 0.9354 and can be fitted to zero order.

Table 4.22 The reaction order types of phenol (10 mg/l, 750 W/m<sup>2</sup>, pH = 7)

	0 <sup>th</sup> order		1 <sup>st</sup> order		2 <sup>nd</sup> order	
	k <sub>0</sub> (mg/l.min)	R <sup>2</sup>	k <sub>1</sub> (min <sup>-1</sup> )	R <sup>2</sup>	k <sub>2</sub> (Lmg <sup>-1</sup> min <sup>-1</sup> )	R <sup>2</sup>
<b>KLTO Surface Coating</b>	0.0097	0.9699	0.00115	<b>0.9747</b>	0.000137	0.9724
<b>Ref.</b>	0.00353	<b>0.3088</b>	0.00037	0.3022	3.952*10 <sup>-5</sup>	0.2956
<b>TiO<sub>2</sub> Nanopowder</b>	0.0333	<b>0.9354</b>	0.025	0.7756	0.666	0.4529

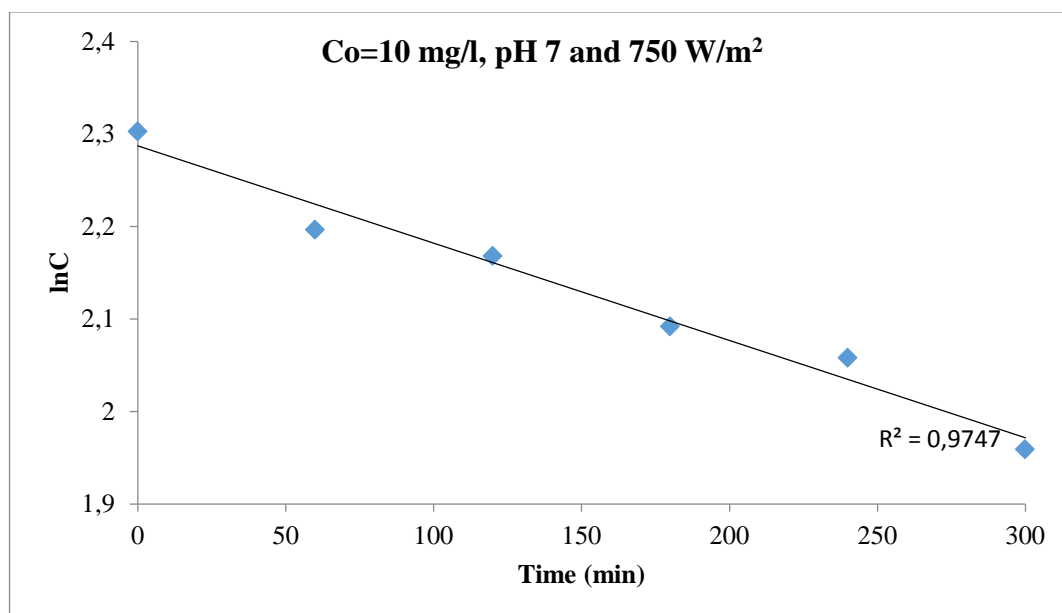


Figure 4.25 Concentration vs. time for first order degradation of phenol (KLTO Surface Coating).

For KLTO surface coating, the degradation curve of phenol (100 mg/l, 750 W/m<sup>2</sup>, pH 7) can be fitted to a zero order reaction rate and for TiO<sub>2</sub> it is first order which can be seen in Table 4.23 and the curve of the KLTO surface coating is in Figure 4.26. The R<sup>2</sup> are 0.8615 and 0.9587, respectively.

Table 4.23 The reaction order types of phenol (100 mg/l, 750 W/m<sup>2</sup>, pH = 7)

	0 <sup>th</sup> order		1 <sup>st</sup> order		2 <sup>nd</sup> order	
	k <sub>0</sub> (mg/l.min)	R <sup>2</sup>	k <sub>1</sub> (min <sup>-1</sup> )	R <sup>2</sup>	k <sub>2</sub> (Lmg <sup>-1</sup> min <sup>-1</sup> )	R <sup>2</sup>
<b>KLTO Surface Coating</b>	0.0395	<b>0.8615</b>	0.00042	0.8514	4.5*10 <sup>-6</sup>	0.8410
<b>TiO<sub>2</sub> Nanopowder</b>	0.333	0.5604	0.033	<b>0.9587</b>	0.667	0.4545

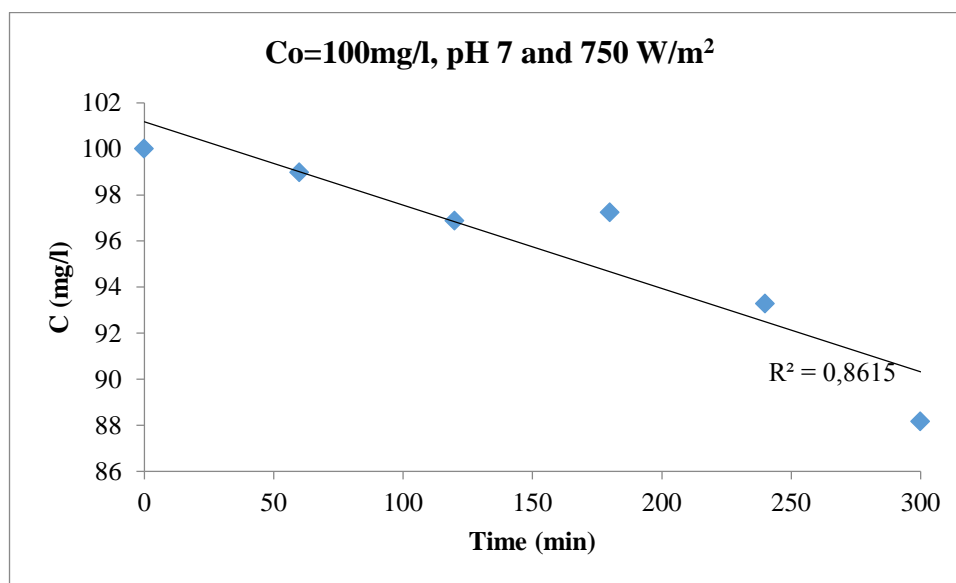


Figure 4.26 Concentration vs. time for zero order degradation of phenol (KLTO Surface Coating).

As a result of the phenol tests at 750 W/m<sup>2</sup>, if the phenol initial concentration is increasing from 10 mg/l to 100 mg/l, the reaction order is changed by using KLTO surface coating. When the phenol initial concentration increases, the reaction rate constants is increased but the correlation constants are decreased.

Photocatalytic degradation experiments for cyanide ( $C_0 = 100 \text{ mg/l}$ ,  $250 \text{ W/m}^2$  and  $\text{pH} = 10$ ) was the second step. KLTO surface coating and  $\text{TiO}_2$  nanopowder studies can be fitted to a first order reaction law. The results of cyanide was shown in Table 4.24 and the lists of the order rate constants calculated and correlation ( $R^2$ ) constants for each order were in table below. The curve of the KLTO Surface Coating was given in Figure 4.27.

Table 4.24 The reaction order types of cyanide ( $100 \text{ mg/l}$ ,  $250 \text{ W/m}^2$ ,  $\text{pH} = 10$ )

	0 <sup>th</sup> order		1 <sup>st</sup> order		2 <sup>nd</sup> order	
	$k_0$ ( $\text{mg/l}\cdot\text{min}$ )	$R^2$	$k_1$ ( $\text{min}^{-1}$ )	$R^2$	$k_2$ ( $\text{Lmg}^{-1}\text{min}^{-1}$ )	$R^2$
<b>KLTO Surface Coating</b>	0.301	0.762	0.0078	<b>0.9487</b>	0.00003139	0.87
<b>Ref.</b>	0.241	0.5695	0.0043	0.6559	0.000314	<b>0.7426</b>
<b>TiO<sub>2</sub> Nanopowder</b>	0.331	0.7065	0.0166	<b>0.9093</b>	0.00709	0.6184

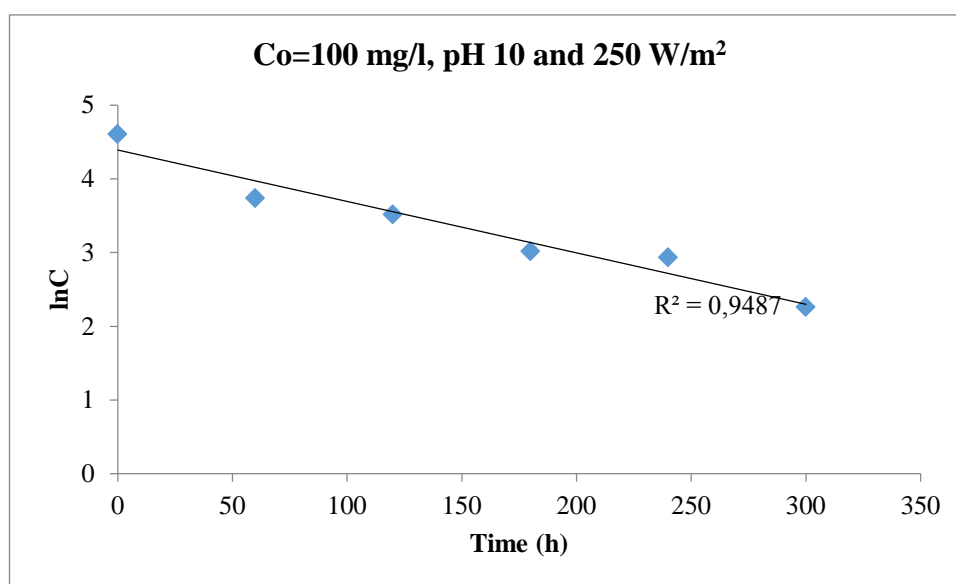


Figure 4.27 Concentration vs. time for first order degradation of cyanide (KLTO Surface Coating).

The degradation curve of cyanide with different conditions (100 mg/l, 750 W/m<sup>2</sup>, pH 10) can be fitted to a zero order reaction rate with KLTO surface coating experiment which can be seen in Table 4.25 and the curve of the coatings is in Figure 4.28. The R<sup>2</sup> is 0.7926. The zero and first order R<sup>2</sup>'s were too close.

Table 4.25 The reaction order types of cyanide (100 mg/l, 750 W/m<sup>2</sup>, pH = 10)

	0 <sup>th</sup> order		1 <sup>st</sup> order		2 <sup>nd</sup> order	
	k <sub>0</sub> (mg/l.min)	R <sup>2</sup>	k <sub>1</sub> (min <sup>-1</sup> )	R <sup>2</sup>	k <sub>2</sub> (Lmg <sup>-1</sup> min <sup>-1</sup> )	R <sup>2</sup>
<b>KLTO Surface Coating</b>	0.3329	<b>0.7926</b>	0.0222	0.7381	0.0260	0.4392
<b>Ref.</b>	0.292	0.8835	0.0069	<b>0.95</b>	0.000235	0.8653
<b>TiO<sub>2</sub> Nanopowder</b>	0.3325	0.6277	0.0201	<b>0.7482</b>	0.2083	0.22

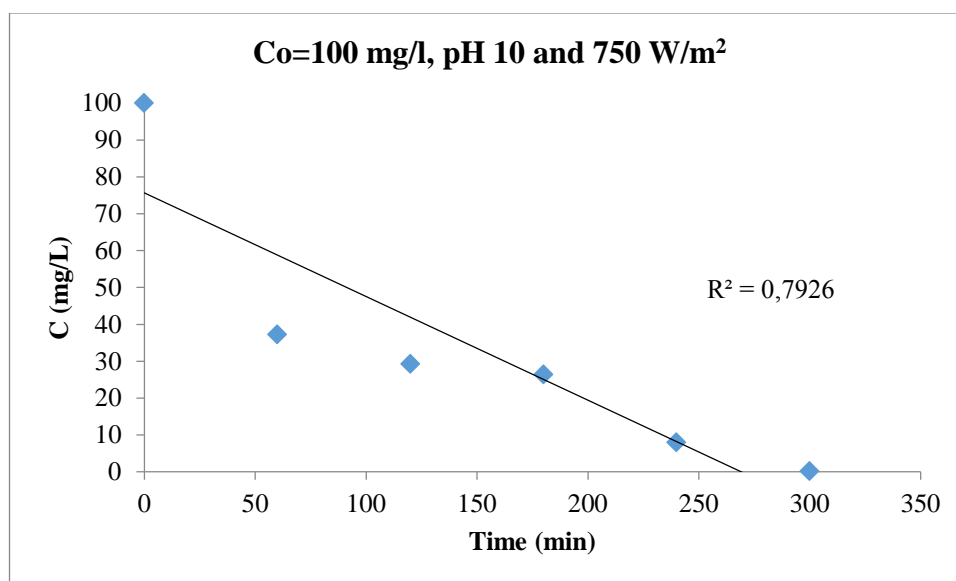


Figure 4.28 Concentration vs. time for zero order degradation of cyanide (KLTO Surface Coating).

As a result of the variation of the light intensity from 250 to 750 W/m<sup>2</sup>, the reaction order is changed by using KLTO surface coating. When the light intensity increases, the reaction rate constants are increased.



Methylene blue was completely treated in 16 minutes with TiO<sub>2</sub> nanopowder. TiO<sub>2</sub> nanopowder is very effective to degrade methylene blue. So, the reaction orders could not found. The table below gives information about KLTO surface coating and arbitration specimen as reference. The reaction order was found second order with KLTO surface coating experiment. The R<sup>2</sup> values and the suitable curve can be seen in Table 4.26 and Figure 4.29, respectively.

Table 4.26 The reaction order types of methylene blue (10<sup>-5</sup> M, 250 W/m<sup>2</sup>, pH = 3)

	0 <sup>th</sup> order		1 <sup>st</sup> order		2 <sup>nd</sup> order	
	k <sub>0</sub> (mg/l.min)	R <sup>2</sup>	k <sub>1</sub> (min <sup>-1</sup> )	R <sup>2</sup>	k <sub>2</sub> (Lmg <sup>-1</sup> min <sup>-1</sup> )	R <sup>2</sup>
<b>KLTO Surface Coating</b>	0.000661	0.6906	0.00167	0.8650	0.00508	<b>0.9718</b>
<b>Ref.</b>	0.000433	0.5506	0.00079	0.6302	0.00508	<b>0.7097</b>

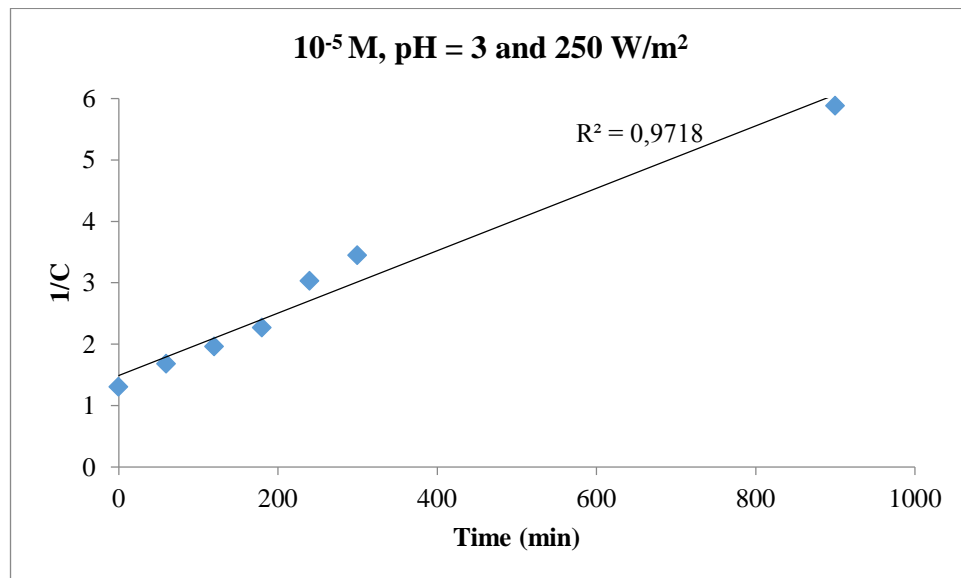


Figure 4.29 Concentration vs. time for second order degradation of methylene blue (KLTO Surface Coating).

At 750 W/m<sup>2</sup> light intensity, methylene blue degradation process was perfect by using KLTO surface coating and TiO<sub>2</sub> nanopowder. For this reason, 2 hours of experiments were enough to see the efficiencies. Even so, the kinetics were taken in Table 4.25 and in Figure 4.31. The kinetics were found zero order law by KLTO surface coating.

Table 4.27 The reaction order types of methylene blue (10<sup>-5</sup> M, 750 W/m<sup>2</sup>, pH = 3)

	0 <sup>th</sup> order		1 <sup>st</sup> order		2 <sup>nd</sup> order	
	k <sub>0</sub> (mg/l.min)	R <sup>2</sup>	k <sub>1</sub> (min <sup>-1</sup> )	R <sup>2</sup>	k <sub>2</sub> (Lmg <sup>-1</sup> min <sup>-1</sup> )	R <sup>2</sup>
<b>KLTO Surface Coating</b>	0.0061	<b>0.9975</b>	0.0262	0.8815	0.2416	0.7762
<b>Ref.</b>	0.0034	0.9027	0.0064	0.9440	0.2416	<b>0.9782</b>

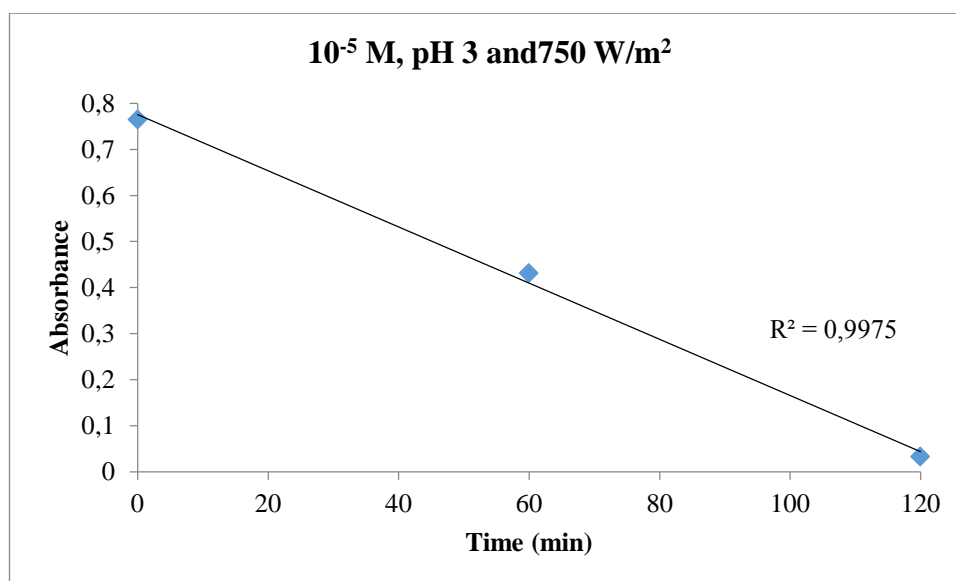


Figure 4.30 Concentration vs. time for zero order degradation of methylene blue (KLTO Surface Coating).

As a result of the methylene blue tests, the methylene blue absorbance variation is observed between 250 W/m<sup>2</sup> to 750 W/m<sup>2</sup> light intensity. The reaction order is changed by using KLTO surface coating.

#### 4.6 Factorial Experimental Design Studies

This section focuses on the designed experiments that include two or three design factors. Phenol, methylene blue and cyanide photocatalytic experiments were done and pH, initial concentration and irradiance ranges are chosen as variable. For phenol and cyanide three factors two replicates factorial design and for methylene blue two factors two replicates factorial design were set up. Each experiment were tested 2 times and totally 16 experiments are done for every single pollutant. The goal of the research problem which identified is to reject or accept the hypothesis and to see if the variables are related with the treatment or not.

Hypothesis test is a confirmation of hypothesis which depends on the information obtained from the samples with a margin of error. Zero hypothesis (null hypothesis) ( $H_0$ ) defends that there is not a relation or difference between the mean and distribution. Contrary, alternative hypothesis stands up that, there is a relation or difference between the mean and distribution.

A research problem which determined and expressed as a hypothesis must reach a solution from the factors which are taking into consideration that are involved and with minimum error. Analysis of variance (ANOVA) is using to compare different groups.

In this study, the significance level is chosen  $\alpha=5\%$  (0.05). In other word, the findings have 95% chance of being true and have a 5% of chance for not being true. If the hypothesis is accepted, the amount of removal rate does not depend on the variable. The Minitab results represent 95% confidence intervals.

If p value  $> 0.05$  ( $\alpha$ ): Cannot reject Null Hypothesis because  $p > 0.05$  (Means are the same).

If p value  $< 0.05$  ( $\alpha$ ): Reject Null Hypothesis because  $p < 0.05$  (Means are different).

Table 4.28 Variables for phenol experimental design

<b>Level</b>	<b>pH</b>	<b>Initial Concentration (mg/l)</b>	<b>Irradiance Ranges (W/m<sup>2</sup>)</b>
<b>Min</b>	7	10	250
<b>Max</b>	10	100	750

Table 4.29 Variables for cyanide experimental design

<b>Level</b>	<b>pH</b>	<b>Initial Concentration (mg/l)</b>	<b>Irradiance Ranges (W/m<sup>2</sup>)</b>
<b>Min</b>	10	100	250
<b>Max</b>	12	300	750

Table 4.30 Variables for methylene blue experimental design

<b>Level</b>	<b>pH</b>	<b>Irradiance Ranges (W/m<sup>2</sup>)</b>
<b>Min</b>	3	250
		750
<b>Mid</b>	7	250
		750
<b>Max</b>	10	250
		750

The variables are chosen as pH, initial concentration and light intensity. A demonstrates pH, B demonstrates initial concentration and C demonstrates light intensity. The test is done to evaluate if pH, initial concentration and/or light intensity significantly affect removal percentage.

Every experiment is replicated 2 times. The variation of the variables is shown in Table 4.28, 4.29 and 4.30. The response is the removal efficiency (%). If Ho's are true, the variances are equal to other variances. ANOVA test is applied to the KLTO Surface Coating test parameters.

As a result of the phenol performance tests, the hypotheses are accepted.

1. pH is not a significant factor on removal.
2. Initial concentration is not a significant factor on removal.

3. Light intensity is a significant factor on removal.
4. It has no interaction. 2 and 3 factor interaction failed.
5. It can be said that catalyst was not very effective on phenol removal.

As a result of the cyanide performance tests, the  $H_{01}$ ,  $H_{04}$ ,  $H_{06}$  and  $H_{07}$  hypotheses are accepted and  $H_{02}$  and  $H_{03}$  are rejected.

1. pH is not a significant factor on removal. So, 10 or 12 pH values have not an effect, the alkali condition is enough for treatment process.
2. Initial concentration is a significant factor on removal. So, it effect by oneself.
3. Light intensity is a significant factor on removal. So, it effect by oneself.
4. pH vs Co, pH vs light intensity and pH vs Co vs light intensity interactions are failed. But Co vs light intensity effect each other, and influence the performance.
5. That is why; pH is ineffective, but initial concentration and light intensity are influential. According to the findings, initial concentration and light intensity are important.

As a result of the methylene blue performance tests, the hypotheses are rejected.

1. pH is a significant factor on removal. Because different pH values (3-7-10) are applied.. So, it effect by oneself.
2. Light intensity is a significant factor on removal. So, it effect by oneself.
3. There is interaction. That is why; pH and light intensity effect each other, and have an influence on performance.

The result tables of the ANOVA tests can be seen in Appendix A.

Table 4.31 A briefly comparison of the variables and their effects by KLTO Surface Coating

<b>Effects</b>	<b>Phenol</b>		<b>Cyanide</b>		<b>Metyhlene Blue</b>	
<b>pH</b>	7-10	No effect	10-12	No effect	3-7-10	Effective
<b>Initial Concentration (Co)</b>	10-100 mg/l	Effective	100-300 mg/l	Effective	10 <sup>-5</sup> M	Co is not selected as a variable
<b>Light intensity</b>	250-750 W/m <sup>2</sup>	No effect	250-750 W/m <sup>2</sup>	Effective	250-750 W/m <sup>2</sup>	Effective
<b>pH x Co</b>	No effect		No effect		Co is not selected as a variable	
<b>pH x Light intensity</b>	No effect		No effect		Effective	
<b>Co x Light intensity</b>	No effect		Effective		Co is not selected as a variable	
<b>pH x Co x Light intensity</b>	No effect		No effect		Co is not selected as a variable	
<b>Conclusion of the treatment process</b>	Any of the variables have no effect		pH has not effective, alkali condition is adequate		The variables are effective to treat the methylene blue	

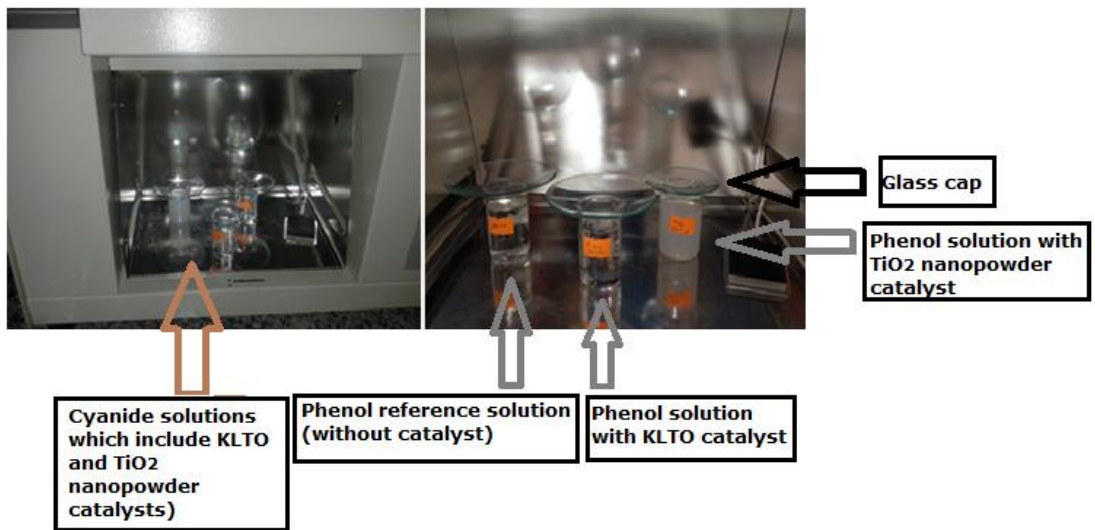
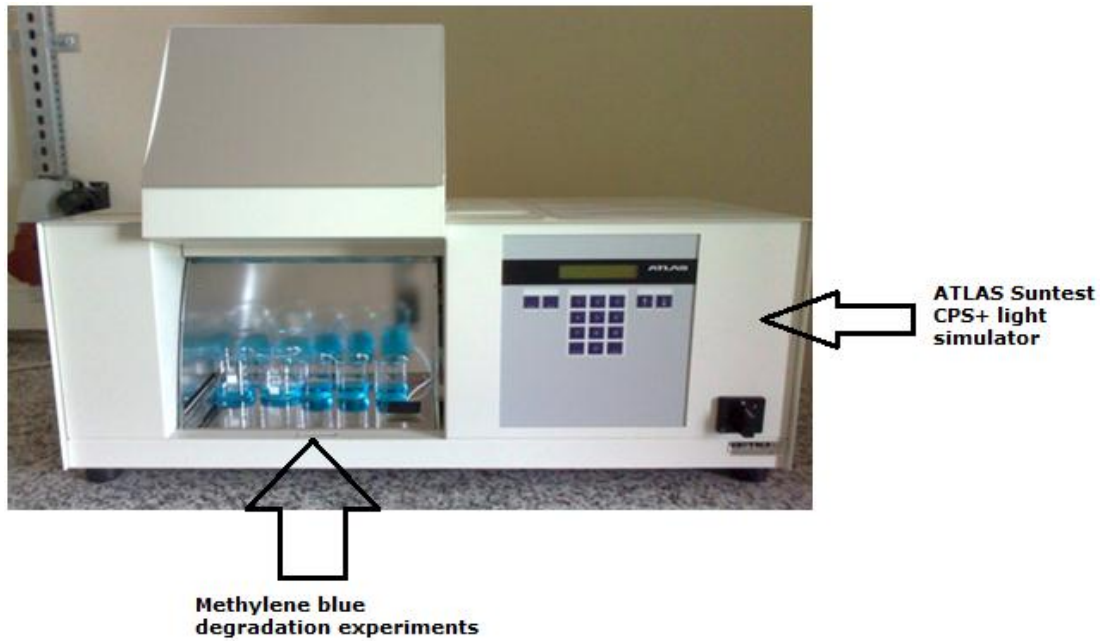


Figure 4.31 Some photos from experimental studies.

## CHAPTER FIVE

### CONCLUSION AND RECOMMENDATIONS

#### 5.1 General Results

The main objective of this study is to see the photocatalytic degradation of the persistent pollutants in wastewater with using the new generation photocatalytic materials (potassium lanthanum titanates). The effect of pH, initial pollutant concentration and light intensity are investigated. The reaction orders and the rate constants were also investigated.

According to the findings; pH, initial concentration and light intensity can influence the photocatalytic degradation rates of phenol, methylene blue and cyanide. The results from the experimental studies are given below.

1. The pH, turbidity values, rheological properties and contact angle were measured to understand the Ce - based and K, La, Ti based solution properties of the catalyst. According to turbidity test, the solutions were homogeny and adequately transparent with 53.36 NTU and 77.06 NTU, respectively. The pH value of the solutions demonstrated acidic condition. Ce-based solution pH value is 4.44 and K, La and Ti based solution pH value is 3.51. The elasticity and viscous modulus obtained at 25°C. And to find the wetting capacity, contact angles evaluated. As a result of the measurement, the contact angles measured 4° and 3°, respectively.
2. To make a decision of heat treatment and to optimize the characterization, DTA-TG and FTIR analysis were done. The optimum KLTO xerogel phase was composed and beginning temperature, ending temperature of the reactions and reaction types were found by DTA-TG curves. The optimum annealing temperature for the phase transformation is obtained at 850°C and 1200°C. The absorbance spectrum of the samples was found at 25°C between



the wavelengths of 600-4000  $\text{cm}^{-1}$ . FTIR results were regularly conformed to DTA-TG results.

3. To constitute the film characterization, XRD, SEM, XPS and AFM devices were used. According to the XRD result, the KLTO phase obtained by using 0.1 gram K precursor. To understand the coating surface morphology, the surface photographed. The surface area is covered by the needless dense coating particle. The elemental analysis results of the XPS and XRD were consentaneously. The roughness of the film surface is found 445.69 nm and 900.27 nm, respectively for two different sites.
4.  $\text{K}_2\text{La}_2\text{Ti}_3\text{O}_{10}$  was produced with using sol-gel method. Spin coating method and buffer layer application was performed. The dimensions of the KLTO surface coating photocatalysts which are used are 2x2 cm.
5. Phenol, methylene blue and cyanide are selected as pollutants in wastewater. The aim of this selection is to evaluate an organic (phenol), azo dye (methylene blue) and inorganic (cyanide) substances.
6. Material Safety Data Sheets (MSDS) of the commercial chemicals which are used as pollutants (phenol, methylene blue and cyanide) and  $\text{TiO}_2$  nanopowder catalyst can be seen in Appendix D.
7. To prevent the evaporation of the wastewater, a glass cap was putted above the beaker which can be seen at Figure 4.31. For every experiment step, the beakers were filled till 25 ml and it was placed on ATLAS Suntest CPS+.
8. The experiments were done with KLTO thin film, and 0.01 g  $\text{TiO}_2$  nanopowder (Sigma-Aldrich). To see the difference and to make a deduction, an arbitration specimen was carried out for every experiment.

9. Every experiment carried out 2 times to ensure the accuracy and to make statistical evaluation.
10. During the treatment of phenol, methylene blue and cyanide, the degradation rates were observed for 5 hours operation and with different pH, initial concentration and light intensity.
11. The highest degradation rate of phenol was obtained 40.04% after five hours by using KLTO surface coating catalyst. The conditions are as below: pH at 7, 100 mg/l for initial concentration and with a  $750 \text{ W/m}^2$  light intensity. Pardeshi & Patil (2008) were found 47% of maximum degradation rate of phenol by using aqueous zinc oxide as photocatalyst. This value was obtained when the phenolic solution was 75 ppm and with visible light of 1000 W Xenon lamp within nine hours. According to these studies, when the amount of photocatalysts increases, the photodegradation rate also increases. The sunlight intensity changed between  $500$  and  $700 \text{ W/m}^2$ . Phenol degradation rate was higher when the natural sunlight was used as a light source. Phenol solutions were completely mineralized by photocatalytic degradation of ZnO under solar light irradiation. According to the results of Guo, Ma & Li (2006), the degradation efficiencies of phenol is obtained 16% and 76% in the presence of  $\text{TiO}_2$  and was also obtained 40% and 81.6% in the absence of  $\text{TiO}_2$  for 3 and 12 hours, respectively. For these experiments Guo et al. used 100 mg/l initial concentration of phenol under UV radiation. The results of the KLTO surface coating catalysts are approached to these results. As a result of a few experiments, the degradation efficiencies of the arbitration specimen (without any catalyst) are higher than KLTO surface coating catalyst results. It can be seen the natural sunlight is very effective to degrade the phenolic compounds.
12. Throughout the treatment studies of methylene blue by using KLTO surface coating catalyst, the maximum degradation rate was observed 99.87% with  $10^{-5} \text{ M}$  at pH 10 and  $750 \text{ W/m}^2$  light intensity after five hours treatment

process by using ATLAS Suntest CPS+. Rizzo et al. (2011) were prepared TiO<sub>2</sub> nanofilm by using sol-gel method. The experiment realized in the photocatalytic reactor under UV lamp (335 nm) radiation. At pH 9, the degradation efficiency was obtained 80% after 10 minutes.

13. With the experiments of cyanide, the maximum degradation rate was measured 99.87% by using KLTO surface coating catalyst. pH value was 10, light intensity value was 750 W/m<sup>2</sup> and the initial concentration was 100 mg/l. Aguado et al. investigated different TiO<sub>2</sub> catalysts like Degussa-P25, anatase phase. According to the results, 96% obtained to remove cyanide by using Degussa P-25 within 4 hours and at initial pH 11.
14. According to the phenol, methylene blue and cyanide findings, the reaction kinetics was investigated. Different conditions were examined in detail. Each test was carried out by using the KLTO Surface Coating catalyst and commercial nanopowder TiO<sub>2</sub> (Sigma-Aldrich) catalysts. The performances of the catalysts were evaluated by comparison of the samples which exposure only light intensity. Phenol degradation curve is fitted to different reaction orders in different conditions. Different conditions are examined. Cyanide degradation kinetics was also changeable. Methylene blue test performance was investigated at pH=3 and light intensity at 250 W/m<sup>2</sup> and 750 W/m<sup>2</sup>. The results can be seen in the Table 5.1.
15. To enhance the degradation rates, some dopants/precursors should be added and their effect should be investigated.

Table 5.1 Summary table of the reaction order

<b>Catalyst</b>	<b>Pollutant</b>	<b>pH</b>	<b>Initial Concentration</b>	<b>Light Intensity (W/m<sup>2</sup>)</b>	<b>Reaction Order and R<sup>2</sup></b>
<b>KLTO Surface Coating</b>	Phenol	7	10 mg/l	250	2nd (0.5550)
		7	10 mg/l	750	1st (0.9747)
		7	100 mg/l	250	0th (0.8259)
		7	100 mg/l	750	0th (0.8615)
<b>Arbitration Specimen (Reference)</b>	Phenol	7	10 mg/l	250	2nd (0.5176)
		7	10 mg/l	750	0th (0.3088)
<b>TiO<sub>2</sub> Nano powder</b>	Phenol	7	10 mg/l	250	2nd (0.9827)
		7	10 mg/l	750	0th (0.9354)
		7	100 mg/l	250	1st (0.9244)
		7	100 mg/l	750	1st (0.9587)
<b>KLTO Surface Coating</b>	Cyanide	10	100 mg/l	250	1st (0.9487)
		10	100 mg/l	750	0th (0.7976)
<b>Arbitration Specimen (Reference)</b>	Cyanide	10	100 mg/l	250	2nd (0.7426)
		10	100 mg/l	750	1st (0.95)
<b>TiO<sub>2</sub> nano powder</b>	Cyanide	10	100 mg/l	250	1st (0.9093)
		10	100 mg/l	750	1st (0.7482)
<b>KLTO Surface Coating</b>	Methylene Blue	3	10 <sup>-5</sup> M	250	2nd (0.9718)
		3	10 <sup>-5</sup> M	750	2nd (0.9975)
<b>Arbitration Specimen (Reference)</b>	Methylene Blue	3	10 <sup>-5</sup> M	250	2nd (0.7097)
		3	10 <sup>-5</sup> M	750	2nd (0.9782)

16. Commercial TiO<sub>2</sub> nanopowder (Sigma-Aldrich Titanium (IV) oxide, 718467) was very effective to degrade the pollutants in the wastewater. It was effective in all degradation experiments as a result of its powder feature and it takes big surface area in the liquid. The efficiencies were always approximately 100%. But the nanopowder materials create another problem like separation technique from water and the particles may be threatened the human health. TiO<sub>2</sub> nanoparticles were separated by centrifugation from wastewater. The supernatant (the liquid which remain after centrifuge) was tested.
17. The results of phenol, cyanide and methylene blue degradation was tested with ANOVA test for different variables.
18. According to the phenol degradation results, different pH (7 - 10), initial concentration (10 - 100 mg/l) and light intensity (250 W/m<sup>2</sup> and 750 W/m<sup>2</sup>) values selected as variables. As a result of the ANOVA test, the light intensity is more effective to degrade phenolic compound.
19. The variables of cyanide test were chosen like phenol experiment, but the range of pH and initial concentration were different. pH values were selected as 10 and 12 to obtain CN<sup>-</sup> ions in aqueous solution. It means only alkali conditions were examined due to the cyanide property. Initial concentration fixed on 100 and 300 mg/l. As a result of the cyanide ANOVA test, the amount of the degradation does not depend in this ranges of pH, in other words the alkali condition is enough for the degradation process. But the degradation rate is depending on initial concentration of cyanide, light intensity and the interaction of initial concentration and light intensity.
20. To monitor the decrease of the methylene blue, Shimadzu spectrophotometer was used. The maximum absorbance was measured 664 nm. According to the ANOVA test results, pH and light intensity have an effect on the degradation

efficiency. And also the efficiency is depending on the interaction of both pH and light intensity.

21. The advantage of the KLTO surface coating includes short reaction times in comparison with only exposed light intensity and it does not require an additional operation as separation or filtration. It does not produce waste and it is more environmental friendly.

## **5.2 Recommendations**

The photocatalysis must be enhanced and the optimum phase should be re - investigated. Thin film photocatalysts are more eco - friendly and less harmful than particulate catalysts. The difficulties of particulate catalysts are the separation of the particles from wastewater. For this reason, this study is realized. The new generated KLTO film production should be investigated and examined for the treatment of wastewaters.

In the future, researches should focus on the development of an effective photocatalyst and a photo reactor should be modeled to apply this study on industrial fields.

## REFERENCES

- Abdelwahab, O., Amin, N.K., & El-Astoukhy, E-S.Z. (2009). Electrochemical removal of phenol from oil refinery wastewater. *Journal of Hazardous Materials*, 163 (2-3), 711-716.
- Aguado, J., Grieken, R., Lopez, M. J., & Marugan, J. (2002). Removal of cyanides in wastewater by supported TiO<sub>2</sub> – based photocatalysts. *Catalysis Today*, 75, 95-102.
- Asahi, R., Morikawa, T., Ohwaki, T., Aoki, K., & Taga, Y. (2001). Visible-light photocatalysis in nitrogen-doped titanium oxides. *Science*, 293 (5528), 269 – 271.
- Babuponnusami, A., & Muthukumar, K. (2012). Advanced oxidation of phenol: A comparison between Fenton, electro-Fenton, sono-electro-Fenton and photo-electro-Fenton processes. *Chemical Engineering Journal*, 183, 1-9.
- Bahnemann, D. (2004). Photocatalytic water treatment: Solar energy applications. *Solar Energy*, 77 (5), 445–459.
- Barakat, M.A., Schaeffer, H., Hayes, G., & Ismat-Shah, S. (2005). Photocatalytic degradation of 2-chlorophenol by Co-doped TiO<sub>2</sub> nanoparticles. *Applied Catalysis B: Environmental*, 57 (1), 23-30.
- Basics notions about solids*. (n.d.). Retrieved October 10, 2013, from <http://www.porous-35.com/electrochemistry-semiconductors-3.html>.
- Baycan, N., (2005). *Advanced oxidative treatment of chlorinated hydrocarbons*. Doctoral Dissertation, Graduate School of Natural and Applied Sciences of Dokuz Eylül University, İzmir.
- Beydoun, D., Amal, R., Low, G., & McEvoy, S. (1999). Role of nanoparticles in photocatalysis. *Journal of Nanoparticle Research*, 1 (4), 439-458.

- Bozkaya, Y. (2006). *Nanoteknoloji ve uygulamaları*. Anadolu Üniversitesi İleri Teknolojiler Araştırma Birimi.
- Chatterjee, S., Kumar, A., Basu, S., & Dutta, S. (2012). Application of Response Surface Methodology for Methylene Blue dye removal from aqueous solution using low cost adsorbent. *Chemical Engineering Journal*, 181-182, 289-299.
- Chen, W., Dong, X., Chen, Z., Chen, S., & Lin, W. (2009). Effect of Fe<sup>3+</sup> doping on photocatalytic activity of K<sub>2</sub>La<sub>2</sub>Ti<sub>3</sub>O<sub>10</sub> for water decomposition to hydrogen under visible light. *Acta Physico-Chimica Sinica*, 25 (6), 1107-1110.
- Chin, P. (2008). *Kinetics of photocatalytic degradation using titanium dioxide*. Doctoral dissertation, Graduate Faculty of North Carolina State University, Raleigh, North Carolina.
- Chiou, C-H., Wu, C-Y., & Juang, R-S. (2008). Photocatalytic degradation of phenol and *m*-nitrophenol using irradiated TiO<sub>2</sub> in aqueous solutions. *Separation and Purification Technology*, 62 (3), 559-564.
- Cui, W., Liu, L., Feng, L., Xu, C., Li, Z., Lu, S., et al. (2006). Preparation of Pt/K<sub>2</sub>La<sub>2</sub>Ti<sub>3</sub>O<sub>10</sub> and its photo-catalytic activity for hydrogen evolution from methanol water solution. *Science in China: Series B Chemistry*, 49 (2), 162-168.
- Çakıroğlu, E. (2011). *Titanyumdioksit esaslı (TiO<sub>2</sub>) Fotokatalizör Kullanılarak Toksik Madde İçerikli Atıksuların Detoksifikasyonu*. Master Thesis, Dokuz Eylül University, Graduate School of Applied Science, Izmir, Turkey.
- Çatalkaya, E.Ç., Bali, U., & Şengül F. (2004). Fenolün fotokimyasal yöntemlerle parçalanması ve mineralizasyonu. *Su Kirlenmesi Kontrolü Dergisi*, 14 (3), 31-41.
- Environmental Protection Agency/ U.S. EPA (1998). *Hazardous waste management system; identification and listing of hazardous waste; solvents; final rule*. Federal Register 63 FR 64371- 402.



- Evcin, A. (2006). *Kaplama teknikleri ders notları*. Retrieved November 21, 2013 from <http://www.kimmuh.com/evcin/coating/coating8.pdf>.
- Evcin, A. (nd). *Sol-jel prosesleri ders notları*. Afyon Kocatepe University Materials Science and Engineering Department.
- Evcin, A.(n.d.). *İleri sol jel prosesleri*. Retrieved November 20, 2013, from <http://www.kimmuh.com/evcin/sol-gel/solgel5.pdf>.
- Fahlman, B.D. (2011). *Materials chemistry* (2nd ed.). New York: Springer.
- Faure, B., Salazar - Alvarez, G., Ahniyaz, A., Villaluenga, I., Berriozabal, G., Migueal, Y.R.D., et al. (2013). Dispersion and surface functionalization of oxide nanoparticles for transparent photocatalytic and UV-protecting coatings and sunscreens. *Science and Technology of Advanced Materials*, 14 (2), 023001.
- Fotokatalitik TiO<sub>2</sub> tozu üretimi. (n.d.). Retrieved January 6, 2014, from [http://www.atilim.edu.tr/shares/atilim/files/haberler/6\\_Jongee%20-%20TiO2%20At%C4%B1%C4%B1m%20Poster.pdf](http://www.atilim.edu.tr/shares/atilim/files/haberler/6_Jongee%20-%20TiO2%20At%C4%B1%C4%B1m%20Poster.pdf).
- Guo, Z., Ma, R., & Li, G., (2006). Degradation of phenol by nanomaterial TiO<sub>2</sub> in wastewater. *Chemical Engineering Journal*, 119 (1), 55-59.
- Gümüő, G. (2001). *Siyanür tayini için yeni bir spektrofotometrik yöntem*. Doctoral Dissertation, Graduate School of Natural and Applied Sciences of İstanbul Technical University, İstanbul, Turkey.
- Güneőin elektromanyetik spektrumu*. (n.d.). Retrieved January, 2014, from <http://www.meteor.gov.tr/FILES/arastirma/ozonuv/gunesspectrumu.pdf>.
- Hoffman, R.V., (2004). *Organic chemistry* (2nd ed.), Hoboken, New Jersey: John Wiley & Sons Press.
- Huang, Y., Wei, Y., Cheng, S., Fan, L., Li, Y., Lin, J., et al. (2010). Photocatalytic property of nitrogen-doped layered perovskite K<sub>2</sub>La<sub>2</sub>Ti<sub>3</sub>O<sub>10</sub>. *Solar Energy Materials & Solar Cells*, 94, 761–766.

- Ikeda, S., Hara, M., Kondo, J.N., Domen, K., Takahashi, H., Okuba, T., et al. (1997). Preparation of a high active photocatalyst  $K_2La_2Ti_3O_{10}$  by polymerized complex method and its photocatalytic activity of water splitting. *Journals of Materials Research*, 13 (4), 852-855.
- Kaili, L., Jiayong, P., Yiwei, C., & Rongming, C. (2009). Study the adsorption of phenol from aqueous solution on hydroxyapatite nanopowders. *Journal of Hazardous Materials*, 161 (1), 231-240.
- Kakahana, M., & Domen, K. (2000). The synthesis of photocatalysts using the polymerizable- complex method. *MRS Bulletin*, 25 (9), 27-31.
- Kaneko, M., & Okura, I. (Eds.). (2002). *Photocatalysis: Science and technology* (2nd ed.). New York: Springer.
- Kargı, F., & Pala A. (2009). *Kimyasal prosesler ders notları*. Dokuz Eylül University Environmental Engineering Department.
- Khakpash, N., Simchi, A., & Jafari, T., (2012). Adsorption and solar light activity of transition- metal doped  $TiO_2$  nanoparticles as semiconductor photocatalyst. *Journal of Material Science: Materials in Electronics*, 23 (3), 659-667.
- Kiriloy, M., Koumanova, B., Spasoy, L., & Petrov, L. (2006). Effects of Ag And Pd modifications of  $TiO_2$  on the photocatalytic degradation of p- chlorophenol in aqueous solution, *Journal of the University of Chemical Technology and Metallurgy*, 41 (3), 343-348.
- Kodama, F., & Suzuki, J., (2007). How Japanese Companies have used scientific advances to restructure their business: The receiver-active national system of innovation. *World Development*, 35 (6), 976-990.
- Kohtani, S., Yoshioka E., & Miyabe, H. (2012). Photocatalytic hydrogenation on semiconductor particles. In *Hydrogenation* (1st ed.) (Chapter 12). Intech Publisher.

- Krishna, V., Noguchi, N., Koopman, B., & Moudgil, B., (2006). Enhancement of titanium dioxide photocatalysis by water-soluble fullerenes. *Journal of Colloid and Interface Science*, 304, 166-171.
- Kusvuran, E., Samil, A., Atanur, O. M., & Erbatur, O. (2005). Photocatalytic degradation kinetics of di- and tri-substituted phenolic compounds in aqueous solution by TiO<sub>2</sub>/UV. *Applied Catalysis B: Environmental*, 58 (3-4), 211,216.
- Larsen, D. (n.d.). *Chem-Wiki: The dynamic chemistry e-textbook*, Retrieved October 10, 2013, from [http://chemwiki.ucdavis.edu/Physical\\_Chemistry/Quantum\\_Mechanics/Electronic\\_Structure/Intrinsic\\_Semiconductors](http://chemwiki.ucdavis.edu/Physical_Chemistry/Quantum_Mechanics/Electronic_Structure/Intrinsic_Semiconductors).
- Ma, D.Y., Wang, X.H., Song, C., Wang, S.G., Fan, M.H., & Li, X.M. (2011). Aerobic granulation for methylene blue biodegradation in a sequencing batch reactor. *Desalination*, 276 (1-3), 233-238.
- Madaeni, S.S., Jamali, Z., & Islami, N. (2011). Highly efficient and selective transport of methylene blue through a bulk liquid membrane containing Cyanex 301 as carrier. *Separation and Purification Technology*, 81 (2), 116- 123.
- Metal oxide photocatalysis*. (n.d.). Retrieved March 18, 2013, from <http://photochemistry.wordpress.com/2009/09/30/metal-oxide-photocatalysis/>.
- Miseki, Y., Kato, H., & Kudo, A., (2009). Water splitting into H<sub>2</sub> and O<sub>2</sub> over niobate and titanate photocatalysts with (111) plane-type layered perovskite structure. *Energy & Environmental Science*, 3, 306–314.
- Molva, M. (2004). *Removal of phenol from industrial wastewaters using lignitic coals*. Master Thesis, Izmir Institute of Technology, Izmir, Turkey.
- Montgomery, C., & Runger, G.C. (2010). *Applied statistics and probability for engineers*, (3rd ed.). Arizona: John Wiley&Sons, Inc.

- Moussavi, G., & Khosravi, R. (2010). Removal of cyanide from wastewater by adsorption onto pistachio hull wastes: Parametric experiments, kinetics and equilibrium analysis. *Journal of Hazardous Materials*, 183 (1-3), 724-730.
- Moussavi, G., Barikbin, B., & Mahmoudi, M. (2010). The removal of high concentrations of phenol from saline wastewater using aerobic granular SBR. *Chemical Engineering Journal*, 158 (3), 498-504.
- Nakamura R, Tanaka T., & Nakato Y., (2004). Mechanism for visible light responses in anodic photocurrents at N-doped TiO<sub>2</sub> film electrodes. *The Journal of Physical Chemistry B*, 108 (30), 10617 – 10620.
- Nano-Zone FAQ. (n.d.). Retrieved October 5, 2013, from <http://www.nano-zone.net/faq.php>.
- Niederberger, M., & Pinna, N. (2009). *Metal oxide nanoparticles in organic solvents engineering materials and processes* (1st edition). London: Springer.
- Nimetoğlu, Z. (2011). *Yeni nesil fotokatalitik filmlerin üretilmesi ve atıksulardaki organik kirleticilerin temizlenmesinde kullanılması*. Dissertation Thesis Dokuz Eylül University, Izmir, Turkey.
- Ohtani, B. (2010). Photocatalysis A to Z—what we know and what we do not know in a scientific sense. *Journal of Photochemistry and Photobiology C: Photochemistry Reviews*, 11, 157-178.
- Oner, G. (2014) *Seventh progress report for Phd thesis studies photocatalytic oxidation of pollutants*. Dokuz Eylül University, Izmir, Turkey.
- Osterloh, F.E., (2008). Inorganic materials as catalysts for photochemical splitting of water. *Chemistry of Materials*, 20, 35–54.
- Özkan, E. (2004). *Fotokatalitik yüzeylerin kaplama yoluyla elde edilmesi ve bir potansiyel uygulanması*. Dissertation Thesis Istanbul Technical University, İstanbul, Turkey.

- Pala, A. (2010). *Veri Değerlendirme ders notları*. Dokuz Eylül University Environmental Engineering Department.
- Pala, A., Çelik, E., Kurşun, G., & Bakal, F. (2013). *Tübitak araştırma projesi gelişme raporu 2*.
- Pardeshi, S.K., & Patil, A.B. (2008). A simple route for photocatalytic degradation of phenol in aqueous zinc oxide suspension using solar energy. *Solar Energy*, 82 (8), 700-705.
- Photocatalysis*. (n.d.). Retrieved 10 March, 2012 from <http://dev.nsta.org/evwebs/1952/photocatalysis.htm>.
- Pilato, L. (Ed.). (2010). *Phenolic resins: A century of progress: a century of progress*, (1st ed.). Verlag Berlin Heidelberg; Springer.
- Qui, X., Alvarez, P.J.J., Li, Q. (2012). Applications of nanotechnology in water and wastewater treatment. *Water Research*, 47 (12), 3931-3946.
- Rizzo, L., Koch, J., Belgiorno, V., & Anderson, M.A. (2007). Removal of methylene blue in a photocatalytic reactor using polymethylmethacrylate supported TiO<sub>2</sub> nanofilm. *Desalination*, 211 (1-3), 1-9.
- Sancinetti, G. P., Sader, L.T., Varesche, B.A., Amorim, E.L.C., Omena, S.P.F., & Silva, E.L. (2010). Phenol degradation in an anaerobic fluidized bed reactor packed with low density support materials. *Brazilian Journal of Chemical Engineering*, 29 (01), 87 - 98.
- Sandoval, R., Cooper, A.M., Aymar, K., Jain, A., & Hristovski, K. (2011). Removal of arsenic and methylene blue from water by granular activated carbon media impregnated with zirconium dioxide nanoparticles. *Journal of Hazardous Materials*, 193, 296-303.

- Sayılkan, F. (2007). *Nano-TiO<sub>2</sub> fotokatalizör sentezi ve fotokatalitik aktivitesinin belirlenmesi*. Doctoral Dissertation, Graduate School of Natural and Applied Sciences of İnönü University, Malatya, Turkey.
- Schimidti, H., & Mennig, M. (2000). *Wet coating technologies for glass*. Retrieved March 21, 2012, from <http://www.solgel.com/articles/Nov00/mennig.htm>.
- Selfcleaning*. (n.d.). Retrieved August 9, 2011, from [http://www.titanshield.co.il/en/p\\_selfcleaning\\_2.php](http://www.titanshield.co.il/en/p_selfcleaning_2.php).
- Shannon, (n.d.). *Titanium Dioxide (TiO<sub>2</sub>) photocatalysis in concrete*. Retrieved December 12, 2013, from [http://pavemaintenance.wikispaces.com/TiO<sub>2</sub>+Photocatalys++Shannon](http://pavemaintenance.wikispaces.com/TiO2+Photocatalys++Shannon).
- Shapley, P. (2012). *Intrinsic semiconductors*. Retrieved March 15, 2014, from <http://butane.chem.uiuc.edu/pshapley/GenChem2/C4/1.html>.
- Shen, Y.H. (2002). Removal of phenol from water by adsorption–flocculation using organobentonite. *Water Research*, 36 (5), 1107-1114.
- Smail, M., Didier, R., Weber J.V., Bouhelassa, M., & Benkhanouche, S., (2009). Photocatalytic degradation of indole in UV/TiO<sub>2</sub>: Optimization and modelling using the response surface methodology (RSM). *Environmental Chemistry Letters*, 7 (1), 45-49.
- Sobczyński, A., Duczmal, L., & Zmudziński, W., (2004). Phenol destruction by photocatalysis on TiO<sub>2</sub>: An attempt to solve the reaction mechanism. *Journal of Molecular Catalysis A: Chemical*, 213, 225-230.
- Sol gel technology*, (n.d.). Retrieved March 20, 2012, from <http://sariyusriati.wordpress.com/2008/10/21/sol-gel-technology/>.
- Spin coating*. (n.d.). Retrieved April 20, 2013 from [http://www.solarnenergy.com/kor/pr\\_service/analyst\\_show.php?sub\\_cat=&bbsId=4953&tbl=column](http://www.solarnenergy.com/kor/pr_service/analyst_show.php?sub_cat=&bbsId=4953&tbl=column).

*Su Kirliliği Kontrolü Yönetmeliği* (2004). Çevre ve Orman Bakanlığı, Ankara.

Suneel, S.D. (n.d.). *Nanotechnology Chapter 3: Synthesis and Processing of Nano Powders- Bottom-up approach*. Retrieved March 21, 2012, from <http://gitam.edu/eresource/nano/NANOTECHNOLOGY/bottamup%20app.htm>.

*Suntest CPS/CPS+Operating Manual*. (n.d.). Retrieved from [http://www.atlasmtt.net/ist/data/ger/manuals/UM\\_suntest\\_cps\\_plus.pdf](http://www.atlasmtt.net/ist/data/ger/manuals/UM_suntest_cps_plus.pdf).

Şam, E.D., Ürgen, M., & Tepehan, F.Z. (2007). TiO<sub>2</sub> fotokatalistleri. *İtüdergisi/d*, 6 (5-6), 81-92.

Takata, T., Shinohara, K., Tanaka, A., Hara, M., Kondo, J. N., & Domen, K. (1997). A highly active photocatalyst for overall water splitting with a hydrated layered perovskite structure. *Journal of Photochemistry and Photobiology A: Chemistry*, 106 (1-3), 45-49.

Tiginyanu, I., Langa, S., Foell, H., & Ursachi, V. (2009). *Porous III-V semiconductors*. Retrieved February 26, 2013, from <http://www.porous-35.com/electrochemistry-semiconductors-3.html>.

Toplan, N. (n.d.). *Sol - jel prosesi ile amorf malzeme üretimi*. Sakarya University Material and Metallurgical Engineering Department.

TS 6227 ISO 6439 (2005). *Phenol Index*.

Turhan, S., & Uzman, S., (2008). Removal of phenol from water using ozone. *Desalination*, 229 (1-3), 257-263.

Wang, B., Li, C., Hirabayashi, D., & K. Suzuki, (2010). Hydrogen evolution by photocatalytic decomposition of water under ultraviolet-visible irradiation over K<sub>2</sub>La<sub>2</sub>Ti<sub>3-x</sub>MxO<sub>10</sub><sup>+</sup> α perovskite. *International Journal of Hydrogen Energy*, 35, 3306-3312.

Wenguan, C., Li, L., Liangrong, F., Zijian, L., Shaojie, L., & Fali, Q. (2006). Preparation of Pt/K<sub>2</sub>La<sub>2</sub>Ti<sub>3</sub>O<sub>10</sub> and its photo-catalytic activity for hydrogen

- evolution from methanol water solution. *Science in China Series B*, 49 (2), 162-168.
- What is Photocatalyst?* (n.d.). Retrieved March 08, 2012 from [http://www.abolinco.com/downloads/downloads/What\\_is\\_Photocatalyst.pdf](http://www.abolinco.com/downloads/downloads/What_is_Photocatalyst.pdf).
- What is PVD coating?* (n.d.). Retrieved April 02, 2013, from <http://www.richterprecision.com/faq.html>.
- Madigan, J. (2011). *What wavelength goes with a color?* Retrieved 15, 2013 from [http://science-edu.larc.nasa.gov/EDDOCS/Wavelengths\\_for\\_Colors.html](http://science-edu.larc.nasa.gov/EDDOCS/Wavelengths_for_Colors.html).
- White, D.M., Pilon, T. A., & Woolard, C.(2000). Biological treatment of cyanide containing wastewater. *Water Research*, 34 (7), 2105-2109.
- Williams, E.A. (Ed.). (2007). *National association of broadcasters engineering handbook* (10th ed.), New York Elsevier Press.
- Yahui, Y., Qiyuan, C., & Jie, L. (2006). Photocatalytic activity of  $K_2La_2Ti_3O_{10}$  doped with boron for hydrogen production from water splitting. *Chinese Journal of Catalysts*, 30, 147-153.
- Yang, Y., Qiu, G., Chen, Q., Feng, Q., & Yin, Z., (2007). Influence of calcination atmosphere on photocatalytic reactivity of  $K_2La_2Ti_3O_{10}$  for water splitting. *Transactions of Nonferrous Metals Society of China*, 17 (4), 836-840.
- Yang, Y., Chen, Q., Yin, Z., & Li, Z. (2009). Study on the photocatalytic activity of  $K_2La_2Ti_3O_{10}$  doped with zinc (Zn). *Applied Surface Science*, 255, 8419–8424.
- Yang, Y., Chen, Q., Yin, Z., & Li, Y., (2009). Study on the photocatalytic activity of  $K_2La_2Ti_3O_{10}$  doped with vanadium (V). *Journal of Alloys and Compounds*, 488, 364–369.
- Yang, Y., Qui, G., Chen, Q., Feng, Q., & Yin, Z. (2007). Influence of calcination atmosphere on photocatalytic reactivity of  $K_2La_2Ti_3O_{10}$  for water splitting. *Transactions of Nonferrous Metals Society of China*, 17 (4), 836-840.



- Yao, J., & Wang, C. (2010). Decolorization of methylene blue with TiO<sub>2</sub> sol via UV irradiation photocatalytic degradation. *International Journal of Photoenergy*, 2010, 6-12.
- Yaşar, S. B., & Özcan, M. (2004). Metilen mavisinin çözücü ekstraksiyonu ile sulu çözeltilerden geri kazanımı. *Balıkesir Üniversitesi Fen Bilimleri Enstitüsü Dergisi*, 6 (2), 51 - 58.
- Yazıcı, D., (2007). *Fosfin metal komplekslerinin fiziksel özellikleri*, Çukurova Üniversitesi Graduate School of Natural and Applied Sciences, Physics Department Doctoral Thesis, Adana.
- Yeddou, A.R., Chergui, S., Chergui, A., Halet, F., Hamza, A.,Nadjemi, B., et al. (2011). Removal of cyanide in aqueous solution by oxidation with hydrogen peroxide in presence of copper-impregnated activated carbon. *Minerals Engineering*, 24 (8), 788-793.
- Yiğit, Z. (2008). *Fotokatalitik arıtmanın doğal organik madde karakterizasyonu ve dezenfeksiyon yan ürünlerine etkisi*. Graduate School of Natural and Applied Sciences of Anadolu University, Eskişehir, Turkey.
- Yuelin, W., Yunfang, H., Haiting, C., & Jihuai, W. (2008). Effect of tantalum substitution for titanium in layered perovskite type K<sub>2</sub>La<sub>2</sub>Ti<sub>3</sub>O<sub>10</sub> photocatalytic property. *Chinese Journal of Materials Research*, 1, 20-24.
- Zhaohui, L., Po-Hsiang, C., Wei-Teh, J., Jiin-Shuh, J., & Hanlie, H. (2011). Mechanism of methylene blue removal from water by swelling clays. *The Chemical Engineering Journal*, 168, 1193-1200.
- Zhu, K., Ren, X., Wei, J., Duan, X., Yao, L., & Zhao, R. (2011). Effective removal of sulphide and cyanide from coking wastewater. *Energy Procedia*, 11, 4687-4695.

## APPENDICES

### Appendix - A ANOVA TESTS RESULTS

#### A.1 Minitab Results of Phenol

##### A.1.1 General Linear Model: Results versus A (pH); B (Co); D (light intensity)

Table A.1 Three Factors Two Replicates Factorial Design for Phenol

Number	A	B	D	AB	AD	BD	ABD	Y
1	-	-	-	+	+	+	-	17.6
2	-	-	-	+	+	+	-	17.8
3	+	-	-	-	-	+	+	23.9
4	+	-	-	-	-	+	+	21.8
5	-	+	-	-	+	-	+	28.84
6	-	+	-	-	+	-	+	18.84
7	+	+	-	+	-	-	-	14.55
8	+	+	-	+	-	-	-	19.61
9	-	-	+	+	-	-	+	29.1
10	-	-	+	+	-	-	+	37.8
11	+	-	+	-	+	-	-	23.5
12	+	-	+	-	+	-	-	36.1
13	-	+	+	-	-	+	-	11.84
14	-	+	+	-	-	+	-	40.04
15	+	+	+	+	+	+	+	34.42
16	+	+	+	+	+	+	+	39.86

Factor	Type	Levels	Values
A (pH)	fixed	2	7; 10
B (Co)	fixed	2	10; 100
D (light)	fixed	2	250; 750

##### Analysis of Variance for Results, using Adjusted SS for Tests

Source	DF	Seq SS	Adj SS	Adj MS	F	F( $\alpha=0,05$ )	
A (pH)	1	8,82	8,82	8,82	0,12	< 5,32	accept
B (Co)	1	0,01	0,01	0,01	0,00	< 5,32	accept
D (light)	1	503,10	503,10	503,10	6,77	> 5,32	reject
A (pH)*B (Co)	1	2,16	2,16	2,16	0,03	< 5,32	2 factor
B (Co)*D (light)	1	0,07	0,07	0,07	0,00	< 5,32	interaction
A (pH)*D (light)	1	20,98	20,98	20,98	0,28	< 5,32	failed
A (pH)*B (Co)*D (light)	1	179,02	179,02	179,02	2,41	< 5,32	3 factor
Error	8	594,67	594,67	74,33			interaction
Total	15	1308,84					failed

Source	P	
A (pH)	0,739 > 0,05	means are same.
B (Co)	0,991 > 0,05	means are same.
C (light)	0,032 < 0,05	means are not same.
A (pH) *B (Co)	0,869 > 0,05	means are same.
B (Co) *C (light)	0,976 > 0,05	means are same.
A (pH) *C (light)	0,610 > 0,05	means are same.
A (pH) *B (Co) *C (light)	0,159 > 0,05	means are same.

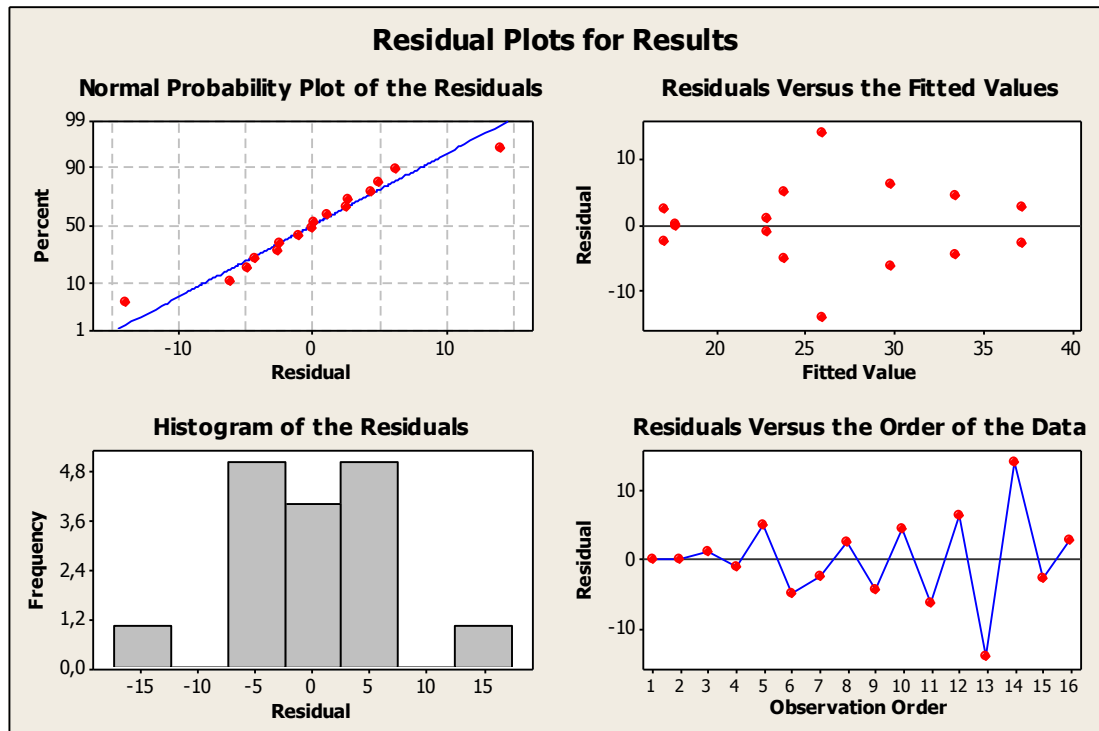


Figure A..1 Residual Plots for Results.

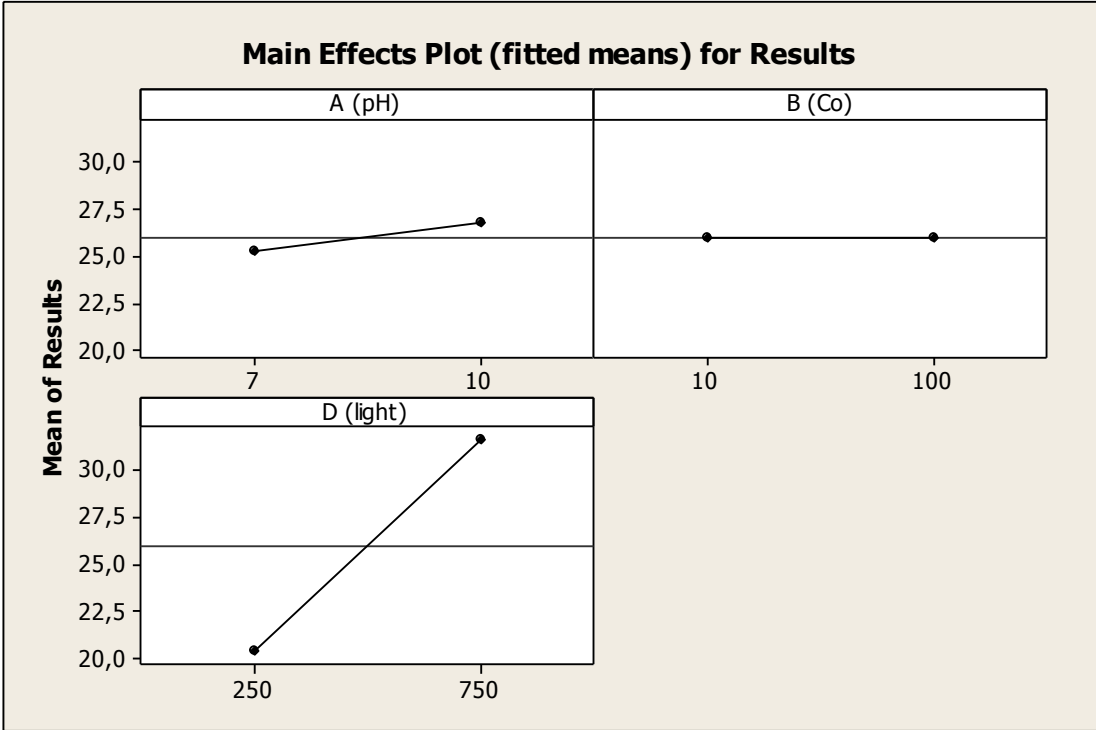


Figure A.2 Main Effects Plot (fitted means) for Results.

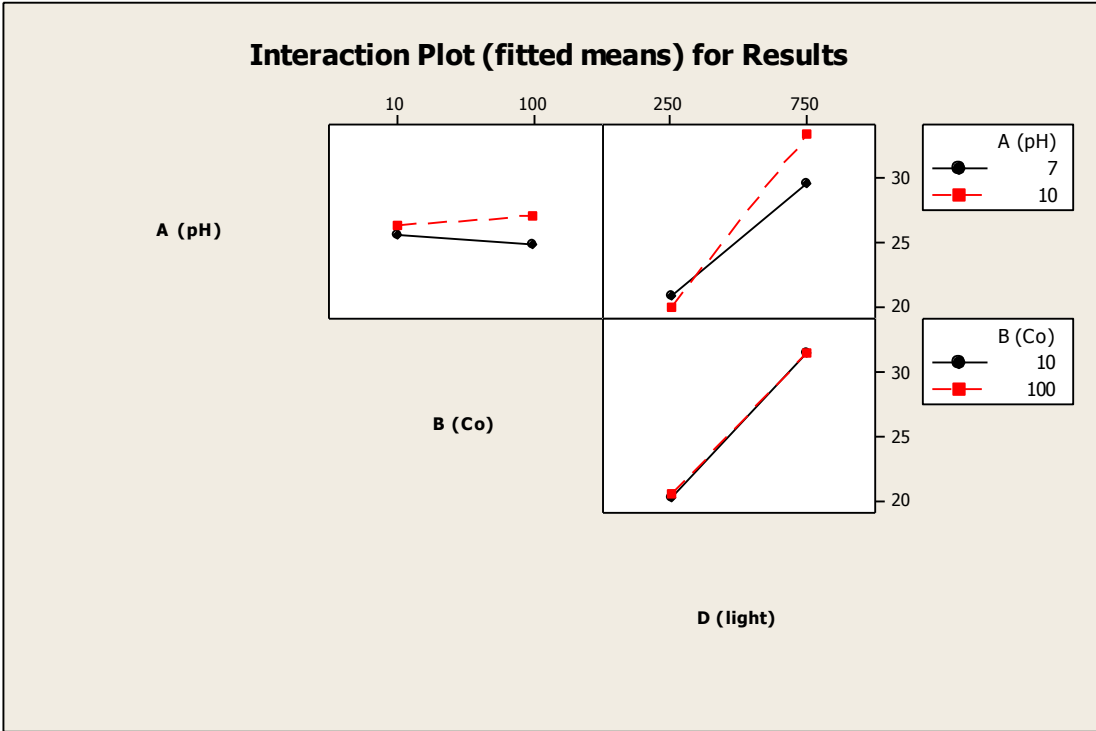


Figure A.3 Interaction Plot (fitted means) for Results.

## A.2 Minitab Results of Methylene Blue

### A.2.1 General Linear Model: Respons versus A (pH); Light intensity

Table A.2 Two Factors Two Replicates Factorial Design for Methylene Blue

	250 W/m <sup>2</sup>	750 W/m <sup>2</sup>
pH = 3	62.09	96.08
	65.88	95.69
pH = 7	65,36	94.77
	64.84	95.69
pH = 10	91.24	98.43
	92.81	99.87

Factor	Type	Levels	Values
A (pH)	fixed	3	3; 7; 10
Light	fixed	2	250; 750

#### Analysis of Variance for Respons, using Adjusted SS for Tests

Source	DF	Seq SS	Adj SS	Adj MS	F	F (α=0,05)	
A (pH)	2	643,88	643,88	321,94	191,52	> 5,14	H <sub>01</sub> = reject
Light	1	1594,14	1594,14	1594,14	948,35	> 5,99	H <sub>02</sub> = reject
A (pH)*Light	2	382,05	382,05	191,03	113,64	> 5,14	H <sub>03</sub> = reject
Error	6	10,09	10,09	1,68			
Total	11	2630,15					

Reject null hypothesis

Source	P	
A (pH)	0,000 > 0,05	means are different.
B (light)	0,000 > 0,05	
A (pH)*B (light)	0,000 > 0,05	

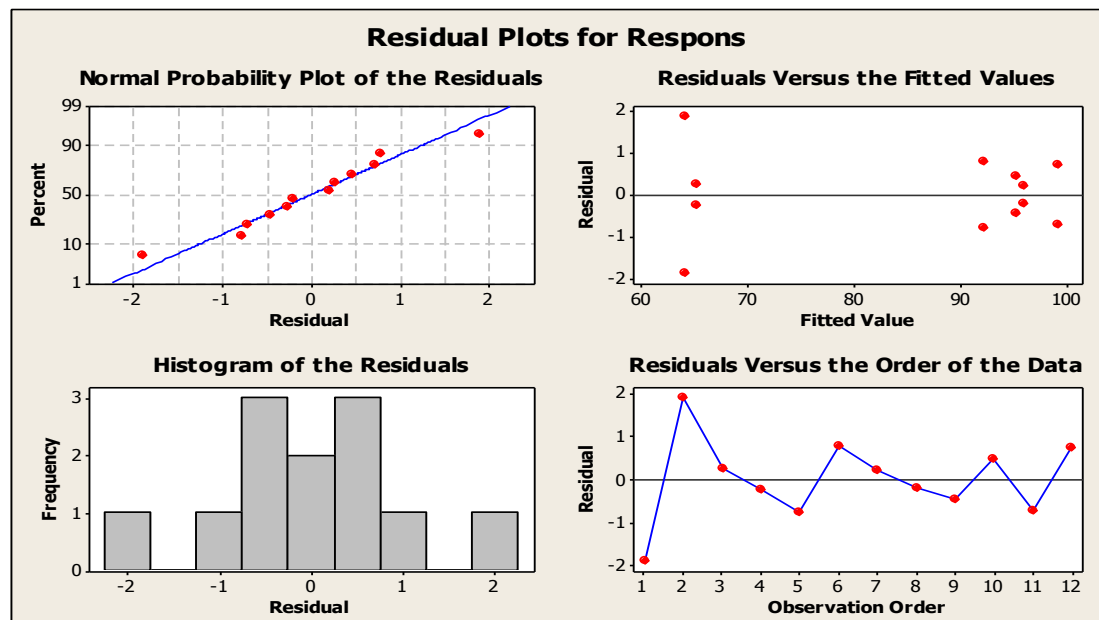


Figure A.4 Residual Plots for Respons.

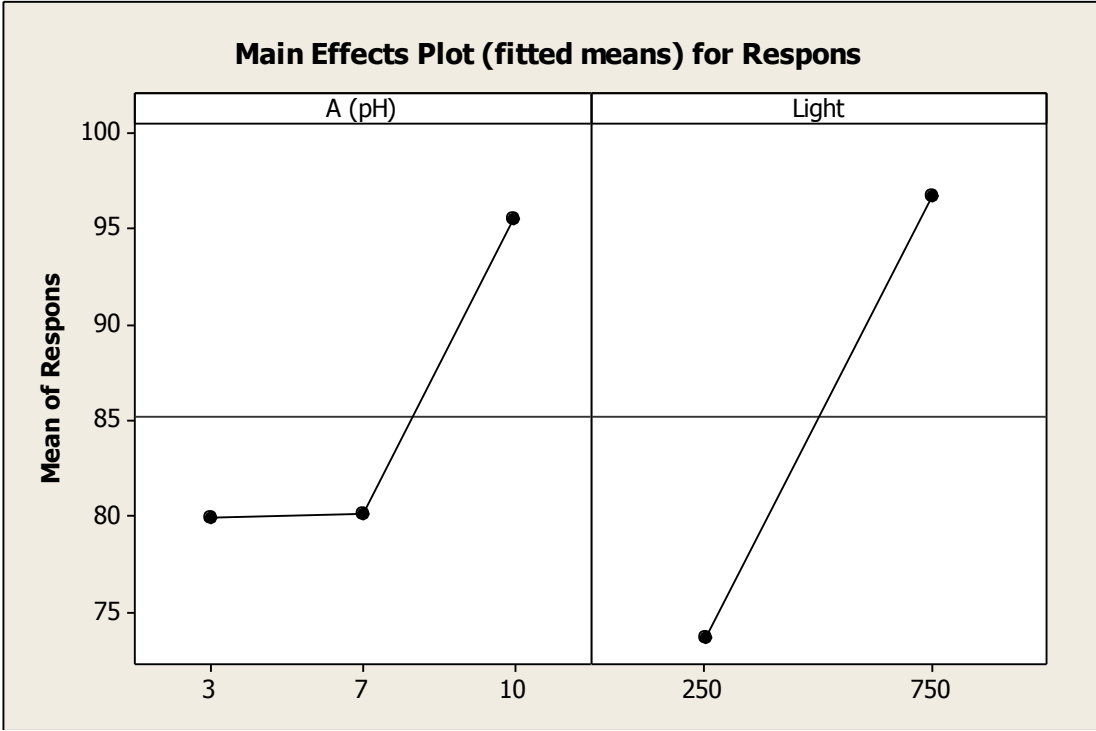


Figure A.5 Main Effects Plot (fitted means) for Respos.

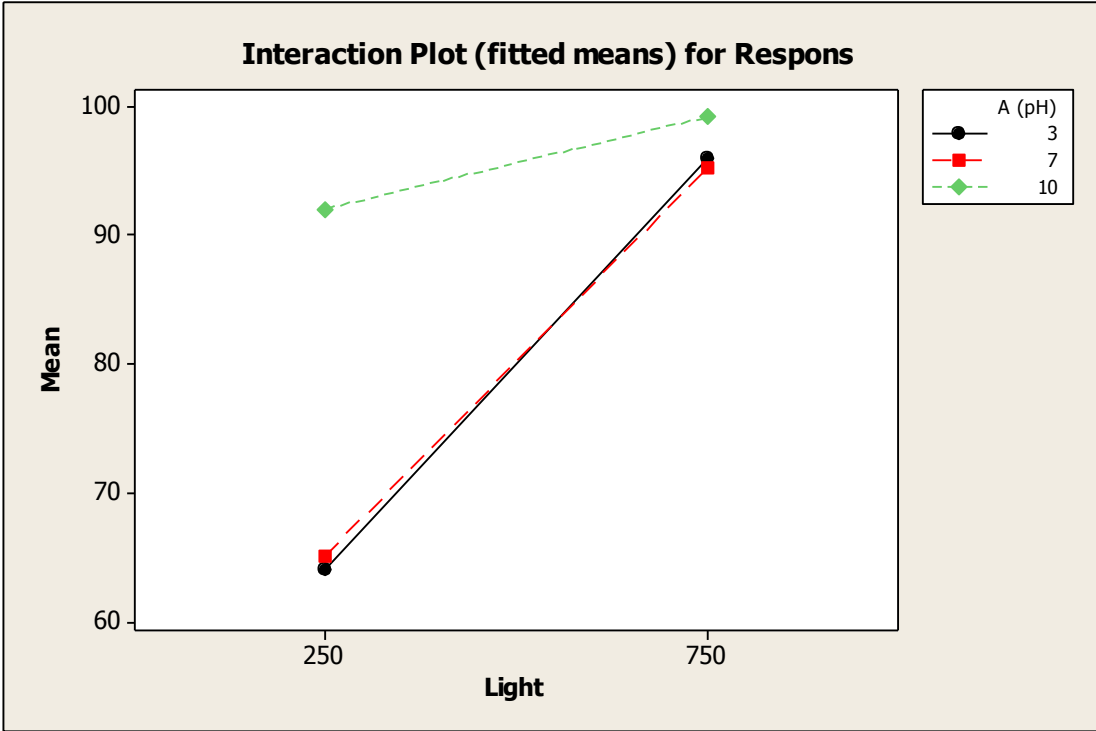


Figure A. 6 Interaction Plot (fitted means) for Respos.

### A.3 Minitab Results of Cyanide

#### A.3.1 General Linear Model: Results versus pH (A); Concentration (B); Light intensity (C)

Factor	Type	Levels	Values
pH (A)	fixed	2	10; 12
Concentration (B)	fixed	2	100; 300
Light intensity (C)	fixed	2	250; 750

#### Analysis of Variance for Results, using Adjusted SS for Tests

Source	DF	Seq SS	Adj SS	Adj MS	F	F( $\alpha=0,05$ )
pH (A)	1	3,67	3,67	3,67	1,81	< 5,32 accept
Concentration (B)	1	71,32	71,32	71,32	35,17	> 5,32 reject
Light intensity (C)	1	836,94	836,94	836,94	412,69	> 5,32 reject
pH (A)*Concentration (B)	1	7,05	7,05	7,05	3,48	< 5,32 accept
Concentration (B)* Light intensity (C)	1	45,02	45,02	45,02	22,20	> 5,32 reject
pH (A)*Light intensity (C)	1	0,85	0,85	0,85	0,42	< 5,32 accept
pH (A)*Concentration (B)* Light intensity (C)	1	7,08	7,08	7,08	3,49	< 5,32 accept
Error	8	16,22	16,22	2,03		
Total	15	988,15				

Source	P
pH (A)	0,216 > 0,05 cannot reject null hypothesis
Concentration (B)	0,000 < 0,05 reject null hypothesis
Light intensity (C)	0,000 < 0,05 reject null hypothesis
pH (A)*Concentration (B)	0,099 > 0,05 cannot reject null hypothesis
Concentration (B)* Light intensity (C)	0,002 < 0,05 reject null hypothesis
pH (A)*Light intensity (C)	0,536 > 0,05 cannot reject null hypothesis
pH (A)*Concentration (B)* Light intensity (C)	0,099 > 0,05 cannot reject null hypothesis

Table A.3 Three Factors Two Replicates Factorial Design for Cyanide

Number	A	B	C	AB	AC	BC	ABC	Y
1	-	-	-	+	+	+	-	90.40
2	-	-	-	+	+	+	-	89.70
3	+	-	-	-	-	+	+	86.90
4	+	-	-	-	-	+	+	85.05
5	-	+	-	-	+	-	+	82.01
6	-	+	-	-	+	-	+	77.62
7	+	+	-	+	-	-	-	82.01
8	+	+	-	+	-	-	-	80.10
9	-	-	+	+	-	-	+	99.87
10	-	-	+	+	-	-	+	99.77
11	+	-	+	-	+	-	-	99.75
12	+	-	+	-	+	-	-	98.00
13	-	+	+	-	-	+	-	98.87
14	-	+	+	-	-	+	-	98.14
15	+	+	+	+	+	+	+	98.51
16	+	+	+	+	+	+	+	97.50

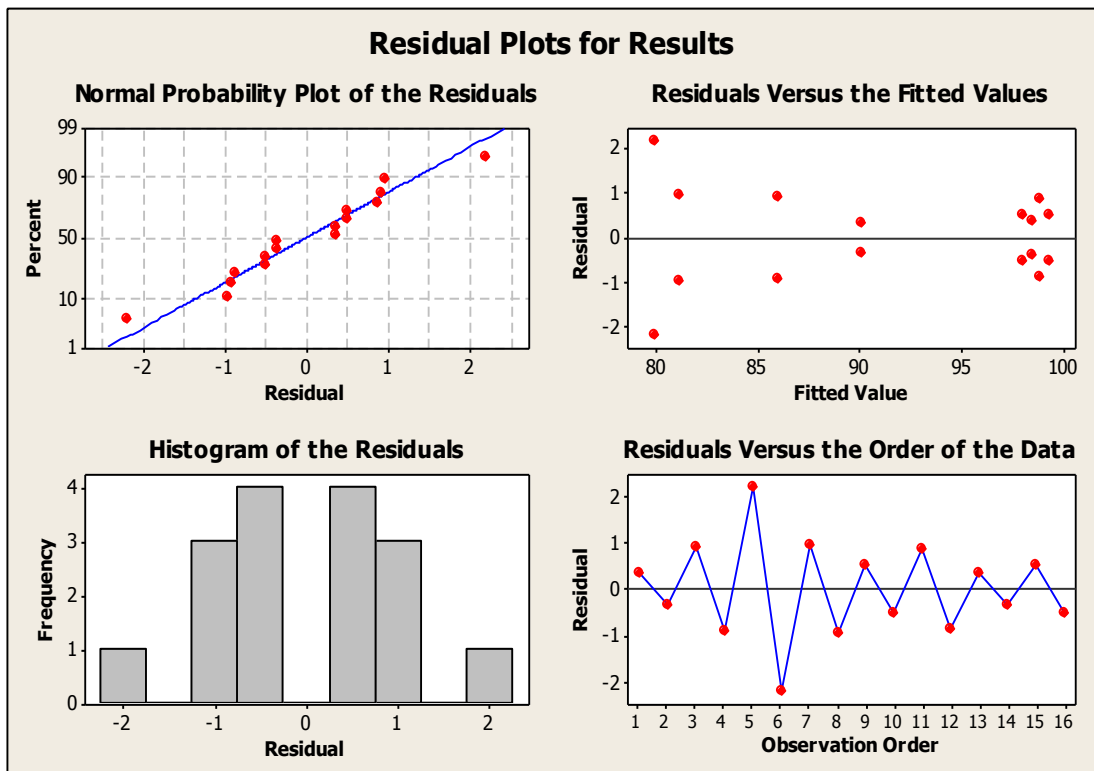


Figure A.7 Residual Plots for Results.

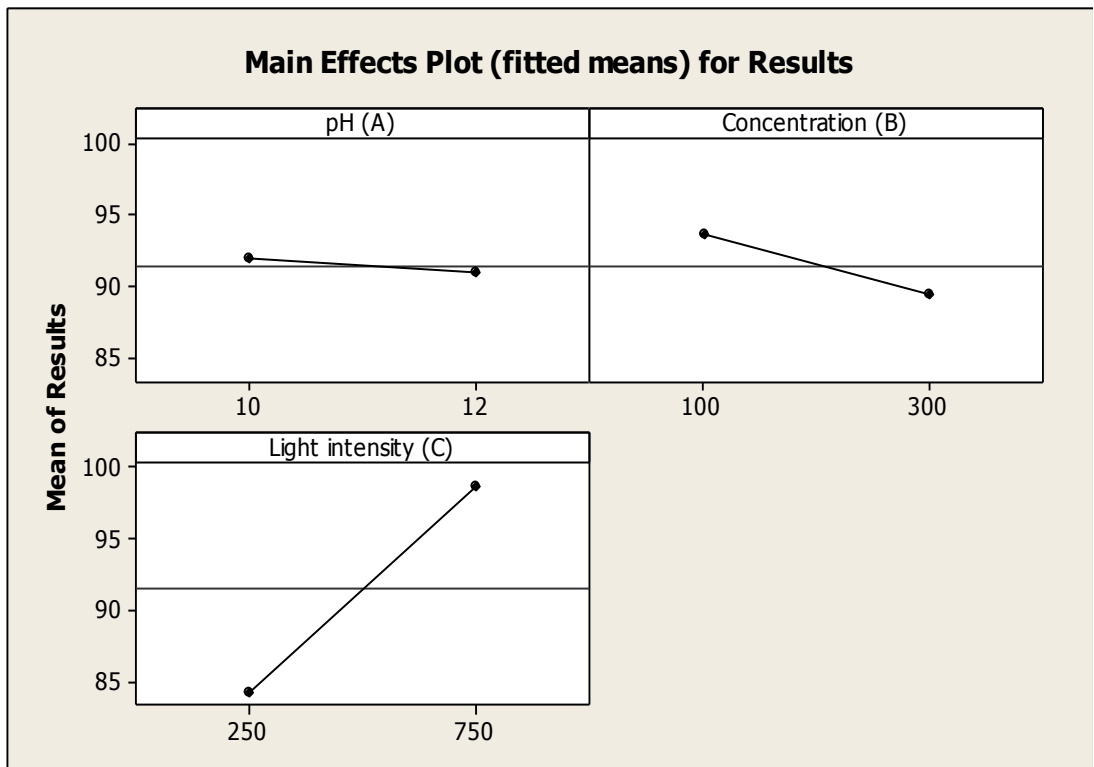


Figure A.8 Main Effects Plot (fitted means) for Results.



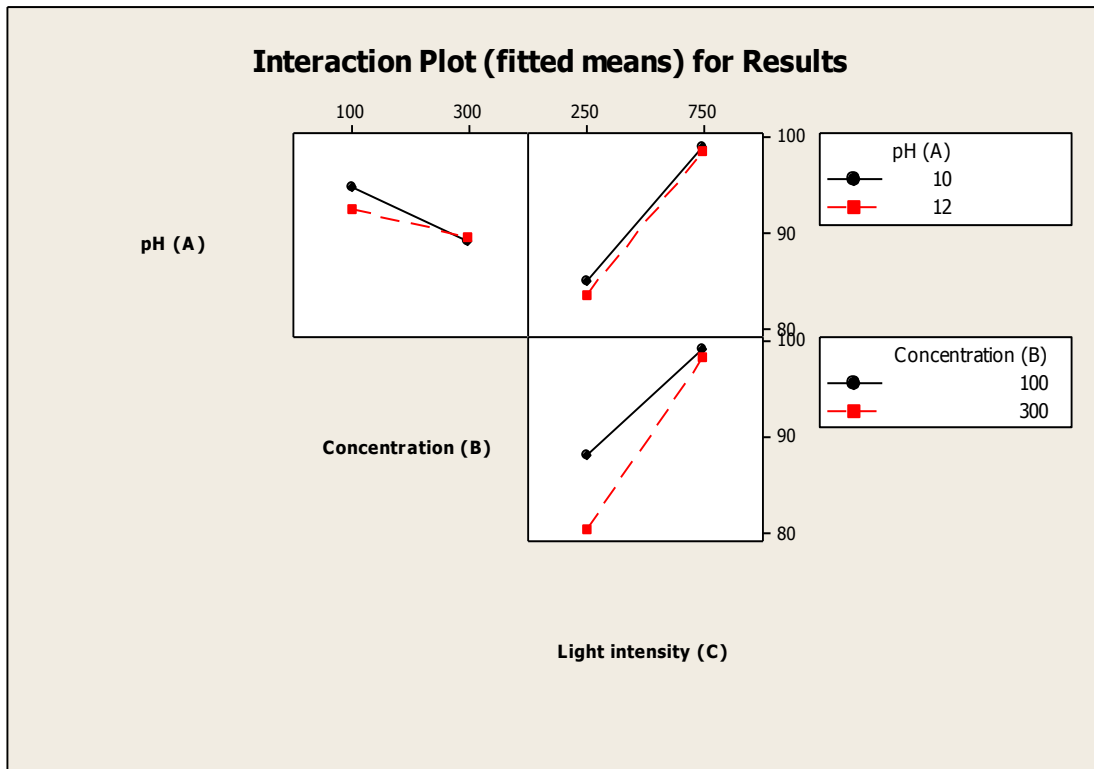


Figure A.9 Interaction Plot (fitted means) for Results.

## **Appendix - B ATLAS SUNTEST CPS + Standard**

- **ASTM D3424** Standard Test Methods for Evaluating the Relative Lightfastness and Weatherability of Printed Matter
- **ASTM D5071** Standard Practice for Exposure of Photodegradable Plastics in a Xenon Arc Apparatus
- **ASTM D6695** Standard Practice for Xenon-Arc Exposures of Paint and Related Coatings
- **ASTM G151** Standard Practice for Exposing Nonmetallic Materials in Accelerated Test Devices that Use Laboratory Light Sources
- **ASTM G155** Standard Practice for Operating Xenon Arc Light Apparatus for Exposure of Non-Metallic Materials
- **ASTM G155** Standard Practice for Operating Xenon Arc Light Apparatus for Exposure of Non-Metallic Materials
- **COLIPA 2011** METHOD FOR THE IN VITRO DETERMINATION OF UVA PROTECTION PROVIDED BY SUNSCREEN PRODUCTS
- **COLIPA 2011** METHOD FOR THE IN VITRO DETERMINATION OF UVA PROTECTION PROVIDED BY SUNSCREEN PRODUCTS
- **DIN EN ISO 4892-2** Plastics - Methods of exposure to laboratory light sources - Part 2: Xenon-arc sources
- **Final Rule FDA-1978-N-0018** Labeling and Effectiveness Testing; Sunscreen Drug Products for Over-the-Counter Human Use
- **ICH Guideline Q1B** Guideline for the photostability testing of new drug substances and products
- **ICH Guideline Q1B** Guideline for the photostability testing of new drug substances and products
- **ISO 10977** Photography - Processed photographic color films and paper prints - Methods for measuring image stability
- **ISO 11431** Building construction - Jointing products - Determination of adhesion/cohesion properties of sealants after exposure to heat, water and artificial light through glass

- **ISO 11979-5** Ophthalmic implants - Intraocular lenses - Part 5: Biocompatibility
- **ISO 4049** Dentistry. Polymer-base filling, restorative and luting materials
- **ISO 4892-1** Plastics - Methods of exposure to laboratory light sources - Part 1: General guidance
- **ISO 4892-2** Plastics - Methods of exposure to laboratory light sources - Part 2: Xenon-arc sources
- **ISO 7491** Dental materials - Determination of colour stability
- **ISO/DIS 24443** Determination of sunscreen UVA photoprotection in vitro
- **VICH GL4** Guideline on Stability Testing - Photostability Testing of New Veterinary Drug Substances and Medicinal Products

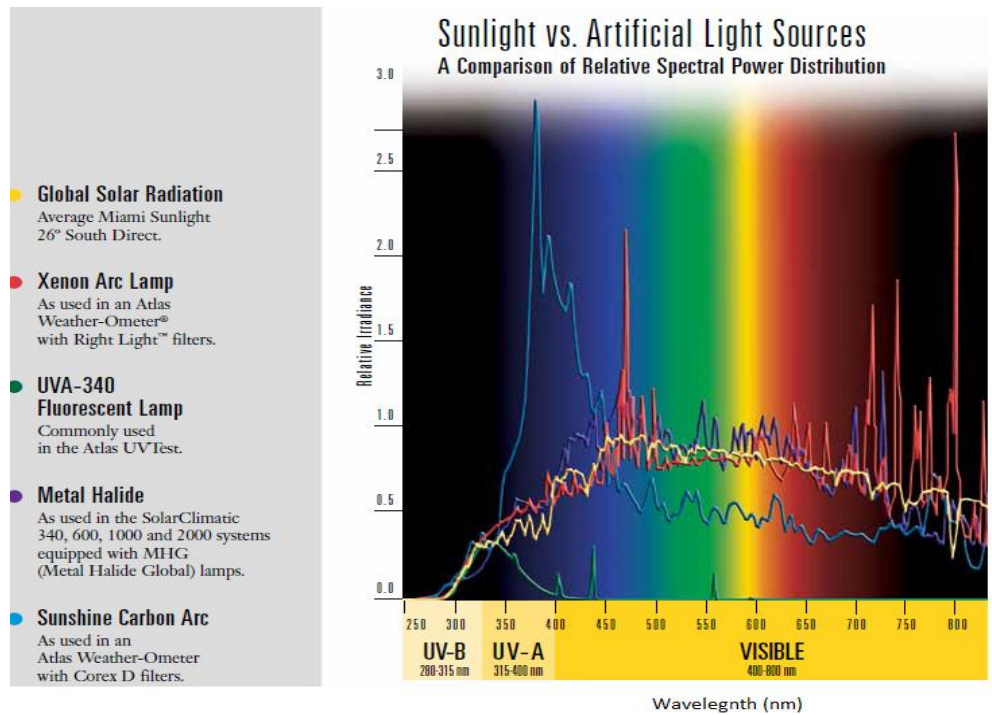


Figure B.1 Sunlight vs. Artificial Light Sources equivalent

## Appendix - C PHENOL AND CYANIDE STANDARDS

### PHENOL INDEX (TS 6227 ISO 6439:2005) DIRECT COLORIMETRIC METHOD

Phenol solution is prepared according to standard (HACH), Lot: A0034, Exp: Feb-13. This method provides to measure colorimetrically phenolic compounds (containing affixes such as carboxyl, halogen, hydroxyl, methoxy, sulphonic acid) which react with 4 - aminoantipyrine as forming colorific compounds and to find the phenol index.

Phenolic compounds are distilled to separate the impurities and the protective materials. The evaporation of the phenolic compounds should be slow. When the pH is  $10 \pm 0.2$  with the presence of the potassium hexacyanoferrate (III), the colorific antipyrine dye is produced by the reaction between phenolic compounds and 4 - aminoantipyrine. The absorbance of colored specimen is measured by the help of spectrophotometer at 510 nm. Phenol index is found as mg phenol ( $C_6H_5OH$ )/l. This method is suitable for the samples whose phenol index is bigger than 0.1 mg/l. The minimum determinable phenol amount is equivalent to 0.01 mg when 50 mm cell and 100 ml sample is used. Distillation apparatus, pH meter and spectrophotometer are using for this method.

#### Reagents:

- Aminoantipyrine solution ( $C_{11}H_{13}N_3O$ ),
- Ammonium chloride solution ( $NH_4Cl$ ),
- Ammonia solution ( $NH_3$  d = 0,90 g/ml),
- Potassium sodium tartrate (Potassium sodium 2,3 - dihydroxybutanedioate (buffer solution)) ( $NaKC_4H_4O_6$ ),
- Copper (II) sulfate pentahydrate solution ( $CuSO_4 \cdot 5H_2O$ ),
- Hydrochloric acid,
- Methyl orange indicator,
- Phenol stock solution (1 g/l  $C_6H_5OH$ ),

- Standard phenol solution (0.01 g/l),
- Standard phenol solution (0.001 g/l),
- Concentrated phosphoric acid (d=1.70 g/ml),
- Phosphoric acid solution,
- Potassium hexacyanoferrite (III) (Potassium ferricyanide) solution ( $K_3Fe(CN)_6$ ),
- Sodium sulfate ( $Na_2SO_4$ , dehydrated, granular),
- Some special reagents; sulphuric acid solution, sodium chloride, sodium hydroxide solution, chloroform ( $CHCl_3$ ).

Samples should be collected in glass bottles. Phenolic compounds in water are exposed to chemical and biochemical oxidation. That is why, if the samples do not analyze within 4 hours, some protective measures should be taken. For example, pH is arranged nearly 4 with addition of phosphoric acid, to prevent the biochemical oxidation, copper (II) sulfate can be added. The samples are kept cool (5 - 10°C) and should be analyze within 24 hours.

100 ml phenol solution is transferred to volumetric flask. To regulate the pH value between 1 and 2, phosphoric acid solution is added (2 - 3 drops). Glass beads are putted in the volumetric flask to provide homogeny boiling. The flask is placed in the distillation apparatus. When 75 ml solution is collected in the beaker, the heater is closed. After the cooling, 25 ml purified water is added into the flask and the heater is reopened until 100 ml distillate is collected. To make the comparison with spectrophotometer, the same process is done but instead of the sample, the purified water is used.

5 ml buffer solution or 5 ml  $NH_4Cl$  solution is added to 100 ml distillate and to adjust the pH between 9 and 10, ammonia solution put in. 2 ml 4 - aminoantipyrin is mixed and blended. After that, 2 ml potassium ferricyanide ( $K_3Fe(CN)_6$ ) solution is added and stirred. The higher absorbance is read at 510 nm. The absorbance readings are done 15 minutes later. Water is using for the reference cell. According to the calibration graph, the phenol content of the sample is estimated.

Waters can include some aliasing distortions such as the bacteria that can degrade the phenol, oxidizing or reducing agents and strong alkali properties of the samples. Biological degradation can prevent with the addition of copper (II) sulfate. The acidic conditions with respect to phosphoric acid can reveal the copper (II) and avoid the chemical changes in strong alkali conditions. Some protective methods are used to avoid the aliasing distortions.

$$\text{Phenol Index, mg/l} = \frac{m}{V_0} \times 1000$$

m = The equivalent phenol amount from calibration graph (mg)

V<sub>0</sub> = Test sample volume of distilled (ml)

Reference: TS 6227 ISO 6439/March 2005

## **THE DETERMINATION OF TOTAL CYANIDE STANDARD METHOD 4500 C/E:2005**

### **TOTAL CYANIDE STANDARD METHOD 4500 - CN<sup>-</sup> C**

HCN can be released by distillation and air cleaning from acidic sample. HCN gas is collected through NaOH solution. The cyanide concentration can be determined by titrimetric and colorimetric procedures. Boiling flask, inlet tube, water-cooled condenser, gas absorber, gas dispersion tube, heating element are used as apparatus.

Reagents:

- NaOH solution,
- MgCl<sub>2</sub> reagent (optional): MgCl<sub>2</sub>.6H<sub>2</sub>O,
- H<sub>2</sub>SO<sub>4</sub> 1+1,
- PbCO<sub>3</sub>,
- Sulphamic acid (NH<sub>2</sub>SO<sub>3</sub>H).

### **STANDARD METHOD 4500-CN<sup>-</sup> E. COLORIMETRIC METHOD**

CN<sup>-</sup> within the alkali distillate from preliminary preparation step transformed to CNCl with chloramines - T reaction but without hydrolyze to CNO<sup>-</sup> under pH<8

condition. After the completion of the reaction, CNCl constitutes to a red - blue color form by the addition of pyridine - barbituric acid reagent. CN<sup>-</sup> concentration is determined at 578 nm by using a spectrophotometer. This method is applied to samples whose concentrations are bigger than 1 mg/l. Interferences were removed or minimized with distillation.

Reagents:

- Chlorine - amine - T solution,
- Cyanide stock solution,
- Standard silver nitrate solution (AgNO<sub>3</sub>),
- Standard cyanide solution,
- Pyridine - barbituric acid reagent,
- Astatine buffer (NaC<sub>2</sub>H<sub>3</sub>O<sub>2</sub>.3H<sub>2</sub>O),
- NaOH dilute solution.

A tube which contains 0.1 N NaOH is putted to the end of the portion of the distillation apparatus. Glass bead is added to CN<sup>-</sup> flask to provide the homogeny. The heater is fixed to 100<sup>0</sup>C for 1 hour. The perimeters are flushed with some reagent. The tube which is at the end of the apparatus contains CN<sup>-</sup> and this CN<sup>-</sup> is transformed to NaOH solution and diluted. A far amount of absorption solution is putted to 50 ml volumetric flask with pipette. 1 ml acetate buffer and 2 ml chlorine - amine - T solution is added and mixed. 2 minutes is allowed to precipitate. 5 ml pyridine - barbituric acid reagent is putted and completed with distilled water and waited 8 minutes. The absorbance is estimated at 578 nm. The same process is done for reference. Instead of using sample, 40 ml diluted water is putted.

#### **THE DETERMINATION OF METHYLENE BLUE (LABORATORY METHOD)**

Methylene blue is determined in certain wavelength by measuring the color as absorbance with using a spectrophotometer. The solubility of methylene blue at room temperature is 4 g/l, and in methanol the solubility is 15 g/l. Practically, 10<sup>-5</sup> M of methylene blue is preferable. The experiments are examined at 664 nm. This wavelength is a part of visible spectrum.

## Appendix - D MSDS

### MSDS of POLLUTANTS and TiO<sub>2</sub> PHOTOCATALYS

**Titanium(IV) oxide - nanopowder, 21 nm particle size (TEM), ≥99.5% trace metals basis**

Aldrich - 718467

**SIGMA-ALDRICH** *sigma-aldrich.com*

#### SAFETY DATA SHEET

According to Regulation (EC) No. 1907/2006

Version 5.1 Revision Date 29.03.2013

Print Date 18.02.2014

GENERIC EU MSDS - NO COUNTRY SPECIFIC DATA - NO OEL DATA

#### **SECTION 1: Identification of the substance/mixture and of the company/undertaking**

##### **1.1 Product identifiers**

Product name: Titanium(IV) oxide

Product Number: 718467

Brand: Aldrich

REACH No. : A registration number is not available for this substance as the substance or its uses are exempted from registration, the annual tonnage does not require a registration or the registration is envisaged for a later registration deadline.

CAS-No. : 13463-67-7

##### **1.2 Relevant identified uses of the substance or mixture and uses advised against**

Identified uses: Laboratory chemicals, Manufacture of substances

##### **1.3 Details of the supplier of the safety data sheet**

Company: Sigma-Aldrich Chemie GmbH Riedstrasse 2 D-89555 STEINHEIM

Telephone: +49 89-6513-1444

Fax: +49 7329-97-2319

E-mail address: eurtechserv@sial.com

##### **1.4 Emergency telephone number**

Emergency Phone #: +49 7329-97-2323

#### **SECTION 2: Hazards identification**



## **2.1 Classification of the substance or mixture**

Not a hazardous substance or mixture according to Regulation (EC) No. 1272/2008.

This substance is not classified as dangerous according to Directive 67/548/EEC.

## **2.2 Label elements**

The product does not need to be labelled in accordance with EC directives or respective national laws.

## **2.3 Other hazards - none**

## **SECTION 3: Composition/information on ingredients**

### **3.1 Substances**

Formula: O<sub>2</sub>Ti

Molecular Weight: 79,87 g/mol

CAS-No. : 13463-67-7

EC-No. : 236-675-5

No components need to be disclosed according to the applicable regulations.

## **SECTION 4: First aid measures**

### **4.1 Description of first aid measures**

#### **General advice**

Consult a physician. Show this safety data sheet to the doctor in attendance.

#### **If inhaled**

If breathed in, move person into fresh air. If not breathing, give artificial respiration.

Consult a physician.

#### **In case of skin contact**

Wash off with soap and plenty of water. Consult a physician.

#### **In case of eye contact**

Flush eyes with water as a precaution.

#### **If swallowed**

Never give anything by mouth to an unconscious person. Rinse mouth with water.

Consult a physician.

### **4.2 Most important symptoms and effects, both acute and delayed**

The most important known symptoms and effects are described in the labelling (see section 2.2) and/or in section 11

### **4.3 Indication of any immediate medical attention and special treatment needed**

no data available

## **SECTION 5: Firefighting measures**

### **5.1 Extinguishing media**

#### **Suitable extinguishing media**

Use water spray, alcohol-resistant foam, dry chemical or carbon dioxide.

### **5.2 Special hazards arising from the substance or mixture**

Titanium/titanium oxides

### **5.3 Advice for firefighters**

Wear self contained breathing apparatus for fire fighting if necessary.

### **5.4 Further information**

no data available

## **SECTION 6: Accidental release measures**

### **6.1 Personal precautions, protective equipment and emergency procedures**

Use personal protective equipment. Avoid dust formation. Avoid breathing vapours, mist or gas. Ensure adequate ventilation. Avoid breathing dust.

For personal protection see section 8.

### **6.2 Environmental precautions**

Do not let product enter drains.

### **6.3 Methods and materials for containment and cleaning up**

Pick up and arrange disposal without creating dust. Sweep up and shovel. Keep in suitable, closed containers for disposal.

### **6.4 Reference to other sections**

For disposal see section 13.

## **SECTION 7: Handling and storage**

### **7.1 Precautions for safe handling**

Provide appropriate exhaust ventilation at places where dust is formed.

For precautions see section 2.2.

### **7.2 Conditions for safe storage, including any incompatibilities**

Store in cool place. Keep container tightly closed in a dry and well-ventilated place.

### **7.3 Specific end use(s)**

A part from the uses mentioned in section 1.2 no other specific uses are stipulated

## **SECTION 8: Exposure controls/personal protection**

## **8.1 Control parameters**

### **Components with workplace control parameters**

## **8.2 Exposure controls**

### **Appropriate engineering controls**

Handle in accordance with good industrial hygiene and safety practice. Wash hands before breaks and at the end of workday.

### **Personal protective equipment**

#### **Eye/face protection**

Safety glasses with side-shields conforming to EN166 Use equipment for eye protection tested and approved under appropriate government standards such as NIOSH (US) or EN 166(EU).

#### **Skin protection**

Handle with gloves. Gloves must be inspected prior to use. Use proper glove removal technique (without touching glove's outer surface) to avoid skin contact with this product. Dispose of contaminated gloves after use in accordance with applicable laws and good laboratory practices.

Wash and dry hands.

The selected protective gloves have to satisfy the specifications of EU Directive 89/686/EEC and the standard EN 374 derived from it.

Full contact

Material: Nitrile rubber

Minimum layer thickness: 0,11 mm

Break through time: 480 min

Material tested: Dermatril® (KCL 740 / Aldrich Z677272, Size M)

Splash contact

Material: Nitrile rubber

Minimum layer thickness: 0,11 mm

Break through time: 480 min

Material tested: Dermatril® (KCL 740 / Aldrich Z677272, Size M)

Data source: KCL GmbH, D-36124 Eichenzell, phone +49 (0)6659 87300, e-mail sales@kcl.de, test method: EN374

If used in solution, or mixed with other substances, and under conditions which differ from EN 374, contact the supplier of the CE approved gloves. This recommendation is advisory only and must be evaluated by an industrial hygienist and safety officer familiar with the specific situation of anticipated use by our customers. It should not be construed as offering an approval for any specific use scenario.

### **Body Protection**

Choose body protection in relation to its type, to the concentration and amount of dangerous substances, and to the specific work-place., The type of protective equipment must be selected according to the concentration and amount of the dangerous substance at the specific workplace.

### **Respiratory protection**

Respiratory protection is not required. Where protection from nuisance levels of dusts are desired, use type N95 (US) or type P1 (EN 143) dust masks. Use respirators and components tested and approved under appropriate government standards such as NIOSH (US) or CEN (EU).

### **Control of environmental exposure**

Do not let product enter drains.

## **SECTION 9: Physical and chemical properties**

### **9.1 Information on basic physical and chemical properties**

a) Appearance Form: powder

Colour: white

b) Odour: odourless

c) Odour: Threshold no data available

d) pH: no data available

e) Melting point/freezing point: Melting point/range: 1.850 °C

f) Initial boiling point and boiling range: no data available

g) Flash point: not applicable

h) Evaporation rate: no data available

i) Flammability (solid, gas): no data available

j) Upper/lower flammability or explosive limits: no data available

k) Vapour pressure: no data available

- l) Vapour density: no data available
- m) Relative density: no data available
- n) Water solubility: no data available
- o) Partition coefficient: noctanol/water: no data available
- p) Auto-ignition temperature: no data available
- q) Decomposition temperature: no data available
- r) Viscosity: no data available
- s) Explosive properties: no data available
- t) Oxidizing properties: no data available

## **9.2 Other safety information**

no data available

## **SECTION 10: Stability and reactivity**

### **10.1 Reactivity**

No data available

### **10.2 Chemical stability**

Stable under recommended storage conditions.

### **10.3 Possibility of hazardous reactions**

No data available

### **10.4 Conditions to avoid**

No data available

### **10.5 Incompatible materials**

Strong acids

### **10.6 Hazardous decomposition products**

Other decomposition products - no data available

In the event of fire: see section 5

## **SECTION 11: Toxicological information**

### **11.1 Information on toxicological effects**

#### **Acute toxicity**

LD50 Oral - rat - > 10.000 mg/kg

LD50 Dermal - rabbit - > 10.000 mg/kg

#### **Skin corrosion/irritation**

Skin - Human

Result: Mild skin irritation - 3 h

**Serious eye damage/eye irritation**

Eyes - rabbit

Result: No eye irritation

**Respiratory or skin sensitisation**

Will not occur

**Germ cell mutagenicity**

Hamster ovary

Micronucleus test

Hamster

Lungs

DNA inhibition

Hamster ovary

Sister chromatid exchange mouse

Micronucleus test

**Carcinogenicity**

Carcinogenicity - rat - Inhalation

Tumorigenic: Carcinogenic by RTECS criteria. Lungs, Thorax, or Respiration:  
Tumors.

Carcinogenicity - rat - Intramuscular

Tumorigenic: Neoplastic by RTECS criteria.

Blood: Lymphomas including Hodgkin's disease.

Tumorigenic: Tumors at site or application.

No data available

IARC: No component of this product presents at levels greater than or equal to 0.1%  
is identified as probable, possible or confirmed human carcinogen by IARC.

**Reproductive toxicity**

No data available

**Specific target organ toxicity - single exposure**

No data available

**Specific target organ toxicity - repeated exposure**

No data available

**Aspiration hazard**

No data available

**Additional Information**

RTECS: XR2275000

To the best of our knowledge, the chemical, physical, and toxicological properties have not been thoroughly investigated.

**SECTION 12: Ecological information****12.1 Toxicity**

Toxicity to fish LC50 - other fish - > 1.000 mg/l - 96 h

Toxicity to daphnia and other aquatic invertebrates:

EC50 - Daphnia magna (Water flea) - > 1.000 mg/l - 48 h

EC0 - Daphnia magna (Water flea) - 1.000 mg/l - 48 h

**12.2 Persistence and degradability**

No data available

**12.3 Bioaccumulative potential**

No data available

**12.4 Mobility in soil**

No data available

**12.5 Results of PBT and vPvB assessment**

PBT/vPvB assessment not available as chemical safety assessment not required/not conducted

**12.6 Other adverse effects**

No data available

**SECTION 13: Disposal considerations****13.1 Waste treatment methods****Product**

Offer surplus and non-recyclable solutions to a licensed disposal company. Dissolve or mix the material with a combustible solvent and burn in a chemical incinerator equipped with an afterburner and scrubber.

**Contaminated packaging**

Dispose of as unused product.

**SECTION 14: Transport information**

**14.1 UN number**

ADR/RID: - IMDG: - IATA: -

**14.2 UN proper shipping name**

ADR/RID: Not dangerous goods

IMDG: Not dangerous goods

IATA: Not dangerous goods

**14.3 Transport hazard class(es)**

ADR/RID: - IMDG: - IATA: -

**14.4 Packaging group**

ADR/RID: - IMDG: - IATA: -

**14.5 Environmental hazards**

ADR/RID: no IMDG Marine pollutant: no IATA: no

**14.6 Special precautions for user**

No data available

**SECTION 15: Regulatory information**

This safety datasheet complies with the requirements of Regulation (EC) No. 1907/2006.

**15.1 Safety, health and environmental regulations/legislation specific for the substance or mixture****Authorisations and/or restrictions on use****15.2 Chemical Safety Assessment**

For this product a chemical safety assessment was not carried out

**SECTION 16: Other information****Further information**

Copyright 2013 Sigma-Aldrich Co. LLC. License granted to make unlimited paper copies for internal use only.

The above information is believed to be correct but does not purport to be all inclusive and shall be used only as a guide. The information in this document is based on the present state of our knowledge and is applicable to the product with regard to appropriate safety precautions. It does not represent any guarantee of the properties of the product. Sigma-Aldrich Corporation and its Affiliates shall not be held liable for any damage resulting from handling or from contact with the above product. See [www.sigmaaldrich.com](http://www.sigmaaldrich.com) and/or the reverse side of invoice or packing slip for additional terms and conditions of sale.



**SIGMA-ALDRICH** *sigma-aldrich.com*

**SAFETY DATA SHEET**

According to Regulation (EC) No. 1907/2006

Version 5.1 Revision Date 06.08.2013

Print Date 28.02.2014

GENERIC EU MSDS - NO COUNTRY SPECIFIC DATA - NO OEL DATA

**SECTION 1: Identification of the substance/mixture and of the company/undertaking**

**1.1 Product identifiers**

Product name: Methylene blue

Product Number: M9140

Brand: Sigma-Aldrich

REACH No. : A registration number is not available for this substance as the substance or its uses are exempted from registration, the annual tonnage does not require a registration or the registration is envisaged for a later registration deadline.

CAS-No. : 7220-79-3

**1.2 Relevant identified uses of the substance or mixture and uses advised against**

Identified uses: Laboratory chemicals, Manufacture of substances

**1.3 Details of the supplier of the safety data sheet**

Company: Sigma-Aldrich Chemie GmbH

Riedstrasse 2

D-89555 STEINHEIM

Telephone: +49 89-6513-1444

Fax: +49 7329-97-2319

E-mail address: eurtechserv@sial.com

**1.4 Emergency telephone number**

Emergency Phone #: +49 7329-97-2323

**SECTION 2: Hazards identification**

**2.1 Classification of the substance or mixture**

**Classification according to Regulation (EC) No 1272/2008**

Acute toxicity, Oral (Category 4), H302

Skin irritation (Category 2), H315

Eye irritation (Category 2), H319

Specific target organ toxicity - single exposure (Category 3), H335

For the full text of the H-Statements mentioned in this Section, see Section 16.

### **Classification according to EU Directives 67/548/EEC or 1999/45/EC**

Xn Harmful R22, R36/37/38

For the full text of the R-phrases mentioned in this Section, see Section 16.

## **2.2 Label elements**

### **Labelling according Regulation (EC) No 1272/2008**



Pictogram

Warning

Signal word

Warning

Hazard statement(s)

H302 Harmful if swallowed.

H315 Causes skin irritation.

H319 Causes serious eye irritation.

H335 May cause respiratory irritation.

Precautionary statement(s)

P261 Avoid breathing dust/ fume/ gas/ mist/ vapours/ spray.

P305 + P351 + P338 IF IN EYES: Rinse cautiously with water for several minutes.

Remove Contact lenses, if present and easy to do. Continue rinsing.

Supplemental Hazard Statements - none

Safety data sheet available on request.

### **2.3 Other hazards - none**

## **SECTION 3: Composition/information on ingredients**

### **3.1 Substances**

Synonyms: Tetramethylthionine chloride

3,7-bis(Dimethylamino)phenazathionium chloride

Basic Blue 9

Formula:  $C_{16}H_{18}ClN_3S \cdot 3H_2O$

Molecular Weight: 373,90 g/mol

CAS-No. : 7220-79-3

EC-No. : 200-515-2

### Hazardous ingredients according to Regulation (EC) No 1272/2008

Component	Classification	Concentration
<b>Methylthioninium chloride</b>		
CAS-No. 7220-79-3	Acute Tox. 4; Skin Irrit. 2;	<= 100 %
EC-No. 200-515-2	Eye Irrit. 2; STOT SE 3; H302, H315, H319, H335	

### Hazardous ingredients according to Directive 1999/45/EC

Component	Classification	Concentration
<b>Methylthioninium chloride</b>		
CAS-No. 7220-79-3	Xn, R22 - R36/37/38	<= 100 %
EC-No. 200-515-2		

CAS-No. 7220-79-3

EC-No. 200-515-2

For the full text of the H-Statements and R-Phrases mentioned in this Section, see Section 16

#### SECTION 4: First aid measures

##### 4.1 Description of first aid measures

###### General advice

Consult a physician. Show this safety data sheet to the doctor in attendance.

###### If inhaled

If breathed in, move person into fresh air. If not breathing, give artificial respiration.

Consult a physician.

###### In case of skin contact

Wash off with soap and plenty of water. Consult a physician.

###### In case of eye contact

Rinse thoroughly with plenty of water for at least 15 minutes and consult a physician.

###### If swallowed

Never give anything by mouth to an unconscious person. Rinse mouth with water. Consult a physician.

#### **4.2 Most important symptoms and effects, both acute and delayed**

The most important known symptoms and effects are described in the labelling (see section 2.2) and/or in section 11

#### **4.3 Indication of any immediate medical attention and special treatment needed**

No data available

### **SECTION 5: Firefighting measures**

#### **5.1 Extinguishing media**

##### **Suitable extinguishing media**

Use water spray, alcohol-resistant foam, dry chemical or carbon dioxide.

#### **5.2 Special hazards arising from the substance or mixture**

Carbon oxides, nitrogen oxides (NO<sub>x</sub>), Sulphur oxides, Hydrogen chloride gas

#### **5.3 Advice for firefighters**

Wear self contained breathing apparatus for firefighting if necessary.

#### **5.4 Further information**

No data available

### **SECTION 6: Accidental release measures**

#### **6.1 Personal precautions, protective equipment and emergency procedures**

Use personal protective equipment. Avoid dust formation. Avoid breathing vapours, mist or gas. Ensure adequate ventilation. Evacuate personnel to safe areas. Avoid breathing dust.

For personal protection see section 8.

#### **6.2 Environmental precautions**

Do not let product enter drains.

#### **6.3 Methods and materials for containment and cleaning up**

Pick up and arrange disposal without creating dust. Sweep up and shovel. Keep in suitable, closed containers for disposal.

#### **6.4 Reference to other sections**

For disposal see section 13.

### **SECTION 7: Handling and storage**

#### **7.1 Precautions for safe handling**

Avoid contact with skin and eyes. Avoid formation of dust and aerosols.

Provide appropriate exhaust ventilation at places where dust is formed. Normal measures for preventive fire protection.

For precautions see section 2.2.

### **7.2 Conditions for safe storage, including any incompatibilities**

Store in cool place. Keep container tightly closed in a dry and well-ventilated place.

### **7.3 Specific end use(s)**

A part from the uses mentioned in section 1.2 no other specific uses are stipulated

## **SECTION 8: Exposure controls/personal protection**

### **8.1 Control parameters**

#### **Components with workplace control parameters**

### **8.2 Exposure controls**

#### **Appropriate engineering controls**

Handle in accordance with good industrial hygiene and safety practice. Wash hands before breaks and at the end of workday.

#### **Personal protective equipment**

##### **Eye/face protection**

Safety glasses with side-shields conforming to EN166 Use equipment for eye protection tested and approved under appropriate government standards such as NIOSH (US) or EN 166(EU).

##### **Skin protection**

Handle with gloves. Gloves must be inspected prior to use. Use proper glove removal technique (without touching glove's outer surface) to avoid skin contact with this product. Dispose of contaminated gloves after use in accordance with applicable laws and good laboratory practices.

Wash and dry hands.

The selected protective gloves have to satisfy the specifications of EU Directive 89/686/EEC and the standard EN 374 derived from it.

Full contact

Material: Nitrile rubber

Minimum layer thickness: 0,11 mm

Break through time: 480 min

Material tested: Dermatril® (KCL 740 / Aldrich Z677272, Size M)

Splash contact

Material: Nitrile rubber

Minimum layer thickness: 0,11 mm

Break through time: 480 min

Material tested: Dermatril® (KCL 740 / Aldrich Z677272, Size M)

Data source: KCL GmbH, D-36124 Eichenzell, phone +49 (0)6659 87300, e-mail sales@kcl.de,

Test method: EN374

If used in solution, or mixed with other substances, and under conditions which differ from EN 374, contact the supplier of the CE approved gloves. This recommendation is advisory only and must be evaluated by an industrial hygienist and safety officer familiar with the specific situation of anticipated use by our customers. It should not be construed as offering an approval for any specific use scenario.

### **Body Protection**

Complete suit protecting against chemicals, The type of protective equipment must be selected according to the concentration and amount of the dangerous substance at the specific workplace.

### **Respiratory protection**

For nuisance exposures use type P95 (US) or type P1 (EU EN 143) particle respirator. For higher level protection use type OV/AG/P99 (US) or type ABEK-P2 (EU EN 143) respirator cartridges.

Use respirators and components tested and approved under appropriate government standards such as NIOSH (US) or CEN (EU).

### **Control of environmental exposure**

Do not let product enter drains.

## **SECTION 9: Physical and chemical properties**

### **9.1 Information on basic physical and chemical properties**

a) Appearance Form: powder

Colour: dark green

b) Odour: no data available

- c) Odour: Threshold no data available
- d) pH no data available
- e) Melting point/freezing point: Melting point/range: 190 °C
- f) Initial boiling point and boiling range: no data available
- g) Flash point: no data available
- h) Evaporation rate: no data available
- i) Flammability (solid, gas): no data available
- j) Upper/lower flammability or explosive limits: no data available
- k) Vapour pressure: no data available
- l) Vapour density: no data available
- m) Relative density: no data available
- n) Water solubility: soluble
- o) Partition coefficient: noctanol/water: no data available
- p) Auto-ignition temperature: no data available
- q) Decomposition temperature: no data available
- r) Viscosity: no data available
- s) Explosive properties: no data available
- t) Oxidizing properties: no data available

## **9.2 Other safety information**

no data available

## **SECTION 10: Stability and reactivity**

### **10.1 Reactivity**

No data available

### **10.2 Chemical stability**

Stable under recommended storage conditions.

### **10.3 Possibility of hazardous reactions**

No data available

### **10.4 Conditions to avoid**

No data available

### **10.5 Incompatible materials**

Strong oxidizing agents

### **10.6 Hazardous decomposition products**

Other decomposition products - no data available

In the event of fire: see section 5

## **SECTION 11: Toxicological information**

### **11.1 Information on toxicological effects**

#### **Acute toxicity**

No data available

#### **Skin corrosion/irritation**

No data available

#### **Serious eye damage/eye irritation**

no data available

#### **Respiratory or skin sensitisation**

No data available

#### **Germ cell mutagenicity**

No data available

#### **Carcinogenicity**

IARC: No component of this product presents at levels greater than or equal to 0.1% is identified as probable, possible or confirmed human carcinogen by IARC.

#### **Reproductive toxicity**

No data available

#### **Specific target organ toxicity - single exposure**

Inhalation - May cause respiratory irritation.

#### **Specific target organ toxicity - repeated exposure**

No data available

#### **Aspiration hazard**

No data available

#### **Additional Information**

RTECS: SP5740000

Absorption into the body leads to the formation of methemoglobin which in sufficient concentration causes cyanosis. Onset may be delayed 2 to 4 hours or longer. Vomiting, Diarrhoea, to the best of our knowledge, the chemical, physical, and toxicological properties has not been thoroughly investigated.

## **SECTION 12: Ecological information**



### **12.1 Toxicity**

No data available

### **12.2 Persistence and degradability**

No data available

### **12.3 Bioaccumulative potential**

No data available

### **12.4 Mobility in soil**

No data available

### **12.5 Results of PBT and vPvB assessment**

PBT/vPvB assessment not available as chemical safety assessment not required/not conducted

### **12.6 Other adverse effects**

No data available

## **SECTION 13: Disposal considerations**

### **13.1 Waste treatment methods**

#### **Product**

Offer surplus and non-recyclable solutions to a licensed disposal company. Contact a licensed professional waste disposal service to dispose of this material. Dissolve or mix the material with a combustible solvent and burn in a chemical incinerator equipped with an afterburner and scrubber.

#### **Contaminated packaging**

Dispose of as unused product.

## **SECTION 14: Transport information**

### **14.1 UN number**

ADR/RID: -          IMDG: -          IATA: -

### **14.2 UN proper shipping name**

ADR/RID: Not dangerous goods

IMDG: Not dangerous goods

IATA: Not dangerous goods

### **14.3 Transport hazard class(es)**

ADR/RID: -          IMDG: -          IATA: -

### **14.4 Packaging group**

ADR/RID: -           IMDG: -                           IATA: -

#### **14.5 Environmental hazards**

ADR/RID: no           IMDG Marine pollutant: no    IATA: no

#### **14.6 Special precautions for user - No data available**

### **SECTION 15: Regulatory information**

This safety datasheet complies with the requirements of Regulation (EC) No. 1907/2006.

#### **15.1 Safety, health and environmental regulations/legislation specific for the substance or mixture - No data available**

#### **15.2 Chemical Safety Assessment**

For this product a chemical safety assessment was not carried out

### **SECTION 16: Other information**

#### **Full text of H-Statements referred to under sections 2 and 3.**

Acute Tox. : Acute toxicity    Eye Irrit. : Eye irritation    Skin Irrit. : Skin irritation

H302: Harmful if swallowed.

H315: Causes skin irritation.

H319: Causes serious eye irritation.

H335: May cause respiratory irritation.

#### **Full text of R-phrases referred to under sections 2 and 3**

Xn: Harmful

R22: Harmful if swallowed.

R36/37/38 : Irritating to eyes, respiratory system and skin.

#### **Further information**

Copyright 2013 Sigma-Aldrich Co. LLC. License granted to make unlimited paper copies for internal use only.


The above information is believed to be correct but does not purport to be all inclusive and shall be used only as a guide. The information in this document is based on the present state of our knowledge and is applicable to the product with regard to appropriate safety precautions. It does not represent any guarantee of the properties of the product. Sigma-Aldrich Corporation and its Affiliates shall not be held liable for any damage resulting from handling or from contact with the above product. See [www.sigmaaldrich.com](http://www.sigmaaldrich.com) and/or the reverse side of invoice or packing slip for additional terms and conditions of sale.

**Merck Millipore**  
**104965 Potassium cyanide**



<b>Product information</b>	
<b>Synonyms</b>	Cyanogen potassium
<b>Hill Formula</b>	CKN
<b>Chemical formula</b>	KCN
<b>HS Code</b>	2837 19 00
<b>EC number</b>	205-792-3
<b>Molar mass</b>	65.12 g/mol
<b>EC index number</b>	006-007-00-5
<b>CAS number</b>	151-50-8
<b>Chemical and physical data</b>	
<b>Solubility</b>	716 g/l (25 °C)
<b>Melting point</b>	634 °C
<b>Molar mass</b>	65.12 g/mol
<b>Density</b>	1.55 g/cm <sup>3</sup> (20 °C)
<b>Bulk density</b>	750 kg/m <sup>3</sup>

<b>pH value</b>	11 - 12 (20 g/l, H <sub>2</sub> O, 20 °C)
<b>Boiling point</b>	1625 °C (1013 hPa)
<b>Vapor pressure</b>	(20 °C)

### Safety information according to GHS

<b>Hazard Statement(s)</b>	H300 + H310 + H330: Fatal if swallowed, in contact with skin or if inhaled H410: Very toxic to aquatic life with long lasting effects. EUH032: Contact with acids liberates very toxic gas.
<b>Precautionary Statement(s)</b>	P273: Avoid release to the environment. P280: Wear protective gloves/ protective clothing. P302 + P352: IF ON SKIN: Wash with plenty of soap and water. P304 + P340: IF INHALED: Remove victim to fresh air and keep at rest in a position comfortable for breathing. P309 + P310: IF exposed or if you feel unwell: Immediately call a POISON CENTER or doctor/physician.
<b>Signal Word</b>	Danger
<b>Hazard Pictogram(s)</b>	
<b>RTECS</b>	TS8750000
<b>Storage class</b>	6.1B Non combustible substances, toxic
<b>WGK</b>	WGK 3 highly water endangering
<b>Disposal</b>	6 Sulfides and sulfites as well as other reducing substances, inorganic cyanides and isonitriles: Stir into sodium hypochlorite solution (Cat. No. 105614) and, if necessary, leave to react for several days. Caution: some substances may show a violent reaction! Draw off any toxic or flammable gases that may be formed. Excess oxidant should be neutralized with sodium thiosulfate (Cat. No. 106513). Container D or E.

## Safety information

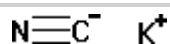
<b>R Phrase</b>	R 26/27/28-32-50/53 Very toxic by inhalation, in contact with skin and if swallowed. Contact with acids liberates very toxic gas. Very toxic to aquatic organisms, may cause long-term adverse effects in the aquatic environment.
<b>S Phrase</b>	S 7-28-29-45-60-61 Keep container tightly closed. After contact with skin, wash immediately with plenty of soap and water. Do not empty into drains. In case of accident or if you feel unwell, seek medical advice immediately (show the label where possible). This material and its container must be disposed of as hazardous waste. Avoid release to the environment. Refer to special instructions/ Safety data sheets.
<b>Categories of danger</b>	very toxic, dangerous for the environment
<b>Hazard Symbol</b>	 Very toxic  Dangerous for the environment

## Transport information

<b>Declaration (railroad and road) ADR, RID</b>	UN 1680 Kaliumcyanid, fest, 6.1, I
<b>Declaration (transport by sea) IMDG-Code</b>	UN 1680 POTASSIUM CYANIDE, SOLID, 6.1, I, Marine Pollutant: P, Segregation Group: 6 (Cyanides)
<b>Declaration (transport by air) IATA-DGR</b>	UN 1680 POTASSIUM CYANIDE, SOLID, 6.1, I

## Toxicological data

LD 50 oral	LD50 rat 5 mg/kg
LD 50 dermal	LD50 rabbit 14.3 - 33.3 mg/kg



## Merck Millipore

### 100206 Phenol

#### Product information



Grade	ACS, Reag. Ph Eur
Synonyms	Hydroxybenzene, Carboic acid
Hill Formula	C <sub>6</sub> H <sub>6</sub> O
Chemical formula	C <sub>6</sub> H <sub>5</sub> OH
HS Code	2907 11 00
EC number	203-632-7
Molar mass	94.11 g/mol
EC index number	604-001-00-2
CAS number	108-95-2

#### Chemical and physical data

Ignition temperature	595 °C
Solubility	84 g/l (20 °C)
Melting point	40.8 °C
Molar mass	94.11 g/mol
Density	1.06 g/cm <sup>3</sup> (20 °C)
Bulk density	620 kg/m <sup>3</sup>
pH value	5 (50 g/l, H <sub>2</sub> O, 20 °C)
Boiling point	181.8 °C (1013 hPa)
Vapor pressure	0.2 hPa (20 °C)
Explosion limit	1.3 - 9.5 % (V)
Flash point	81 °C

#### Safety information according to GHS

	H301 + H311 + H331: Toxic if swallowed, in contact with skin or if inhaled
	H314: Causes severe skin burns and eye damage.
Hazard Statement(s)	H341: Suspected of causing genetic defects. H373: May cause damage to organs (/\$/*_ORGAN_REPEAT/\$/) through prolonged or repeated exposure.
	P280: Wear protective gloves/ protective clothing/ eye protection/ face protection.
Precautionary Statement(s)	P301 + P330 + P331: IF SWALLOWED: Rinse mouth. Do NOT induce vomiting. P302 + P352: IF ON SKIN: Wash with plenty of soap and water.

	<p>P304 + P340: IF INHALED: Remove victim to fresh air and keep at rest in a position comfortable for breathing.</p> <p>P305 + P351 + P338: IF IN EYES: Rinse cautiously with water for several minutes. Remove contact lenses, if present and easy to do. Continue rinsing.</p> <p>P309 + P310: IF exposed or if you feel unwell: Immediately call a POISON CENTER or doctor/physician.</p>
Signal Word	Danger
Hazard Pictogram(s)	
RTECS	SJ3325000
Storage class	6.1A Combustible, acute toxic Cat. 1 and 2 / very toxic hazardous materials
WGK	WGK 2 water endangering 9
Disposal	<p>Carcinogenic compounds and flammable compounds labelled "Highly toxic" or "Toxic": container F. Alkyl sulfates are carcinogenic; Take particular care to avoid inhalation and skin contact. To neutralize alkyl sulfates, add dropwise (from a dropping funnel) to concentrated ice-cool Ammonia solution (Cat.No. 105426) with vigorous stirring. Before placing in container D, check the pH with pH Universal indicator strips (Cat.No. 109535).</p>
R Phrase	<p><b>Safety information</b></p> <p>R 23/24/25-34-48/20/21/22-68</p> <p>Toxic by inhalation, in contact with skin and if swallowed.Causes burns.Harmful: danger of serious damage to health by prolonged exposure through inhalation, in contact with skin and if swallowed.Possible risk of irreversible effects.</p>
S Phrase	<p>S 24/25-26-28-36/37/39-45</p> <p>Avoid contact with skin and eyes.In case of contact with eyes, rinse immediately with plenty of water and seek medical advice.After contact with skin, wash immediately with plenty of soap and water.Wear suitable protective clothing, gloves and eye/face protection.In case of accident or if you feel unwell, seek medical advice immediately (show the label where possible).</p>
Categories of danger	toxic, corrosive, mutagenic
Hazard Symbol	 Toxic



Corrosive

### Transport information

Declaration (railroad and road) ADR, RID UN 1671 Phenol, fest, 6.1, II

Declaration (transport by sea) UN 1671 PHENOL, SOLID, 6.1, II  
IMDG-Code

Declaration (transport by air) UN 1671 PHENOL, SOLID, 6.1, II  
IATA-DGR

### Toxicological data

LD 50 oral LD50 rat 317 mg/kg

LD 50 dermalLD50 rat 525 - 714 mg/kg

